FINAL REPORT

Impact of Clay-DNAPL Interactions on Transport and Storage of Chlorinated Solvents in Low Permeability Zones

SERDP Project ER-1737

FEBRUARY 2015

Avery Demond
University of Michigan

Mark Goltz
Air Force Institute of Technology

Junqi Huang
U.S. Environmental Protection Agency

SERDP
DOD ▪ EPA ▪ DOE

REPORT DOCUMENTATION PAGE

1. REPORT DATE *(DD-MM-YYYY)* 21-04-2014	2. REPORT TYPE Final	3. DATES COVERED *(From - To)*

4. TITLE AND SUBTITLE	5a. CONTRACT NUMBER
Impact of Clay-DNAPL Interactions on Transport and Storage of Chlorinated Solvents in Low Permeability Zones	
	5b. GRANT NUMBER

6. AUTHOR(S)	5c. PROGRAM ELEMENT NUMBER
Demond, Avery H.	
Goltz, Mark N.	5d. PROJECT NUMBER
Huang, Junqi	ER-1737
	5e. TASK NUMBER
	5f. WORK UNIT NUMBER

7. PERFORMING ORGANIZATION NAME(S) AND ADDRESS(ES)	8. PERFORMING ORGANIZATION REPORT NUMBER
University of Michigan, Ann Arbor, MI 48109-2125 Air Force Institute of Technology, Wright-Patterson Air Force Base, OH 45433-7765 U.S. Environmental Protection Agency, Ada, OK 74820	

9. SPONSORING / MONITORING AGENCY NAME(S) AND ADDRESS(ES)	10. SPONSOR/MONITOR'S ACRONYM(S)
	11. SPONSOR/MONITOR'S REPORT NUMBER(S)

12. DISTRIBUTION / AVAILABILITY STATEMENT

13. SUPPLEMENTARY NOTES

14. ABSTRACT

The objective of this research was to examine clay-DNAPL waste interactions as a contributor to the accumulation of chlorinated compound contamination in subsurface clay lenses and layers. The results showed that contact between DNAPL waste and Na-smectitic clay materials caused a contraction of the clay's basal space, producing cracking, in a time frame on the order of weeks. The hypothesized mechanism is syneresis, involving the sorption of the surfactants from the waste onto the clay surface and the solvation of the surfactants' aggregates. Numerical simulations suggest that even a small amount of cracking, and the time-variable dissolution of the DNAPL stored in the cracks into the surrounding clay matrix, extends the remediation time by decades.

15. SUBJECT TERMS

aquitard, back diffusion, clay, chlorinated solvents, cracking , diffusion, DNAPL, groundwater contamination , groundwater remediation, hazardous waste sites, permeability, solute transport, tailing, tetrachloroethylene, trichloroethylene

16. SECURITY CLASSIFICATION OF:

a. REPORT			17. LIMITATION OF ABSTRACT	18. NUMBER OF PAGES	19a. NAME OF RESPONSIBLE PERSON
	b. ABSTRACT	c. THIS PAGE			19b. TELEPHONE NUMBER *(include area code)*

Table of Contents

Abstract

Objective: Chlorinated solvents are often disposed of in such a manner that they form pools on subsurface clay layers. There they slowly migrate into the clay layers, accumulating therein over time. Due to the low permeability of these layers, it is assumed that the migration occurs by dissolution and diffusion. However, field evidence suggests that more solvent may be stored in such layers than can be accounted for through this mechanism. The objective of the Statement of Need (SON) by Strategic Environmental Research and Development Program (SERDP) under which the proposal for this research was submitted was to "improve our understanding of how low permeability zone storage occurs, [and] the hydrogeochemical conditions that contribute to this process." Consistent with this SON, the overall objective of the research was to examine the validity of diffusion as the dominant mechanism of transport and to examine the possibility that cracks in low permeability clay layers contribute to the accumulation of contamination therein and the long remediation times associated with these sites.

Technical Approach: Since there are few reported measurements of the diffusion coefficient in clayey soils for contaminants of interest, steady-state measurements using the time-lag method were made in silt and silt-clay mixtures (75% silica silt and 25% Na-montmorillonite). Changes in clay structure for smectitic clays were measured using x-ray diffraction and through macroscopic observations of crack apertures. The mechanism of cracking was examined using x-ray diffraction, FTIR and sorption measurements. The impact of cracking and dissolution rates on down gradient concentrations and remediation time frames was evaluated using numerical simulation.

Results: The diffusion measurements showed that the diffusion coefficient for trichloroethylene in a silt-clay mixture was at least two to four fold smaller than estimates used in field studies. Calculations based on the measurements obtained in this research suggest that there is an even greater discrepancy between the amount of mass storage in low permeability layers and that which can be attributed to diffusion. To account for this enhanced transport, it was postulated that direct contact between the waste and these layers altered the structure of the clay, and consequently the transport properties. Measurements using x-ray diffraction showed that contact with chlorinated field wastes decreased the basal spacing of water-saturated smectites from 19 Å to 15 Å, accompanied by cracks with apertures as large as 1 mm, within weeks. Calculations showed that even minimal cracking could easily account for the enhanced mass storage observed in the field.

To investigate the mechanism of basal spacing decrease, a set of screening experiments were performed, which identified a nonionic surfactant, an anionic surfactant, and a chlorinated solvent, as the minimum waste components necessary for cracking to occur. Sorption measurements showed enhanced synergistic sorption of the surfactants in the presence of the chlorinated solvent, while Fourier transform infrared spectroscopy suggested a displacement of water from the interlayer space. Based on all the accumulated evidence, it was hypothesized that

the nonionic surfactant sorbs on the margins of the interlayer space, displacing some of the interlayer water. The anionic surfactant sorbs via an interaction with the nonionic surfactant and enhances the dehydration of the interlayer space through the solvation of water in micellar aggregates. Thus, the reduction in basal spacing is predominantly through a process of syneresis.

The numerical simulations showed that the presence of cracks in a clay layer has a significant effect on down gradient concentrations, with the storage of the contaminant as a dense nonaqueous phase liquid (DNAPL) in the cracks and the rate of dissolution being key. In particular, if DNAPL is present in the cracks, it is the process of DNAPL dissolution which drives the contaminant farther into the clay matrix that impacts the down gradient concentration temporal history. Simulations comparing the influence of constant and variable dissolution rates showed that when the dissolution rate depends on the DNAPL saturation, the mass of DNAPL that persists in the clay is greater, extending the remediation time by decades.

Benefits: The results of this research directly address the statement of need in that it specifically focused on how significant amounts of low permeability storage may occur. This research suggests that contact between DNAPLs and clay minerals in the low permeability layers alters the structure of the clay, resulting in the formation of cracks. Calculations performed as part of this research indicated that even small cracks (naturally occurring or forming as a result of contact with DNAPLs) can significantly increase the amount of storage in these low permeability layers. Numerical simulations showed that extended remediation times may be associated with DNAPL residing in cracks, the dissolution of which serves to drive the contaminant farther into the low permeability matrix. These results indicate that conventional remediation, even if effective in removing contaminant from high permeability areas, will fail to decrease contaminant concentrations below the maximum contaminant level (MCL) for decades, suggesting lengthy and costly cleanups for contaminated sites where the remedial objective is meeting the MCL.

List of Tables

List of Figures

List of Acronyms

AFB   Air Force Base

AOT   Aerosol OT

ATR   attenuated total reflectance

CEC   cation exchange capacity

CMC   critical micelle concentration

CTAB   cetyltrimethylammonium bromide

$C_{12}E_6$ hexaethylene glycol monododecyl ether

DoD   Department of Defense

DNAPL   dense nonaqueous phase liquid

ELSD   evaporative light scattering detector

FTIR   Fourier transform infrared

ESTCP   Environmental Security Technology Certification Program

GC   gas chromatography

GMS   Ground Water Modeling System (Department of Defense)

HPLC   high performance liquid chromatography

ID   internal diameter

ISA   ionic strength adjuster

MCL   maximum contaminant level

MS   mass spectroscopy

PCE   tetrachloroethylene

RCF   relative centrifugal force

TCE   trichloroethylene

TOT   tetrahedral-octahedral-tetrahedal

SERDP   Strategic Environmental Research and Development Program

SON   statement of need

XRD   x-ray diffraction

Keywords

aquitard

back diffusion

clay

chlorinated solvents

cracking

diffusion

DNAPL

groundwater contamination

groundwater remediation

hazardous waste sites

permeability

solute transport

tailing

tetrachloroethylene

trichloroethylene

Acknowledgements

1.0   Introduction and Objectives

The chlorinated ethenes, trichloroethylene (TCE) and tetrachloroethylene (PCE) are used extensively as cleaning solvents in processes such as degreasing and dry cleaning because of their ability to dissolve grease and oil effectively (Williams-Johnson et al., 1997). Their improper disposal has resulted in their introduction to the subsurface environment, resulting in the fact that these compounds are two of the organic contaminants most commonly found at Superfund sites (SERDP and ESTCP, 2006). As they are denser than water and relatively insoluble in water, they travel vertically in the subsurface as a separate organic liquid (also known as a denser-than-water nonaqueous phase liquid or DNAPL), pooling on top of low permeability lenses and layers. Due to the long-term contact between the DNAPLs and the low permeability geologic strata, the latter can accumulate a significant mass of contaminants over time, essentially becoming contaminant storage zones (Sale et al., 2008a; Stroo et al., 2012). Once the original source is removed, these zones release contamination into the surrounding groundwater, serving as long-term secondary contamination sources. Studies such as that by Parker et al. (2008) suggest that even a clay layer as thin as 0.2 m can result in groundwater concentrations above permissible levels for decades after the original source is isolated or removed.

The mechanism of transport into and out of these low permeability zones is thought to be diffusion (Mackay and Cherry, 1989; Ball et al., 1997; Wilson, 1997; Chapman and Parker, 2005; Parker et al., 2008). However, it has been reported that the detected quantity of contaminants in some clay layers is higher than what can be attributed to diffusion only (Sale et al., 2007). Similarly, Ball et al. (1997) observed that the effective diffusion rates of organic compounds, including TCE, through unweathered clay were 1.6 to 5 times higher than that estimated for diffusional transport. Thus, there is circumstantial evidence that pure diffusion may not be the only mechanism of transport into and out of these low permeability zones.

The objective of the Statement of Need (SON) by Strategic Environmental Research and Development Program (SERDP) under which the proposal for this research was submitted was to "improve our understanding of how low permeability zone storage occurs, [and] the hydrogeochemical conditions that contribute to this process." Consistent with this SON, the overall objective of the research was to examine the validity of diffusion as the dominant mechanism of transport and to examine the possibility that cracks in low permeability clay layers contribute to the accumulation of contamination therein and the long remediation times associated with these sites. These cracks may be naturally occurring, or, it is hypothesized, may actually result from the contact of DNAPLs with the low permeability layers. This research project was originally divided into three tasks:

Task 1. Modification of clay structure due to contact with chlorinated DNAPLs;

Task 2. Measurement of enhanced transport due to the contact with chlorinated DNAPLs;

Task 3. Modeling the impact of enhanced transport on the longevity of the dissolved phase plume.

During the course of the project, a fourth task was added:

Task 4. Determination of mechanism of clay structure modification.

However, to present the research performed for this project in a more logical fashion, it was reorganized here as follows:

Task 1. Diffusion of solutes in saturated low permeability soil materials;

Task 2. Modification of soil structure due to contact with chlorinated DNAPLs;

Task 3. Determination of mechanism of clay structure modification;

Task 4. Modeling the impact of enhanced transport on the longevity of the dissolved phase plume.

2.0   Diffusion of Solutes in Saturated Low Permeability Soil Materials

2.1.   Introduction

It is often assumed that diffusion is the mechanism governing the transport of compounds such as TCE and PCE into low permeability lenses and layers in the subsurface (Goodall and Quigley, 1977; Johnson et al., 1989; Parker et al., 2004). Despite of the importance of diffusion for the transport of chlorinated organic solutes in low permeability soils, few studies have actually measured the diffusion coefficient of chlorinated organic solutes in saturated low permeability soils. Table 2.1 (Ayral and Demond, 2014) present a summary of measurements from eleven studies for diffusion coefficients for organic solutes in saturated soil, of which eight included chlorinated aliphatics. Because of the relative paucity of measurements, the diffusion coefficient is often estimated. One hypothesis for the higher than anticipated mass storage in low permeability strata is that the reported diffusion coefficients are in error. Table 2.2 gives methods for determining the relative diffusivity in saturated soils, defined as:

$$\frac{D_e}{D_{aq}} \tag{2.1}$$

where D_e is the effective diffusion coefficient, defined by the application of Fick's First Law to the movement of solutes in porous media (written here in one dimension):

$$J_s = D_e \frac{dC}{dx} \tag{2.2}$$

where J_s is the mass flux (per unit area bulk soil), C is the concentration in the aqueous phase and D_{aq} is the diffusion coefficient of the solute in bulk water.

The effective diffusivity is frequently estimated as a power function of porosity:

$$\frac{D_e}{D_{aq}} = \varepsilon^m \tag{2.3}$$

where the value of the exponent m is often taken as 1.3 (Archie, 1942; Millington and Quirk, 1960, 1961). Although this value gives reasonable estimates for the diffusion of inorganic solutes in sandy soils, it has been noted in the past that methods giving the relative diffusivity as an exponential function of porosity often yield poor estimates for soil media containing greater than 25% clay (e.g., Olesen et al., 1999). This conclusion was confirmed for relative diffusivities for organic solutes in clayey soils (Ayral and Demond, 2014). Looking specifically at studies for tracer (tritiated water) diffusion in clayey soils and organic solute diffusion in clayey soils (and fitting equations to the data therein if necessary) yielded the relationships in Table 2.2. The average percent relative errors for the estimation of the relative diffusivities reported in Table 2.1, using the methods from Table 2.2, are given in Table 2.3. These statistics suggest that the methods based on diffusion measurements of tritiated water give the best estimates for clayey soils (>25% clay), with the method by Bourg et al. (2006) giving the lowest overall error.

Table 2.1. Summary of Literature Values of Diffusion Coefficients of Organic Solutes in Saturated Clayey Soils

Solute	Soil	Type of measurement	Porosity (-)	D_e (cm²/s *10⁶); D_{aq} (cm²/s *10⁶); [D_e/D_{aq}]	D_{app} (cm²/s *10⁶)	R; [K_d (mL/g)]	Notes	Reference
1,4-DCB 4-CP	Synthetic soil mixture containing silica sand, kaolinite, and bentonite; L = 0.3 - 0.5 cm	"Quasi steady state" (Source and collection reservoirs sampled at 10 and 20 days after an equilibration time of two weeks)	0.40 (2% bent.) 0.43 (4% bent.) 0.48 (4% bent.)	2.41; *8* [0.301] (DCB) 2.34; *8.9* [0.263] (CP) 2.65; *8* [0.331] (DCB) 2.59; *8.9* [0.291] (CP) 3.05; *8* [0.381] (DCB) 3.05; *8.9* [0.343] (CP)	-	-	Confining pressure is 4 psi. Study reported hindrance factor (H) which is defined as D_{aq}/D_e. D_e is calculated as D_{aq}/H.	Mott and Weber (1991)
Lindane	Synthetic soil mixture containing silica sand, kaolinite, and bentonite; L = 0.3 - 0.5 cm	Non-steady state (Columns sectioned at 8, 16, 32 days)	0.46 (avg. of 4% bentonite values is assumed)	2.4; *5.6* [0.429]	-	$K_F = 3.84$ x 10^{-4}; $1/n = 1.17$	Sorption of lindane is described by Freundlich isotherm, parameter values compatible with units of mg/g and mg/L; Confining pressure = 4 psi. Study reported D_e.	Mott and Weber (1991)
Acetone 1,4-Dioxane Aniline Chloroform Toluene	Grey clay soil from Sarnia, Ontario, Canada (45% clay, mainly chlorite and illite);L = 1.6 cm	Non-steady state (Source and collection reservoirs sampled at two day interval over 14 days)	0.39 $\rho_s = 2.73$ g/cm³ $\rho_b = 1.68$ g/cm³	2.2; *12.8* [0.172] 1.6; *9.7* [0.165] 2.7; *10.5* [0.257] 4.3; *10* [0.430] 5.4; *8.5* [0.635]	1.20 0.90 0.40 0.16 0.05	1.8; [0.19] 1.7; [0.17] 6.6; [1.3] 26.8; [6.0] 113.0; [26]	Soil was placed in cell saturated. Study reported D_e. εD_e is reported here in accordance with definition of D_e here. Batch tests indicated linear isotherms. R is calculated from reported values of ρ_b, K_d (fitted to data) and ε. D_{app} is calculated as D_e/R.	Barone et al. (1992)

Table 2.1. Continued

Solute	Soil	Type of measurement	Porosity (-)	D_e (cm²/s *10⁶); D_{aq} (cm²/s *10⁶); [D_e/D_{aq}]	D_{app} (cm²/s *10⁶)	R; [K_d (mL/g)]	Notes	Reference
Benzene TCE Toluene CB	Glaciolacustrine clay from Sarnia, Ontario, Canada (40% clay, mostly chlorite and illite); L = 10 cm	Non-steady state (Source reservoir is sampled over 23 days)	0.34 ρ_b= 1.77 g/cm³	3.5; *10.9* [0.321] 3.5; *9.4* [0.372] 3.0; *8.5* [0.353] 2.9; *8.7* [0.333]	0.11 0.06 0.04 0.03	32.3 58.4 74 98.4	Soil used directly from soil sampler. Study reported D_{app} and R. Batch tests indicated linear isotherms. D_e is calculated from D_{app}*R (fitted to data)	Myrand et al. (1992)
DCM	Silty-clay glacial till from Sarnia, Ontario, Canada (38% clay, mainly chlorite and muscovite); L = 9 cm	Non steady state (Column sectioned at two weeks)	0.34 ρ_b= 1.71 g/cm³	3.5; *11.5* [0.304]	2.94	1.19	Soil used directly from soil sampler. Study reported D_e and R. D_{app} was calculated as D_e /R.	Parker (1996)
1-Naphthol	Weathered shale (43 % clay, mainly montmorillo-nite) L = 0.4 cm	Steady state (Collection reservoir sampled over about 30 days; steady-state reached in 21 days)	(avg) ρ_b =1.26 g/cm³ ρ_b =1.40 g/cm³ ρ_b =1.57 g/cm³	(avg) 0.17; *7.5* [0.023] 0.20; *7.5* [0.027] 0.067; *7.5* [0.009]	(avg) 0.0019 0.0017 0.00044	(avg) 94 [39] 116 [39] 151 [39]	Sample was partially saturated, compacted to a particular ρ_b, and then fully saturated. Batch tests indicated linear isotherms. Study reported D_e and R. Reported values of D_{es} were taken as D_e.	Sawatsky et al. (1997)

Table 2.1. Continued

Solute	Soil	Type of measurement	Porosity (-)	D_e (cm²/s *10⁶); D_{aq} (cm²/s *10⁶); [D_e/D_{aq}]	D_{app} (cm²/s *10⁶)	R; [K_d (mL/g)]	Notes	Reference
Naphthalene	Weathered shale (43 % clay, mainly montmorillonite) L = 0.4 cm		ρ_b =1.26 g/cm³ (avg) ρ_b =1.40 g/cm³ (avg) ρ_b =1.57 g/cm³ (avg)	0.024; 7 [0.003]	0.00025	94 [27]	D_{app} was calculated as D_{es} /R.	Sawatsky et al. (1997)
Naphthalene	Montmorillonite (reference clay from Source Clay Repository, Columbia, MS, all cations were replaced with Ca²⁺ prior to use) L = 0.4 cm		ρ_b =1.49 g/cm³ (avg) ρ_b =1.45 g/cm³ (avg)	0.069; 7 [0.010]	0.069 (avg)			
TCE	- Jurassic clay from Frommern, Germany (52% clay);	Steady state (Collection reservoir sampled up to 20 days)	(Avg) 0.45; ρ_s =2.67	(Avg) 0.89; 9.4 [0.095]	(Avg) 0.27	(Avg) 3.3	Material was pressed tightly into the diffusion cell ring. Study reported D_e, D_{app} and α. R was calculated as α/ε. D_{app} was calculated as D_e /R.	Grathwohl (1998)
	- Jurassic clay from Lustnau, Germany (41% clay);		0.41; ρ_s =2.65	1.37; 9.4 [0.146]	0.24	5.8		
	- Triassic clay from Haigerloch Germany, (55% clay);		0.46 ρ_s =2.7	0.72; 9.4 [0.077]	0.73	1.0		

6

Table 2.1. Continued

Solute	Soil	Type of measurement	Porosity (-)	D_e (cm²/s *10⁶); D_{aq} (cm²/s *10⁶); $[D_e/D_{aq}]$	D_{app} (cm²/s *10⁶)	R; [K_d (mL/g)]	Notes	Reference
TCE	- Activated Na-bentonite from Friedland, Germany (87% clay);		0.55; ρ_s=2.65	0.21; *9.4* [0.022]	0.52	0.4		Grathwohl (1998)
	-Silt-clayey soil from Darmstadt, Germany (6% clay) L = 1 cm		0.34; ρ_s=2.65	1.25; *9.4* [0.133]	1.08	1.2		
TCE Aniline	Mixture of locally sourced soil (45% finer 75 micron) and 6% bentonite L = 11.8 cm (avg)	Non-steady state (Diffusion coefficient is determined by fitting the adv-dispersion equation to column exp'ts which last 25-49 days)	0.33 (avg)	1.27; *9.4* [0.135] (avg) 0.81; *10.5* [0.077] (avg)	0.99 0.62	1.28; [0.051] 1.25; [0.044]	Soil was wet uniformly and placed into cell and saturated by increasing the pressure from 28 to 315 kPa. Study reported D_e/ε. D_e was calculated as $D_e/\varepsilon * \varepsilon$. R was calculated from K_d (fitted to data), ρ_b and ε.	Khandelwal et al. (1998)
PCE 1,2,4-TCB	Silty clay loam from Dover AFB, DE (35% clay, clay minerals identified were kaolinite and chlorite) L = 25 cm Diffusion distance = 0.59 cm	Non-steady state (Diffusion coefficient determined by fitting dual domain model to breakthrough experiments lasting 11 to 112 days)	0.43 ρ_b= 1.51 g/cm³	1.8; *8.7* [0.207] 2.0; *6.7* [0.299]	0.918 0.344	1.96 5.82	Material moistened at 20%, packed and then saturated for three weeks. Study reported D_e and R (fitted to data). D_{app} was calculated as D_e /R.	Young and Ball (1998)

7

Table 2.1. Continued

Solute	Soil	Type of measurement	Porosity (-)	D_e (cm²/s *10⁶); D_{aq} (cm²/s *10⁶); [D_e/D_{aq}]	D_{app} (cm²/s *10⁶)	R; [K_d (mL/g)]	Notes	Reference
Benzene	Silty clay from Regina, Saskatchewan, Canada (70 % clay, mainly smectite) L = approx. 3 cm	Non-steady state (Source and collection reservoirs sampled over 36 days; column sectioned at end of exp'ts)	0.57 (avg) ρ_s =2.81 g/cm³	1.8; *10.9* [0.165]	0.577	3.12 [1.0]	Soil was saturated and consolidated. Batch tests indicated linear isotherms. Study reported D_e. εD_e was reported here in accordance with definition of D_e here. R was calculated from K_d (fitted to data), ρ_b and ε. D_{app} was calculated as D_e/R.	Donahue et al. (1999)
Benzene Toluene 2-FT	Synthetic soil mixture (85% sand, 12% bentonite, 3% organophilic clay) L = approx. 3 cm	Non-steady state (The source reservoir was sampled daily for the first two weeks and then twice weekly up to 56 or 72 days)	0.34 ρ_b= 1.74 g/cm³	1.6; *10.9* [0.144] 0.8; *8.5* [0.093] 1.1; *8.3* [0.133]	0.0076 0.0011 0.0015	206 [40] 717 [140] 717 [140]	Soil was compacted at a water content of 15% and vacuum-saturated under a pressure of 70 kPa for three days. Study reported D_e. D_e for toluene and 2-fluorotoluene are values in a three-component mixture. R was calculated from K_d (fitted to data), ρ_b and ε. D_{app} was calculated as εD_e /R.	Headley et al. (2001)

Table 2.1. Continued

Solute	Soil	Type of measurement	Porosity (-)	D_e (cm²/s *10⁶); D_{aq} (cm²/s *10⁶); [D_e/D_{aq}]	D_{app} (cm²/s *10⁶)	R; [K_d (mL/g)]	Notes	Reference
MEK TCE Toluene	Reconstituted clay (Londonderry clay from Sydney, New South Wales, Australia) (95% finer than 75 μm, mainly kaolinite and illite) L = 1.25 – 2.97 cm	Non-steady state (Source and collection reservoirs sampled over 15-27 day	Reconst. 0.41 (avg) ρ_b= 1.51 g/cm³ (avg)	1.02; *9.4* [0.109] (MEK) 0.83; *9.4* [0.088] (TCE) 0.88; *8.5* [0.104] (Toluene)	1.02 0.53 0.57	1 [0] 1.5 [0.15] 1.5 [0.15]	Reconstituted sample mixed with distilled water at a moisture content of 40%, then placed in cell and compressed at 100 kPa to achieve field densities. Undisturbed samples used directly from corers. Study reported D_e. ϵD_e was reported here in accordance with definition of D_e here. R was calculated from K_d (fitted to data), ρ_b and ε. D_{app} was calculated as ϵD_e /R.	Itakura et al. (2003)
	Undisturbed clay (50% finer than 75 μm, mainly kaolinite and illite) L= 1.25 cm		Undist. 0.36 (avg) ρ_b= 1.68 g/cm³ (avg)	1.02; *9.4* [0.108] (MEK) 0.91; *9.4* [0.097] (TCE) 1.19; *8.5* [0.140] (Toluene)	0.70 0.54 0.61	1.46 [0.10] 1.69 [0.15] 1.92 [0.2]		

CB: Chlorobenzene, CP: Chlorophenol, DCB:Dichlorobenzene, DCM: Dichloromethane, FT: Fluorotoluene, MEK: Methyl ethyl ketone, TCB:Trichlorobenzene, TCE: Trichloroethylene, PCE: Tetrachloroethylene.

D_e: Effective diffusion coefficient; D_{aq}: Aqueous diffusion coefficient (Montgomery, 2000); D_{app}: Apparent diffusion coefficient; R: Retardation factor; K_d: Distribution coefficient; K_F and n: Freundlich isotherm fitting parameters; L: Thickness of sample; ρ_s: Soil particle density; ρ_b: Dry bulk density.

Table 2.2. Methods for Estimating the Relative Diffusivity in Clayey Materials

Method	Reference
Gas/Inorganic Diffusion in Saturated Sandy Soils	
$\varepsilon^{4/3}$	Millington and Quirk (1960, 1961)
Tritiated Water Diffusion in Saturated Clayey Soils	
$10^{(-0.8549\rho_b - 0.0868)}$	Log-linear fit to data for tritiated water from Miyahara et al. (1991), Sato et al. (1992) and Garcia-Gutierrez et al. (2004)
$\dfrac{(1 - f_{interlayer}) + \delta_{interlayer} f_{interlayer}}{G}$	Bourg et al. (2006)
Organic Solute Diffusion in Saturated Clayey Soils	
0.25	Johnson et al. (1989)
$-0.4619\varepsilon^2 + 0.926\varepsilon + 0.0764$	Parker et al. (1994)
0.7	Ball et al. (1997)
$10^{(2.2517\rho_b - 4.3364)}$	Grathwohl (1998)

ρ_b = dry bulk density, δ = constrictivity of the interlayer space taken as equal to 0.3, G = geometric factor taken as equal to 4.0, $f_{interlayer}$ = fraction of porosity in the interlayer of clay minerals which can be evaluated by: $f_{interlayer} = 0.87\rho_b - 0.348$, for $1 < \rho_b < 1.3$ g/cm^3 ; $f_{interlayer} = 0.78$, for $1.3 < \rho_b < 1.5$ g/cm^3 ; $f_{interlayer} = 0.9\rho_b - 0.58$, for $1.5 < \rho_b < 1.7$ g/cm^3 (equations fitted to point values provided in Bourg et al. [2006]).

Table 2.3. Average Percent Relative Error for Estimation of Relative Diffusivities Reported in the Literature

Methods	Average Percent Relative Error			
	Overall	Soil clay content <25% clay	Soil clay content >25% clay	On average
Millington and Quirk (1960, 1961)	140	52	165	overestimate
Log-linear fit to data for tritiated water from Miyahara et al. (1991), Sato et al. (1992) and Garcia-Gutierrez et al. (2004)	67	82	63	underestimate
Bourg et al. (2006)	23	48	16	underestimate
Johnson et al. (1989)	89	47	101	overestimate
Parker et al. (1994)	189	212	106	overestimate
Ball et al. (1997)	430	311	464	overestimate
Grathwohl (1998)	55	45	92	overestimate

This analysis suggests that if common correlations are used to calculate diffusive fluxes of chlorinated compounds in the field, an overestimation of the flux is likely. However, there are sufficiently few measurements of effective diffusion coefficients for chlorinated compounds, it is difficult to make such a statement with certainty.

2.2.   Materials and Methods

Diffusion measurements were made using two different types of porous media prepared from silica silt and clay minerals. The first porous medium was silica silt with a median diameter of 10 µm, and a SiO_2 content of 99.7% (U.S. Silica, Frederick, MD). The second porous medium was a combination of silica silt and pure Na-montmorillonite clay (SWy-2; Clay Minerals Society, Chantilly, VA) (with a cation exchange capacity of 76.4 meq/100 g [Van Olphen and Fripiat, 1979]) to represent the presence of reactive clay minerals in subsurface layers and lenses. The determination of the relative quantities of each was based on quantities cited as occurring in field aquitards and the swelling potential. Ball et al. (1997) reported a clay fraction of 17-35% in the aquitard at Dover AFB, and Murray and Quirk (1982) stated that soil mixtures with a clay content of less than 30% can accommodate volume changes within the pores of the matrix. To satisfy both criteria, 25% was chosen as the clay fraction for the silt-clay mixtures. To minimize particle segregation issues during packing and saturation, a well-graded soil mixture was constructed. Figure 2.1 shows the particle size distribution obtained with a hydrometer (151H) using ASTM D422-63 (ASTM, 2007a). The median grain diameter was 5 µm, a bit smaller than the median diameter of 9 µm reported for the aquitard at Dover AFB (Ball et al., 1997).
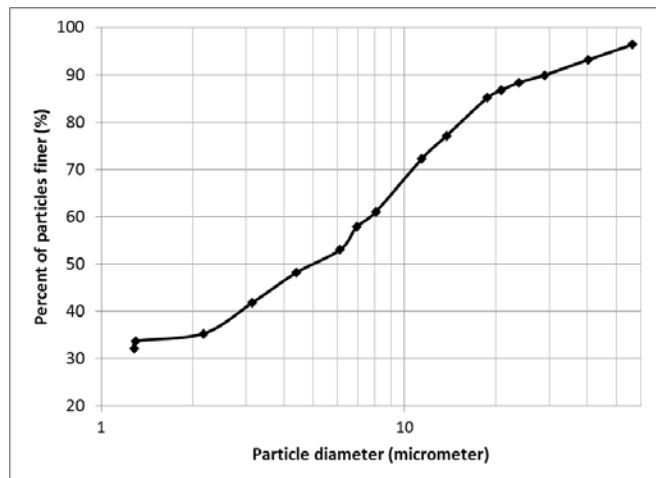
Figure 2.1. Particle size distribution of silt-clay mixture used in diffusion measurements.

The silt was packed dry in a ring (I.D: 5 cm, height: 1 cm) in seven layers, compacting each layer with a 2.5 cm diameter wooden rod in accordance with a procedure outlined by Oliveira et al. (1996) for producing homogeneous columns. The dry bulk density was calculated from the mass of the material packed in the ring (around 35 grams) and the volume of the ring (22.5 cm^2). The porosity of the samples was then determined from the bulk dry density, assuming that the solid density was equal to 2.65 g/cm^3. The ring then was placed on top of a reservoir filled with a 0.005 M $CaSO_4$ solution for saturation. A 0.005 M $CaSO_4$ solution was used rather than distilled water as distilled water has been reported as problematic in hydraulic

conductivity experiments involving clayey soils (ASTM, 2007b). The silt in the ring stayed in contact with water for one day to allow for the spontaneous imbibition of water from the bottom of the sample to the top, and the change in the weight of the ring was recorded. Following that, the water level in the reservoir was raised to induce seepage through the porous medium to eliminate air that might be remaining. At the end of the second day, the weight of the ring was checked again, and, since the change in mass was insignificant, it was considered that saturation had essentially been achieved.

The silt-clay mixtures were packed using the same method described for the silt soil; however, two different approaches were used for saturation. The first one entailed placing a stainless steel block with a weight about 0.5 kg on top of the soil to help ensure even swelling. After ten days of imbibition of water from the bottom, the change in the mass became negligible (change < 1%). Then, the portion of the soil that swelled beyond the top of the ring was scraped off, air dried and then weighed to calculate the porosity of the soil in the ring after expansion. Then, on the tenth day, the level of the reservoir was raised and maintained for another week to displace any remaining air. The second saturation method for silt-clay mixtures restricted the expansion of the soil. The soil mixture in the ring was placed on the reservoir filled with water while confined at the top, so that the sample did not swell beyond the confines of the ring, maintaining the porosity constant. As a result, the porosities of the samples treated in this manner were lower than the porosities of the silt-clay samples which were allowed to expand.

Table 2.4 summarizes the experimental systems for the diffusion measurements. Diffusion experiments were conducted using four different solutes. Iodide was used as an inorganic solute, produced by the dissolution of potassium iodide (Sigma Aldrich, >99.5%) in Milli-Q water, with a resistivity of 18.3 M$\Omega\cdot$cm, created by passing deionized, distilled water through a series of four cartridges to remove impurities (EMD Millipore). Trichloroethylene (TCE) (Fisher Scientific, >99.5%) was chosen as the chlorinated organic solute as it is the solvent base of DNAPL waste from Hill Air Force Base (Hsu, 2005). As surfactants are important components of DNAPL wastes and may diffuse at a different rate than chlorinated solutes based on their considerably larger molecular weights, measurements were also made of the rate of diffusion of an anionic surfactant, Aerosol OT (AOT) (Fisher Scientific) dissolved in Milli-Q water. AOT has a nonpolar tail and polar negatively-charged head, and a molecular weight of 456 g/mol; its structure is given in Figure 2.2. The experiments outlined above were conducted examining the diffusion in water. However, clayey soils in the subsurface are in contact with DNAPL waste for decades. Thus, they may become saturated with an organic solvent. To investigate the possible impact of this on the rate of diffusion, silt soil was packed into the stainless steel ring and saturated with pure tetrachloroethylene (PCE) (Sigma Aldrich, HPLC grade, >99.9%). As the silt was air-dry initially, saturation with PCE appeared to occur within two days, as after that there was negligible mass change. In reality, however, it is unknown the extent to which a DNAPL waste permeates the soil. To more closely replicate the situation in the field, a sample of the 75% silt and 25% clay mixture was compacted and saturated with water, allowing it to expand freely, as explained previously. Then, the water-

saturated soil mixture was put into a diffusion cell with PCE-based DNAPL waste, whose composition is given in Table 2.5, in both the source and collection reservoirs for 18 months prior to the start of the diffusion experiment. For this system, ^{13}C-labeled TCE (Cambridge Isotope Laboratory, MA, >98%) was used as the solute instead of unlabeled TCE because the PCE-based DNAPL waste contained TCE and it was necessary to be able to distinguish between the TCE already in the waste and the TCE diffusing through the sample.

Table 2.4. Experimental Matrix for Diffusion Experiments

Solute	Soil	Saturation liquid
Iodide	Silt	0.005 M $CaSO_4$
Iodide	Silt and clay-expanded	0.005 M $CaSO_4$
Iodide	Silt and clay-confined	0.005 M $CaSO_4$
TCE	Silt	0.005 M $CaSO_4$
TCE	Silt and clay-expanded	0.005 M $CaSO_4$
TCE	Silt and clay-confined	0.005 M $CaSO_4$
AOT	Silt	0.005 M $CaSO_4$
AOT	Silt and clay-expanded	0.005 M $CaSO_4$
AOT	Silt and clay-confined	0.005 M $CaSO_4$
[13]C-labeled TCE	Silt	PCE
[13]C-labeled TCE	Silt and clay-expanded	0.005 M $CaSO_4$ then contacted with PCE-based DNAPL waste for 18 months.
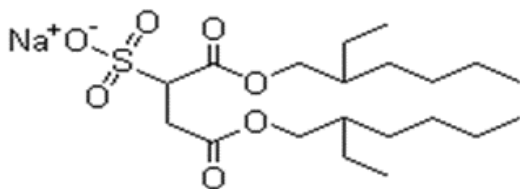
Figure 2.2. Structure of the anionic surfactant, Aerosol OT (AOT).

Table 2.5. Characteristics of DNAPL Field Wastes

	PCE-based DNAPL	TCE-based DNAPL
Source	Dry cleaner, Ann Arbor, MI	Operable Unit 2, Hill Air Force Base, UT
Dominant solvent	Tetrachloroethylene (PCE)	Trichloroethylene (TCE)
Density (g/mL)	1.60	1.30
Interfacial tension with water (dyn/cm)	2 to 3	2 to 3
Dominant surfactant content	nonionic (anionics << 1mM)	anionic
Contact angle at pH 7 (measured through water on quartz)	~30°	~30°

Data from Hsu (2005).

Table 2.1 presents a summary of measurements from the literature of diffusion coefficients for organic solutes in saturated soils containing clay. As the table shows, procedures for measuring the diffusion coefficient vary considerably from one study to another. Nonsteady state experiments seem to be the type most frequently utilized. Many of these involve the fitting of concentrations measured in the source and/or collection reservoirs (Barone et al., 1992; Myrand et al., 1992; Headley et al., 2001; Itakura et al., 2003) to solutions to Fick's Second Law:

$$\frac{\partial c}{\partial t} = D_{app} \frac{\partial^2 c}{\partial x^2} \qquad (2.4)$$

where D_{app} is the observed diffusion coefficient in a nonsteady state situation. D_{app} differs from the effective diffusion coefficient (D_e in Eqn. 2.2) in that D_{app} also reflects sorption characteristics of the solute (Shackelford, 1991), whereas D_e is the diffusion coefficient at steady-state and is theoretically independent of sorption (Grathwohl, 1998). The relationship between D_{app} and D_e is given by:

$$D_{app} = \frac{D_e}{R} \qquad (2.5)$$

where R is the retardation factor, whose relationship to sorption parameters depends on the form of the sorption isotherm. R is then determined independently through, for example, equilibrium batch experiments, which may not reflect the same conditions as in the diffusion cell. Because of the complicating factors posed by evaluating the impact of sorption, steady-state methods may be preferable.

The diffusion through a thin layer of thickness d can be modeled as diffusion into a plane sheet (Figure 2.3). Assuming that the solute is conservative, that C_0, the concentration inside the sheet at time $t = 0$, is equal to 0, and that C_2, the concentration at the exit face of the plane sheet

is also equal to zero, the amount of mass that has passed through the plane sheet is given by (Crank, 1975):

$$M = C_1 d \left(\frac{D_e t}{d^2} - \frac{1}{6} - \frac{2}{\pi^2} \sum_{n=1}^{\infty} \frac{(-1)^n}{n^2} exp \left[\frac{-n^2 \pi^2 D_e t}{d^2} \right] \right)$$ (2.6)

As t $\rightarrow \infty$, the exponential term in Eqn. 2.6 goes to zero, leading to:

$$M = \frac{C_1 D_e}{d} t - \frac{C_1 d}{6}$$ (2.7)

or a linear relation between the cumulative mass that has exited the plane sheet per unit area, M, and time. Eqn. 2.7 can be reorganized to calculate the effective diffusion coefficient as follows:

$$D_e = \frac{d}{C_1} \frac{dM}{dt}$$ (2.8)

This approach to measuring the effective diffusion coefficient is often referred to as the "time-lag" method, with the y-intercept of the linear relationship in Eqn. 2.7, $C_1 d/6$ representing the "time-lag." In the case of a sorbing solute, the time-lag is greater, with its magnitude increasing linearly with R. This method has been used to determine diffusion coefficients in a variety of systems, including gas diffusion in polymers (Barrer and Rideal, 1939; Michaels and Bixler, 1961), ion diffusion in clay soils (Muurinen, 1990; Oscarson, 1994; Boving and Grathwohl, 2001; Garcia-Gutierrez et al., 2004) as well as chlorinated solutes in low permeability porous materials (Grathwohl, 1998). In the studies reported in Grathwohl (1998) and Boving and Grathwohl (2001), steady state was reached in less than three weeks for 1-cm thick samples containing 6-87% clay. The percent relative error was 22% for soil with a porosity of 0.45, and 38% for soil with a porosity of 0.46. Based on this experience, the time-lag method was used in these experiments.

plane
sheet

$C_0 = 0$
at t = 0

x = 0   x = d
$C = C_1$ $C = C_2 = 0$
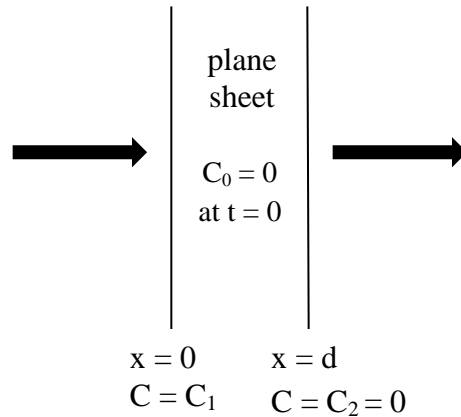
Figure 2.3. Diffusion into a plane sheet. Boundary and initial conditions for Eqn. 2.4, for the solution to diffusion equation given in Eqn. 2.6.

15

The design of the diffusion cells was based on Grathwohl (1998) and Boving and Grathwohl (2001). The diffusion cell for iodide was constructed of Plexiglas and contained three main sections (Figure 2.4). The middle section held the porous medium and consisted of a ring with an internal diameter of 5.0 cm and a height of 1 cm. The lower reservoir served as the source and the top reservoir collected the material that had diffused through the porous medium. Each these reservoirs had a volume of about 350 cm^3. This volume was considered to be large enough to prevent significant concentration changes in the source and collection reservoirs during an experiment (Boving and Grathwohl, 2001), thus maintaining a constant concentration gradient across the sample. Stainless steel mesh with a pore size of 2 µm (TWP, Berkeley, CA) was placed on both the top and the bottom of the ring to prevent the solid particles of the porous medium from entering the reservoirs. The ring containing the compacted and saturated soil was placed on top of the source reservoir filled with a 0.1 M potassium iodide solution in Milli-Q water. The upper reservoir was filled with a 0.1 M potassium nitrate (Sigma Aldrich, >99%) solution, in order to provide a similar osmotic potential in both reservoirs and to minimize the transport of solutes due to an osmotic potential gradient. The upper reservoir was placed on top of the ring and the three components of diffusion cell were assembled by tightening the screws. The diffusion cell was rotated every day to minimize the development of concentration gradients within the reservoirs.
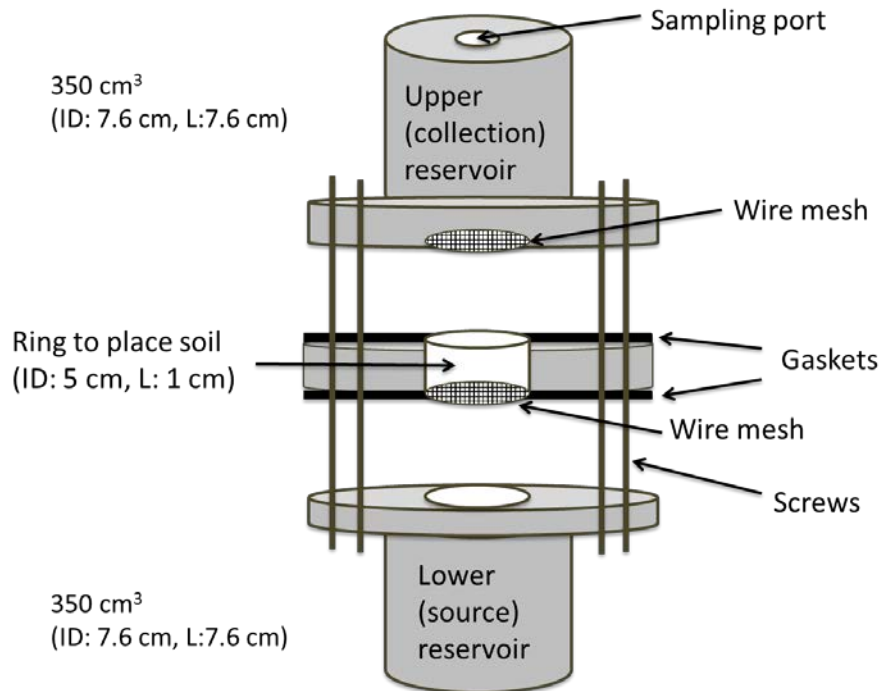
Figure 2.4. Plexiglas cell for measuring iodide diffusion.

Iodide concentrations were measured in the upper collection reservoir over time using an iodide selective probe (Ionplus, Thermo Scientific, Beverly, MA) connected to an Orion Five Star meter (Thermo Scientific, Beverly, MA). The probe was inserted into the collection reservoir and monitored until the reading was steady. After the reading, the probe was removed, rinsed and stored in a beaker containing Milli-Q water. The probe had the capability of measuring concentrations between 5.00×10^{-3} and 1.27×10^{5} mg/L. Calibration standards over the concentration range of 317 - 1269 mg/L were prepared from a 0.1 M iodide standard (Thermo Scientific, Beverly, MA) using Milli-Q water for dilution. The same standard solutions were used throughout the experiment, and the average error was less than 5%. The iodide probe was recalibrated if the error between the standard solution and the reading exceeded 6%. The average calibration slope was -60, a value which fell in the recommended range of -54 to -60. After each run, the reference electrode filling solution was replenished. Although the instruction manual for the probe suggested using an iodide ionic strength adjuster (ISA) to avoid errors caused by the ionic strength of the sample, an ISA was not used because the ionic strength in the collection reservoir had already been adjusted using potassium nitrate. The cumulative mass of iodide in the collection reservoir was calculated from the concentration measured by the iodide probe and the volume of the collection reservoir (350 cm^3). The cumulative mass was divided by the cross-sectional area of the ring containing the soil and the cumulative mass per unit area was plotted as a function of time to obtain D_e using Eqn. 2.8.

The experimental cell for measuring TCE diffusion was also composed of three parts, but it was constructed out of stainless steel for greater chemical resistance (Figure 2.5). The volume of the source reservoir was approximately 10 mL, and it was filled with pure TCE. The aqueous concentration at the lower boundary was taken as the aqueous solubility of TCE equal to 1270 mg/L, as measured by Grathwohl (1998). The collection reservoir (volume of 60 mL) was filled with 20 mL of a 0.005 M $CaSO_4$ solution. Then, the ring, where the compacted, saturated soil resided, was sandwiched in between the source and collection reservoirs. Air from a zero grade air tank (Metro Welding, Detroit, MI) was humidified with Milli-Q water, and the humidified air was bubbled through the collection reservoir at a flowrate of 0.5 mL/min (Figure 2.6). As TCE is a volatile compound, it partitioned into the air, and the TCE that emerged from the collection reservoir was swept into a toluene (Sigma Aldrich, HPLC grade >99.9%) trap with a volume of 20 mL. The continuous removal of TCE from the collection reservoir maintained the concentration therein close to zero.
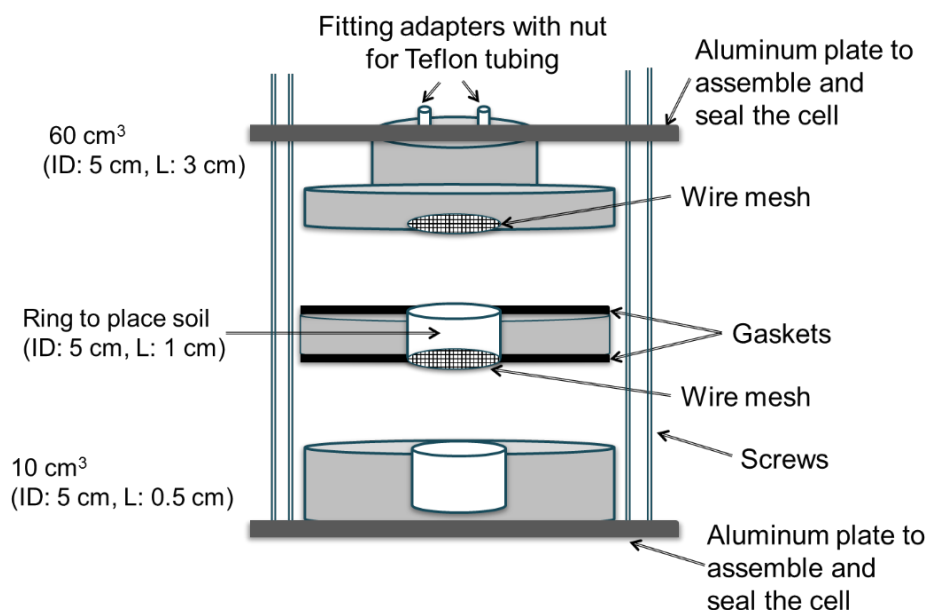
Figure 2.5. Stainless steel cell for measuring TCE diffusion.
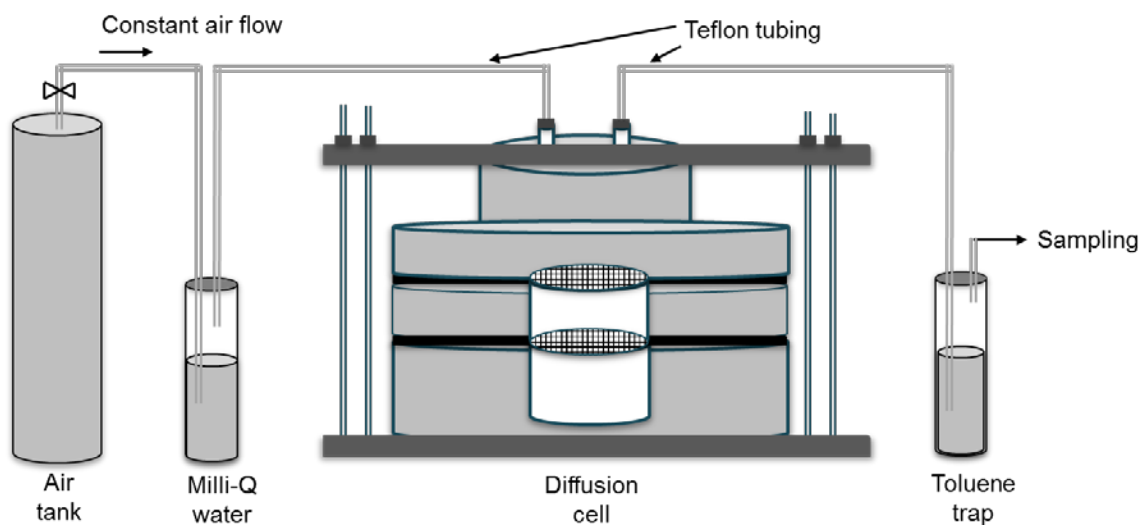
Figure 2.6. Experimental setup used to measure TCE diffusion (after Grathwohl [1998]).

0.5-mL samples were withdrawn from the toluene trap daily over a period of two to three weeks; they were stored in a refrigerator (around 4°C) until they were analyzed using a gas chromatograph (Hewlett Packard 5890) with an electron capture detector. A Phenomenex ZB-5 column (film thickness: 0.25 µm, ID: 0.25mm, L: 30m) was used as the stationary phase and N_2 was used as carrier gas. To prepare the stock solution of TCE in toluene for preparation of calibration standards, toluene was added to a volumetric flask which was then weighed. Then, two or more drops of TCE were added using a 10 µL glass syringe. The flask with toluene and TCE was then reweighed and then the remaining volume was filled with toluene. The

concentration of the stock solution was calculated from the weight and volume of the toluene. Concentrations in the range of 5 to 25 mg/L were used for calibration. In order to decrease the concentration of the stock solution to this range, samples were diluted from 10 to 100 times. As the volume in the toluene trap decreased over time due to sampling, the volume of toluene was adjusted by subtracting the volume of sample (0.5 mL) from the previous volume of toluene. The cumulative mass of TCE was calculated by multiplying the concentration by the modified volume.

The Plexiglas set-up used for iodide diffusion (Figure 2.4) was adapted for use in the experiments examining the diffusion of surfactants in the soils. The source reservoir was filled with a 10^{-3} M AOT solution made up using Milli-Q water. After that, the ring containing the soil and the collection reservoir containing Milli-Q water were placed on top. Two weeks after the start of the experiment, a 1-mL sample was taken from the collection reservoir every other day for four weeks so that the total volume of sample taken from the collection reservoir did not exceed 10% of the total volume of the reservoir (350 cm^3). The experiment was terminated when the concentration in the collection reservoir reached 10% of the concentration in the source reservoir. The samples were analyzed using high-performance liquid chromatography (HPLC) (Hewlett Packard 1090). An Econosphere 3μm silica column (ID: 4.6 mm, L: 150 mm) was used as the stationary phase, and a mixture of Milli-Q water and acetonitrile (> 99.9% [HPLC grade] Fisher Scientific) at a ratio of 20:80, respectively was used as the carrier liquid without a solvent program. An evaporative light scattering detector (ELSD) (Sedere Sedex 55, Richard Scientific, Novato, CA) helped to quantify the concentration of AOT in the samples taken from the collection reservoir. An analytic sequence was initialized once the baseline was stabilized. Calibration standards were made up over the range of 9 - 46 mg/L and run in the same sequence as the samples.

The experimental setup used for measuring the diffusion rate of ^{13}C-labeled TCE was modified from the one used for diffusion of TCE in water-saturated soils (Figures 2.5 and 2.6) by adding a fitting adapter and nut at the bottom of the source reservoir for the injection of ^{13}C-labeled TCE. Both the source and the collection reservoirs were filled with 60 mL PCE or PCE-based DNAPL, and then 0.1 mL ^{13}C-labeled TCE was injected into the source reservoir at the start of the diffusion experiment. The initial concentration in the source reservoir was 14,600 mg/L, which was considered to be high enough to remain constant over the duration of the experiments. The fitting adapters and nuts at the top of the collection reservoir were stoppered with a Viton plug. One of the adapters was untightened to take the 0.1 mL samples from the collection reservoir and was retightened after sampling. Sampling continued until the concentration of ^{13}C-labeled TCE in the collection reservoir reached 10% of the concentration in the source reservoir.

The concentration of ^{13}C-labeled TCE was measured using a gas chromatograph (Hewlett Packard 5890) with a HP 624 column (thickness: 1.4 μm, ID: 0.25 mm, L: 35 m) and H_2 as the carrier gas. A three-minute solvent delay and a decrease in the voltage from 1694 down to 1247 mAV at the sixth minute were used to avoid damaging the detector in the case of liquid injection.

A mass selective detector (Hewlett Packard 5972) was chosen to differentiate the TCE and ^{13}C-labeled TCE, based on a shift of the base peaks. The most abundant mass-to-charge ratios (m/z) of TCE were at 130, 132, and 134 whereas these values shifted to 131, 133, and 135 for ^{13}C-labeled TCE because of the increase in molecular weight of 1 g/mol. Ions at m/z values of 131, 133, and 135 were extracted and used for analysis of the concentration of ^{13}C-labeled TCE. A stock solution was prepared by adding 5 μL of ^{13}C-labeled TCE into 1 mL of PCE. Then, calibration standards were prepared over the range of 146 - 1168 mg/L by diluting this stock solution with PCE.

2.3.   Results and Discussion

2.3.1. Iodide

The main goal of the iodide experiments was to examine the applicability of estimation methods for clayey soils (Table 2.2) and to serve as a comparison for the measurements of diffusion of TCE. Figures 2.7 a, b, and c show plots of the cumulative mass that diffused through the silt, expanded silt-clay mixture and confined silt-clay mixture, respectively, as a function of time. Tables 2.6 and 2.7 summarize the average mass fluxes, with the corresponding effective diffusion coefficients and relative diffusivities. The average effective diffusion coefficient of iodide was determined to be $2.00 \times 10^{-6} \pm 6.04 \times 10^{-8}$ cm^2/sec for silt, and $1.91 \times 10^{-6} \pm 5.39 \times 10^{-8}$ cm^2/sec for the silt-clay mixture that was allowed to expand during saturation. The relative standard deviation between replicates was 3% or lower. These results are not significantly different (p-value > 0.15 at 95% confidence level), suggesting that the presence of 25% clay in and of itself did not reduce the diffusion rate of iodide significantly. However, in the case of the silt-clay mixture that was not allowed to expand freely, the effective diffusion coefficient of iodide decreased significantly (p-value < 0.15) to 1.02×10^{-6} cm^2/sec. Since the silt and confined silt-clay mixture had the same porosity of 0.44, it is apparent that clay content affected the diffusion rate substantially. Thus, estimating the diffusion coefficient just based on porosity would fail to predict the difference. Furthermore, the silt-clay mixtures have the same clay content, yet the diffusion coefficient was reduced in the confined sample, due to the lower porosity of the confined sample ($\varepsilon = 0.45$) compared to that of the expanded mixture ($\varepsilon = 0.68$). Therefore, it appears that neither clay percentage nor porosity alone is sufficient to describe the diffusive characteristics of a clayey soil.
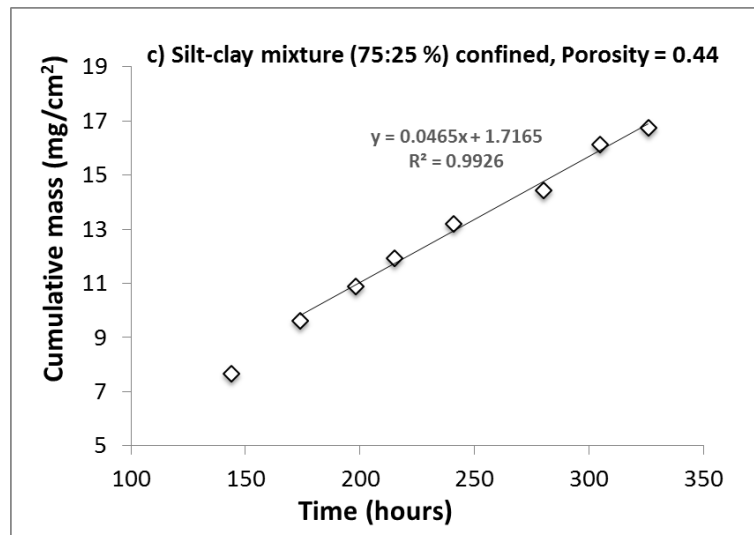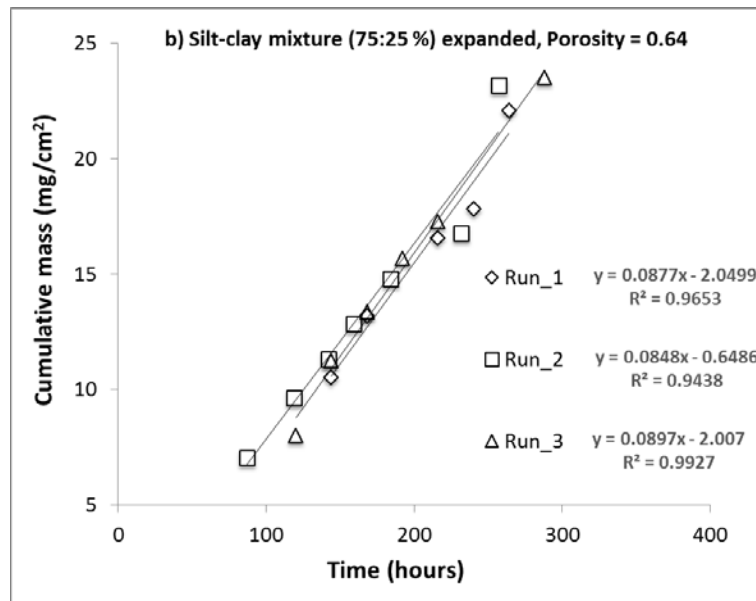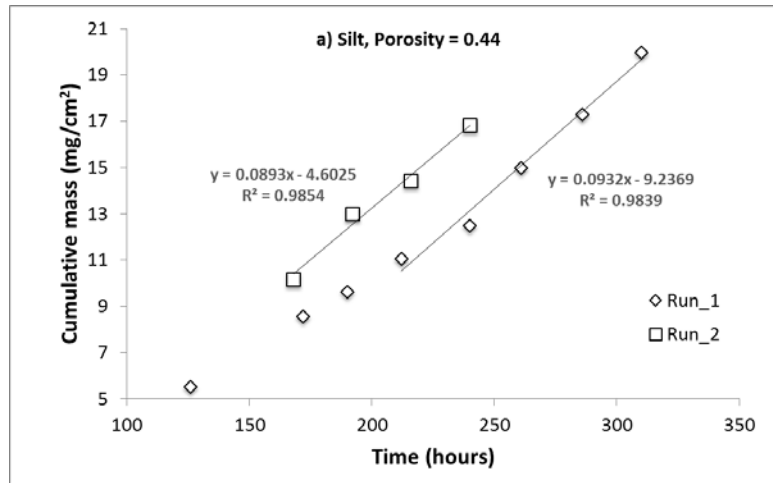
Figure 2.7. Cumulative mass flux of iodide through a) silt, b) expanded silt-clay mixture, and c) confined silt-clay mixture.

21

Table 2.6. Mass Fluxes Obtained from Experimental Data and Calculated Effective Diffusion Coefficients for Iodide

Porous medium	Porosity (-)	Best fit mass flux (dM/dt)[§] (mg/cm^2·hour)	D_e (x 10^6 cm^2/sec)
Silt	0.44	0.0932	2.04
Silt	0.42	0.0893	1.95
Silt and clay mixture, expanded	0.69	0.0877	1.92
Silt and clay mixture, expanded	0.64	0.0848	1.86
Silt and clay mixture, expanded	0.65	0.0897	1.96
Silt and clay mixture, confined	0.43	0.0465	1.02

[§]Based on best-fit lines shown in Figure 2.7.
D_e calculated using Eqn. 2.8, assuming that C_1 = 12690 mg/L (0.1 M KI) and d = 1 cm.

Table 2.7. Average Effective Diffusion Coefficients and Relative Diffusivities for Iodide

Porous Medium	Average porosity	Average D_e (x 10^6 cm^2/sec)	Standard deviation (x 10^8 cm^2/sec)	Relative standard deviation (%)	Average relative diffusivity (D_e/D_{aq})
Silt	0.44	2.00	6.04	3.0	0.12
Silt and clay mixture, expanded	0.64	1.91	5.39	2.8	0.12
Silt and clay mixture, confined	0.44	1.02	NA	NA	0.06

Relative standard deviation = standard deviation/average.
D_{aq} =18.6 x 10^{-6} cm^2/sec (Robinson and Stokes [1955]).
NA = not applicable since only one experimental value.

Table 2.8. Average Percent Relative Errors for Estimated Relative Diffusivities for Iodide

Methods[§]	Predicted Relative Diffusivities (Average percent relative error, %)		
	Silt	Silt-clay expanded	Silt-clay confined
Millington and Quirk (1960, 1961)	0.33 (191%)	0.55 (368%)	0.33 (437%)
Johnson et al. (1989)	0.25 (117%)	0.25 (112%)	0.25 (301%)
Parker et al. (1994)	0.39 (243%)	0.48 (308%)	0.39 (532%)
Ball et al. (1997)	0.70 (508%)	0.70 (495%)	0.70 (1022%)
Grathwohl (1998)	0.10 (12%*)	0.01 (94%*)	0.10 (12%*)
Log-linear fit to data for tritiated water from Miyahara et al. (1991), Sato et al. (1992), and Garcia-Gutierrez et al. (2004)	0.04 (62%*)	0.13 (6%)	0.04 (29*)
Bourg et al. (2006)	0.11 (1%)	0.17 (41%)	0.11 (82%)

[§]Methods given in Table 2.2. *Underestimation.

Table 2.8 summarizes the percent relative error of estimates of relative diffusivities made using the methods from Table 2.2. The methods of Bourg et al. (2006) and the log-linear fit to tritiated water diffusion data, which were suggested as providing more accurate estimates for clayey soils based on literature measurements, performed better in estimating the relative diffusivity of iodide. The log-linear fit to literature results for tritiated water estimated the relative diffusivity of iodide both in expanded and confined in silt-clay mixtures with the smallest relative error (6% overestimation and 29% underestimation, respectively).

2.3.2. TCE

A goal of the diffusion measurements of a chlorinated organic solute was to ascertain whether the few measurements in the literature were reasonable. Additionally, the iodide diffusion experiments supported the conclusion that the estimation methods based on the diffusion of tritiated water in clay provided the best estimates. So, another goal of the organic diffusion experiments was to evaluate if the estimation methods in Table 2.2 could accurately predict the diffusion coefficients in case of an organic solute.

The cumulative mass fluxes for TCE measured using the setup shown in Figure 2.6 are presented in Figure 2.8. The effective diffusion coefficients calculated from these data are given in Table 2.9, with the averages reported in Table 2.10. The effective diffusion coefficients of TCE in silt and in the expanded silt-clay mixture were $1.31 \times 10^{-6} \pm 5.50 \times 10^{-8}$ cm^2/sec and $1.30 \times 10^{-6} \pm 1.49 \times 10^{-8}$ cm^2/sec, respectively. These values are not statistically different from each other and, furthermore, not statistically different (p-value > 0.15) from the results for iodide. On the other hand, the effective diffusion coefficient in the confined silt-clay mixture, which had the same clay content as the expanded sample, but a porosity closer to that of the silt sample, had a significantly reduced diffusion coefficient, $0.70 \times 10^{-6} \pm 6.19 \times 10^{-8}$ cm^2/sec. The relative standard deviations were somewhat higher than those obtained in the case of iodide, but still reasonable.
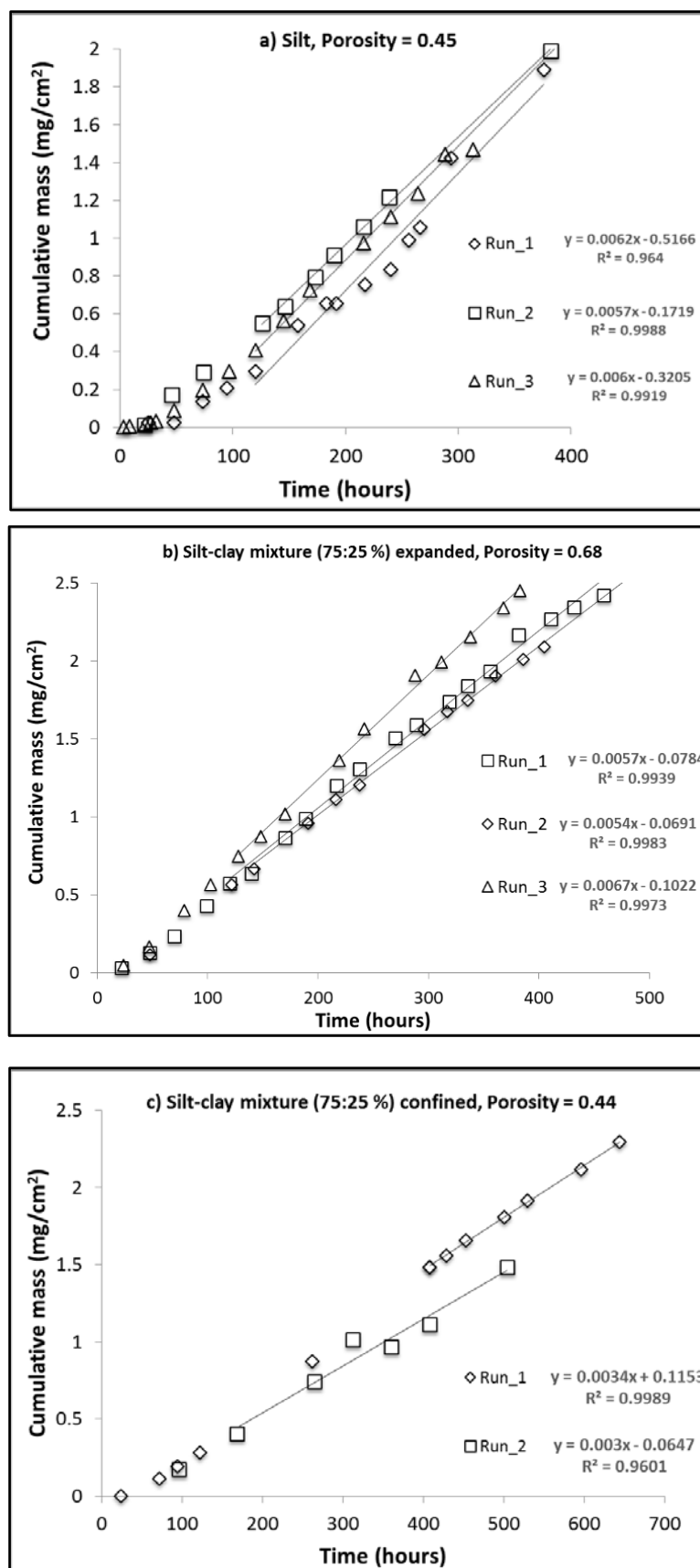
Figure 2.8. Cumulative mass flux of TCE through a) silt, b) expanded silt-clay mixture, and c) confined silt-clay mixture.

Table 2.9. Mass Fluxes Obtained from Experimental Data and Calculated Effective Diffusion Coefficients for TCE

Porous Medium	Porosity (-)	Best-fit mass flux[§] (dM/dt) (mg/cm²·hour)	D_e (x 10^6 cm²/sec)
Silt	0.45	0.0062	1.36
Silt	0.45	0.0057	1.25
Silt	0.43	0.0060	1.31
Silt and clay mixture, expanded	0.68	0.0057	1.25
Silt and clay mixture, expanded	0.64	0.0054	1.18
Silt and clay mixture, expanded	0.60	0.0067	1.47
Silt and clay mixture, confined	0.44	0.0034	0.74
Silt and clay mixture, confined	0.43	0.0030	0.66

[§]Based on best-fit lines shown in Figure 2.8.
D_e calculated using Eqn. 2.8, assuming that C_1 = 1270 mg/L (the solubility limit for TCE, as measured by Grathwohl [1998]) and d = 1 cm.

Table 2.10. Average Effective Diffusion Coefficients and Relative Diffusivities for TCE

Porous Medium	Average porosity	Average D_e (x 10^6 cm²/sec)	Standard deviation (x 10^8 cm²/sec)	Relative standard deviation (%)	Average relative diffusivity (D_e/D_{aq})
Silt	0.45	1.31	5.50	4.2	0.14
Silt and clay mixture, expanded	0.68	1.30	1.49	11.5	0.14
Silt and clay mixture, confined	0.44	0.70	6.19	8.8	0.07

Relative standard deviation = standard deviation/average.
D_{aq} = 9.4x10^{-6} cm²/sec (estimated using method of Hayduk and Laudie [1974]).

Only a few of the studies summarized in Table 2.1 measured the effective diffusion coefficient of TCE in the laboratory. The results from several of these studies seem to agree reasonably well with each other and the results presented here. For example, Khandelwal et al. (1998) measured the value to be 1.27 x 10^{-6} cm²/sec in a soil containing 43% silt and 6% bentonite. Additionally, Itakura et al. (2003) determined the effective diffusion coefficient to be 0.83 x 10^{-6} cm²/sec and 0.91 x 10^{-6} cm²/sec in soils containing 51% and 95% silt, respectively. Using a similar experimental setup to the one employed in these studies, Grathwohl (1998) measured an effective diffusion coefficient of TCE ranging from 1.37 to 0.2 x 10^{-6} cm²/sec for samples whose clay content varied from 6 to 87%, in agreement with the data reported in this study.

On the other hand, Myrand et al. (1992) measured the apparent diffusion coefficient for TCE in clayey soils using a nonsteady method and then measured the retardation factor in batch tests. The effective diffusion coefficient derived from the apparent diffusion coefficient was 3.50 x 10^{-6} cm²/sec, higher than the value obtained here (0.7 x 10^{-6} cm²/sec) and the value

reported by Grathwohl (1998) (1.37 x 10^{-6} cm^2/sec) for systems with a similar clay content and porosity. This discrepancy may stem from the fact that the effective diffusion coefficient was determined from the apparent diffusion coefficient. To do so requires a measure of the retardation coefficient, which, in turn, entails an assumption of equilibrium and a particular model for the sorption isotherm. The lack of agreement highlights the inconsistencies that may ensue when comparing nonsteady-state and steady-state measurements in systems where sorption occurs.

Table 2.11 gives the estimated relative diffusivities for TCE and the associated error for the methods given in Table 2.2. The model developed from the experimental data of Grathwohl (1998) performed the best in estimating the diffusion coefficient of TCE in the confined silt-clay mixture (36% overestimation), whereas its ability in estimating the diffusion of TCE in the expanded silt-clay mixture was much poorer (97% underestimation). The relative diffusivities estimated based on field studies of organic solute diffusion in saturated clay soils (Johnson et al., 1989; Parker et al., 1994; Ball et al., 1997) resulted in an average overestimation of at least 80%. The best estimates for the relative diffusivity of TCE in clayey soils were achieved using the correlations developed based on data for tritiated water or the experimental data for TCE from Grathwohl (1998), depending whether the sample was confined during saturation. It can be concluded that, in situations where the clay content of the soil is more than 25%, models which predict the effective diffusion coefficient based on a log-linear, rather than exponential, relationship with bulk density (or porosity) work better.

Table 2.11. Average Percent Relative Errors for Estimated Relative Diffusivities for TCE

Method[§]	Relative Diffusivities (Average percent relative error)		
	Silt	Silt-clay expanded	Silt-clay confined
Millington and Quirk (1960, 1961)	0.34 (147%)	0.6 (332%)	0.33 (349%)
Johnson et al. (1989)	0.25 (79%)	0.25 (81%)	0.25 (236%)
Parker et al. (1994)	0.40 (187%)	0.49 (256%)	0.39 (430%)
Ball et al. (1997)	0.7 (402%)	0.7 (406%)	0.7 (840%)
Grathwohl (1998)	0.09 (33%*)	0.004 (97%*)	0.10 (36%)
Log-linear fit to data for tritiated water from Miyahara et al. (1991), Sato et al. (1992), and Garcia-Gutierrez et al. (2004)	0.05 (67%*)	0.11 (12%)	0.04 (41%*)
Bourg et al. (2006)	0.11 (19%*)	0.18 (31%)	0.11 (52%)

[§]Methods given in Table 2.2. *Underestimation.

2.3.3. AOT

DNAPL wastes are comprised of both chlorinated solvents and surfactants. However, surfactants are considerably larger molecules and may be comprised of both charged and

uncharged moieties. Based on estimating the aqueous diffusion coefficient of AOT using correlations of Hayduk and Laudie (1974) and Wilke and Chang (1955), the effective diffusion was expected to be around 2-3 times smaller than that of TCE. Figure 2.9 and Table 2.12 show the experimental results obtained here, with the average effective diffusion coefficients and standard deviations given in Table 2.13. The diffusion coefficients were determined to be 0.65 x 10^{-6} ± 9.30 x 10^{-8} cm^2/sec in silt, 0.41 x 10^{-6} ± 18.60 x 10^{-8} cm^2/sec in the expanded silt-clay mixture and 0.23 x 10^{-6} cm^2/sec in the confined silt-clay mixture. The results for the silt and expanded silt-clay samples were not significantly different (p-value<0.15), probably due to the large standard deviation for the expanded silt-clay sample. On the other hand, the diffusion coefficients for the silt and confined silt-clay samples were found to be statistically different.

The effective diffusion coefficient of AOT was two to three times smaller than the comparable measurements for TCE. This reduction is essentially equivalent to the reduction in the aqueous diffusion coefficient. Thus, no additional reduction in the relative diffusivity was observed for AOT, despite its larger size or negatively-charged head. Given the observation that the reduction in the effective diffusion coefficient could be attributed to the reduction in the aqueous diffusion coefficient, similar conclusions as to the best estimation methods were drawn for AOT as for TCE (Table 2.14). For the silt soil, the correlation given by Bourg et al. (2006) gave the best agreement, whereas for the silt-clay mixtures, the log-linear fit of literature data performed the best with a relative error of 10% for the confined silt-clay mixture.

Table 2.12. Mass Fluxes Obtained from Experimental Data and Calculated Effective Diffusion Coefficients for AOT

Porous Medium	Porosity (-)	Best-fit mass flux[§] (dM/dt) (mg/cm^2.hour)	D_e (x 10^6 cm^2/sec)
Silt	0.41	0.0011	0.67
Silt	0.43	0.0012	0.73
Silt	0.42	0.0009	0.55
Silt and clay mixture, expanded	0.62	0.0010	0.61
Silt and clay mixture, expanded	0.73	0.0006	0.36
Silt and clay mixture, expanded	0.69	0.0004	0.24
Silt and clay mixture, confined	0.47	3.87x10^{-4}	0.24
Silt and clay mixture, confined	0.44	3.56x10^{-4}	0.22

[§]Based on best-fit lines shown in Figure 2.9.
D_e calculated using Eqn. 2.8, assuming that C_1 = 456 mg/L (1 mM AOT) and d = 1 cm.
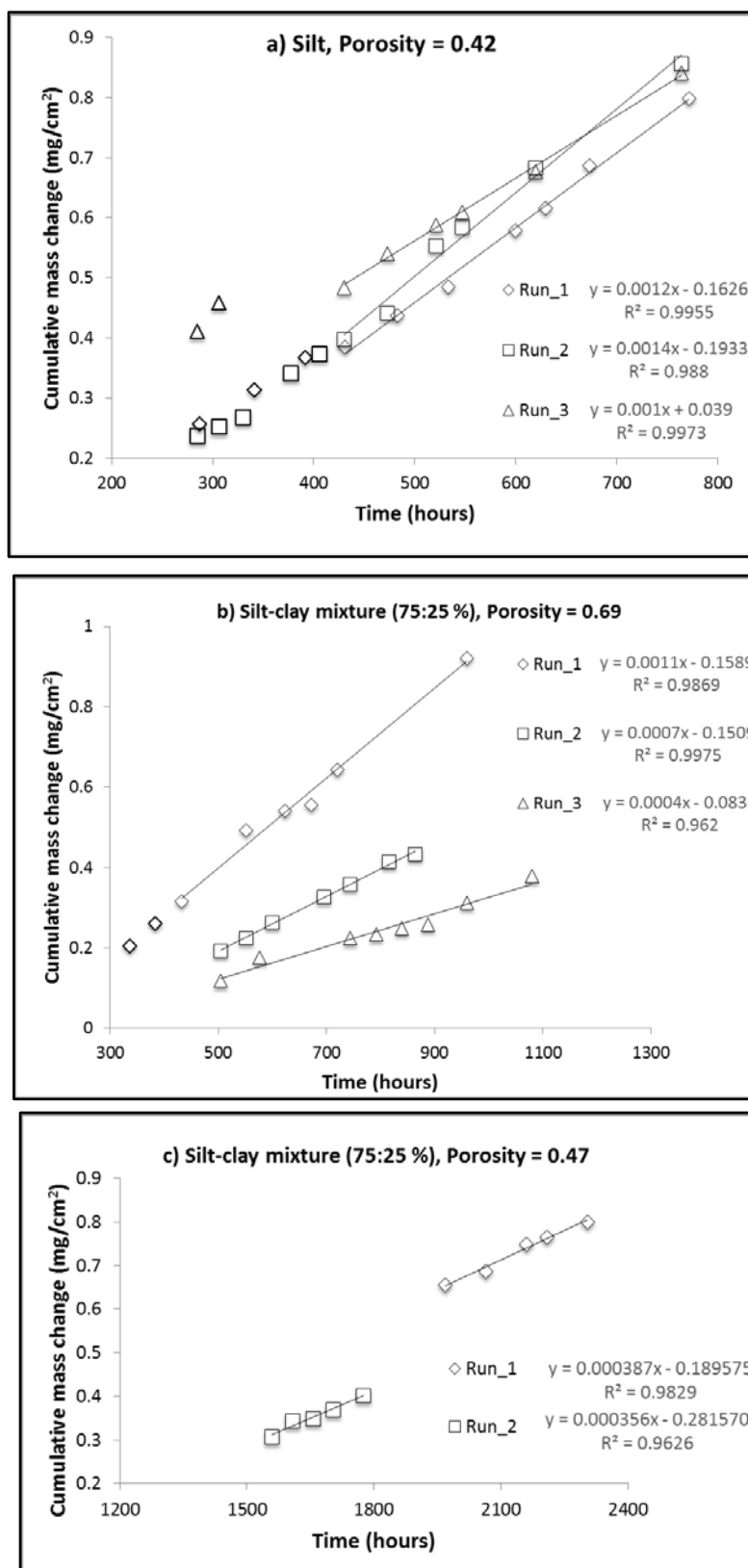
Figure 2.9. Cumulative mass flux of AOT through a) silt, b) expanded silt-clay mixture, and c) confined silt-clay mixture.

Table 2.13. Average Effective Diffusion Coefficients and Relative Diffusivities for AOT

Porous Medium	Average porosity	Average D_e (x 10^6 cm^2/sec)	Standard deviation (x 10^8 cm^2/sec)	Relative standard deviation (%)	Average relative diffusivity (D_e/D_{aq})
Silt	0.42	0.65	9.3	14.3	0.17
Silt and clay mixture, expanded	0.69	0.41	18.6	45.8	0.11
Silt and clay mixture confined	0.47	0.23	1.3	5.9	0.06

Relative standard deviation = standard deviation/average.
D_{aq} = 3.8 x 10^{-6} cm^2/sec (estimated using the method of Hayduk and Laudie [1974]).

Table 2.14. Average Percent Relative Errors for Estimated Relative Diffusivities for AOT

Method[§]	Relative Diffusivities (Average percent relative error)		
	Silt	Silt-clay expanded	Silt-clay confined
Millington and Quirk (1960, 1961)	0.31 (82%)	0.61 (459%)	0.37 (508%)
Johnson et al. (1989)	0.11 (39%*)	0.17 (58%)	0.12 (95%)
Parker et al. (1994)	0.38 (122%)	0.50 (354%)	0.41 (581%)
Ball et al. (1997)	0.7 (70%)	0.7 (343%)	0.7 (447%)
Grathwohl (1998)	0.13 (23%*)	0.003 (97%*)	0.07 (11%)
Log-linear fit to data for tritiated water from Miyahara et al. (1991), Sato et al. (1992) and Garcia-Gutierrez et al. (2004)	0.04 (76%*)	0.17 (57%)	0.05 (10%*)
Bourg et al. (2006)	0.11 (34%*)	0.19 (70%)	0.11 (89%)

[§]Methods given in Table 2.2.
*Underestimation.

2.3.4. ^{13}C-labeled TCE

To more closely emulate conditions in the field, a water-saturated expanded silt-clay sample was contacted with the PCE-based DNAPL waste for 18 months. To differentiate between the diffusion of TCE through the waste and the TCE already present in the PCE-based DNAPL waste, ^{13}C-labeled TCE was used. For a comparison, the diffusion coefficient of ^{13}C-labeled TCE through silt saturated with PCE was measured. To estimate the diffusion coefficient of TCE in PCE, the correlations of Wilke and Chang (1955) and Hayduk and Minhas (1982) were used, employing the value of one as the association factor (as appropriate for an unassociated nonpolar solvent), 165 g/mol as the molecular weight of the solvent, and 0.93 cP as the viscosity of the solvent (Riddick et al., 1986). Using these correlations, the diffusion coefficient of TCE in PCE was estimated to be 19.0×10^{-6} cm^2/sec and 10.3×10^{-6} cm^2/sec, respectively, which are 88% and 9% higher than the diffusion coefficient of TCE in water, respectively.

The experimental results for the diffusion of labelled TCE are given in Figure 2.10.a and in Tables 2.15 and 2.16. The effective diffusion coefficient of TCE through silt saturated with PCE was measured as 1.39×10^{-6} cm^2/sec, only 6% higher than the effective diffusion coefficient of TCE in the silt saturated with water of 1.31×10^{-6} cm^2/sec (Table 2.10). However, this difference was not statistically significant (p-value > 0.15). If the impact of the porous medium on diffusion is similar in both cases, the ratio of the effective diffusion coefficients of TCE in water to that in PCE would be equal to the ratio of the bulk diffusion coefficients in the different liquid phases. The measurements reported here agree with that supposition as the bulk diffusion coefficient of TCE in PCE was calculated to be 9% or 88% higher than the bulk diffusion coefficient of TCE in water. Thus, the increase of 6% could be simply due to the difference in the diffusion coefficients in the different bulk liquids.

The results reported in Section 3.3.2 showed that the effective diffusion coefficients of TCE through silt and through the expanded silt-clay mixture were very similar. Also, the effective diffusion coefficient of TCE through silt saturated with PCE versus that through silt saturated with water were not significantly different. If the situation with the PCE-based waste in contact with an expanded silt-clay mixture is reflective of these cases, then it might be anticipated that the effective diffusion coefficient of ^{13}C-TCE through the expanded silt-clay mixture contacted with PCE waste would be similar to the effective diffusion coefficient of ^{13}C-TCE in silt. The results of the diffusion experiments for ^{13}C-TCE through the expanded silt-clay mixture contacted with PCE waste are presented in Figure 2.10.b and in Tables 2.15 and 2.16. The average diffusion coefficient of ^{13}C-TCE in this situation was equal to 1.14×10^{-8} cm^2/sec, more than two orders of magnitude lower. The reasons behind this low value are currently unknown; however it suggests that, in the case of diffusion from a real DNAPL waste into a saturated soil matrix, the diffusion rate of a chlorinated solute could be substantially lower than that in a clean system involving a single solute into water-saturated soil.
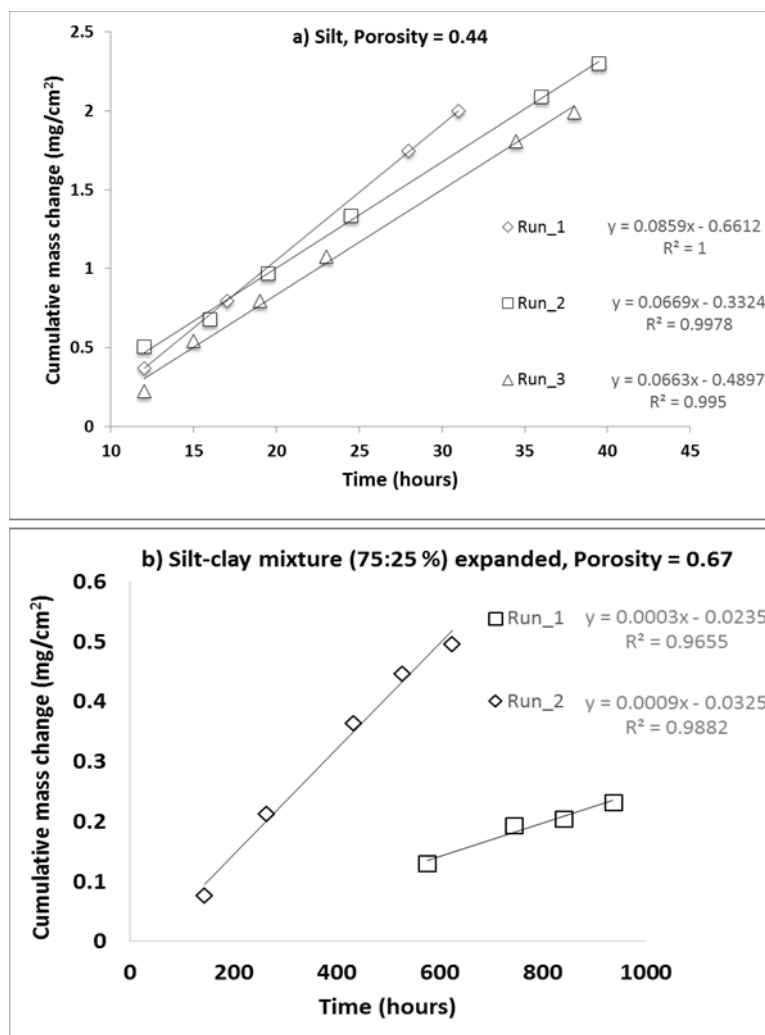
Figure 2.10. Cumulative mass flux of ^{13}C-labeled TCE through a) silt saturated with PCE, and b) expanded silt-clay mixture saturated with water and contacted with PCE-based DNAPL waste for 18 months.

Table 2.15. Mass Fluxes Obtained from Experimental Data and Calculated Effective Diffusion Coefficients for ^{13}C-labeled TCE

Porous Medium	Porosity (-)	Best-fit mass flux[§] (dM/dt) (mg/cm^2·hour)	D_e (cm^2/sec)
Silt saturated with PCE	0.45	0.0859	1.63 x 10^{-6}
Silt saturated with PCE	0.44	0.0669	1.27 x 10^{-6}
Silt saturated with PCE	0.41	0.0663	1.26 x 10^{-6}
Silt and clay mixture, expanded and contacted with PCE-based DNAPL waste	0.68	0.0003	0.57 x 10^{-8}
Silt and clay mixture, expanded and contacted with PCE-based DNAPL waste	0.65	0.0009	1.71 x 10^{-8}

[§]Based on best-fit lines shown in Figure 2.10.

D_e calculated using Eqn. 2.8, assuming that C_1 = 14600 mg/L and d = 1 cm.

Table 2.16. Average Effective Diffusion Coefficients and Relative Diffusivities for ^{13}C-labeled TCE

Porous Medium	Average porosity	Average D_e (cm^2/sec)	Standard deviation (x 10^8 cm^2/sec)	Average relative standard deviation (%)	Average relative diffusivity (D_e/D_{aq})
Silt saturated with PCE	0.44	1.39 x 10^{-6}	21.2	15.3	0.13[§]
Silt and clay mixture, expanded and contacted with PCE-based DNAPL waste	0.65	1.14 x 10^{-8}	0.81	70.7	0.001*

Relative standard deviation = standard deviation/average.
[§]Relative to the diffusion coefficient of TCE in PCE of 10.3 x 10^{-6} cm^2/sec (estimated using the method of Hayduk and Laudie [1974]).
*Relative to the diffusion coefficient of TCE in water of 9.4 x 10^{-6} cm^2/sec (estimated using the method of Hayduk and Laudie [1974]).

2.4.   Conclusions

An accurate determination of diffusion rates is critical to the calculation of rates of transport into and out aquitards and the mass storage therein.   In studies looking at the mass accumulation in aquitards, the effective diffusion coefficient is often estimated because there are few measured values.   Many estimation methods suggest an exponential dependence of the relative diffusivity on the porosity of soil, but these methods were developed originally for inorganic or gas diffusion in sandy soils.   The results reported here, and in Ayral and Demond (2014), suggest that such methods grossly overestimate the diffusion coefficient, especially in soils with a clay content higher than 25%.   Similarly, it was found that the relative diffusivities of TCE based on field studies provide an overestimate of the values measured here.   Two other estimation methods were also explored: a log-linear relationship developed by fitting experimental data for the diffusion of tritiated water in clay soils and a theoretical relation by Bourg et al. (2006) developed for clay soils considering clay variables such as the fraction of interlayer space.   Both of these estimation methods performed better in estimating relative diffusivities of TCE and iodide.

The diffusion coefficient of an anionic surfactant (AOT) was also measured because it is known that field wastes contain surfactants.   It appeared that reductions in the effective diffusion coefficient and aqueous diffusion coefficient were to a similar degree, so no additional decrease in relative diffusivity for AOT was observed despite its larger size.   The log-linear relation developed from literature experimental data for tritiated water and the theoretical relation developed by Bourg et al. (2006) gave the best estimates for AOT, similar to the results for iodide and TCE.

In order to evaluate the diffusion of a chlorinated solvent in a clayey soil in a situation more reflective of the field, the diffusion of ^{13}C-labeled TCE was measured in a silt-clay mixture that had been in contact with a PCE-based DNAPL waste for 18 months.   In this system, the

effective diffusion coefficient was almost two orders of magnitude lower than that for pure TCE through water, suggesting that diffusion from a waste matrix at a field site may be much slower than diffusion of a chlorinated solute from a pure solvent.

2.5. Implications

The effective diffusion coefficient of TCE measured here was 1.30×10^{-6} cm^2/sec for an unconfined saturated silt-clay mixture (75% silt and 25% clay) and 0.7×10^{-6} cm^2/sec for a confined saturated silt-clay mixture. These values are in agreement with those reported by Grathwohl (1998) and others (Khandelwal et al, 1998; Itakura et al., 2003). The diffusion coefficient for the expanded silt-clay sample contacted with field DNAPL waste was 1.14×10^{-8} cm^2/sec which is considerably lower than previously reported values. The diffusion coefficients for TCE measured here are almost four times lower than the ones estimated using Parker et al. (1994)'s data (Table 2.2), and five times lower than the observed diffusion coefficients reported in Johnson et al. (1989) of 3.25×10^{-6} cm^2/sec. As the diffusion coefficient of TCE observed in the field has been reported as 1.7 times higher than the diffusion coefficient of TCE estimated based on the relative diffusivity of chloride (Johnson et al., 1989), the fact that the measured diffusion coefficients are all lower than the estimates magnifies the reported discrepancy between the field observed values and what can be attributed to diffusion.

In order to assess the impact of this discrepancy between measured and field observed diffusion coefficients on mass storage, the diffusion of TCE from a DNAPL waste pool into an aquitard was modeled as diffusion into a plane sheet (Figure 2.11). The amount of mass accumulated over 30 years into a 5-m thick aquitard was estimated by (Crank, 1975):

$$\frac{M_t}{M_\infty} = 1 - \frac{8}{\pi} \sum_{n=0}^{\infty} \frac{1}{(2n+1)} \exp\{-D_e(2n+1)^2\pi^2 \, t/d^2\} \tag{2.9}$$

where M_t is the total amount of diffusing substance which has entered the plane sheet per unit area during time t, and M_∞ is defined by:

$$M_\infty = d\left\{\frac{1}{2}(C_1 + C_2) - C_0\right\} \tag{2.10}$$

where C_1 = the concentration at x = 0; C_2 = concentration at x = d; C_0 = the concentration in the plane at t = 0, assumed to be uniform.
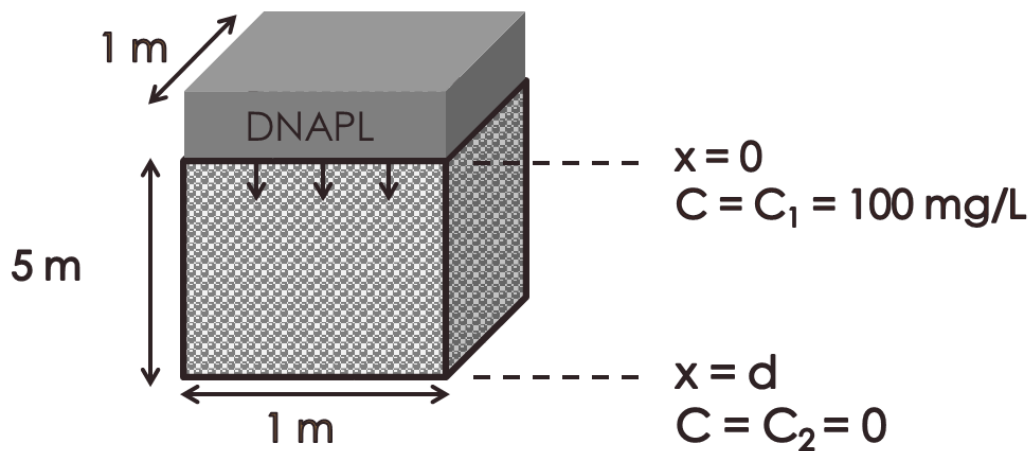
Figure 2.11. DNAPL pool on a unit area of a hypothetical aquitard.

The concentration at $x = 0$ was set equal to 100 mg/L, based on the value of the aqueous phase concentration of TCE for water equilibrated with a PCE-based DNAPL waste of 59±25 mg/L (Dou et al., 2008). Calculations of mass accumulation were made using three values for the effective diffusion coefficient of TCE: 0.7×10^{-6} cm^2/sec (as measured in this study for the confined silt-clay mixture), 1.14×10^{-8} cm^2/sec (the measured diffusion coefficient of ^{13}C-TCE in expanded silt-clay mixture contacted with PCE-based DNAPL waste) and 3.25×10^{-6} cm^2/sec (the diffusion coefficient for TCE based on the field study by Johnson et al. [1989]). The calculations, summarized in Table 2.17, show that using the value of the effective diffusion coefficient for the confined silt-clay mixture measured here results in a halving of the estimate of the mass storage in the aquitard due to diffusion. Using the slower diffusion rate of TCE from the experiment involving a silt-clay mixture contacted with DNAPL waste, the estimated mass that accumulated in the aquitard was 17 times smaller than the field observation. Given that it is thought that the observed diffusion coefficients already underpredicted the mass stored in the aquitard, these results suggest that transport rates in the field cannot be solely attributed to diffusion into a competent clay layer and it is necessary to consider other transport mechanisms.

Table 2.17. Mass of TCE Accumulated in a Hypothetical Aquitard after 30 Years of Diffusion Based on Measured and Field-Observed Effective Diffusion Coefficients

Source of Effective Diffusion Coefficient	D_e (cm^2/sec)	Mass (g)
Measured in this study (in expanded silt-clay mixture contacted with DNAPL waste)	1.14 x 10-8	3.7
Measured in this study (in confined silt-clay mixture)	0.70×10^{-6}	29.0
Observed in the field by Johnson et al. (1989)	3.25×10^{-6}	62.6

3.0   Modification of Clay Structure Due to Contact with Chlorinated DNAPLs

3.1.   Introduction

The measured diffusion coefficients reported in the previous chapter suggest that simply diffusion into a competent clay layer fails to explain the mass storage in low permeable layers. One hypothesis that might explain enhanced transport into aquitards is the modification of the clayey soils' structure. Data from field sites suggest that aquitards at hazardous waste sites may contain up to 70% clay including considerable amounts of smectites, which change their structure with water content. Additionally, the documented existence of subsurface DNAPL pools is evidence of direct contact between the aquitard and DNAPL waste. Thus, the impact of waste DNAPLs on the structure of clayey soils needs to be examined. If waste DNAPLs can cause the contraction of the structure of the clayey soil and the formation of cracks, higher transport rates into the aquitards might result.

The distance between two adjacent layers of smectite clay minerals, i.e., the basal spacing, varies based on water content. The basal spacing of an air-dry smectitic clay increases from 12 Å (for Na-montmorillonite) or 15 Å (for Ca-montmorillonite) to around 19 Å after full hydration (Brown and Brindley, 1980; Moore and Reynolds, 1997). In addition to changes in contact with water, basal spacing changes in montmorillonite clays may occur in contact with aqueous solutions of organic solvents. Brindley et al. (1969) equilibrated Ca-montmorillonite with solutions of several organic solvents. The general conclusion was that dilute solutions of organic solvents increased the basal spacing of smectites to the same degree as water, whereas their concentrated solutions expanded the structure less. For example, ethanol solutions more concentrated than 35% or methanol solutions more concentrated than 47% increased the basal spacing of Ca-montmorillonite to about 17 Å where more dilute solutions increased the basal spacing to above 19 Å, similar to the basal spacing with water. Even though n-propanol belongs to the same chemical group, the basal spacing of dry clay increased to 18 Å in solutions of propanol more concentrated than 8%; below this volume percent, the basal spacing increased to above 19 Å. Like propanol, diol-group organic liquids did not cause as much swelling (the reported basal spacing was 17-18 Å) as water when the solution's organic liquid fraction was higher than 8%. Consistent with this finding, Brown and Thomas (1987) reported that bentonite clays in dilute water-acetone or water-ethanol solutions had a basal spacing of 19-20 Å, equivalent to the basal spacing of bentonite in contact with water. The basal spacing increased less, only up to 16 Å, when the solution percentage of acetone exceeded 50% or the percentage of ethanol exceeded 75%. Most of the work has been performed using miscible organic solvents. However, more recently, a study by Matthieu et al. (2013) found that the basal spacing of Na-montmorillonite in contact with an aqueous solution saturated with TCE was 18.2 Å, similar to the value reported with water.

In addition to the basal spacing changes observed with aqueous solutions of organic solvents, the impact of pure solvents has also been addressed by several studies. Barshad (1952)

measured the basal spacing of dry Ca and Na-montmorillonite contacted with a variety of organic liquids and found that the organic liquids could not expand the structure of clay as much as water. The degree of swelling was hypothesized to be related to the dielectric constant of the organic liquid. Following this study, the relation between the basal spacing of clay and the dielectric constant of the solvent was analyzed further but no general correlation was derived (Olejnik et al. 1974; Berkheiser and Mortland, 1975; Murray and Quirk, 1982).

Middleton and Cherry (1996) provide a summary of historical measurements of basal spacing for clay minerals in contact with chlorinated organic liquids. These measurements emphasized water-miscible compounds, such as alcohols and acetone, and comparatively few utilized chlorinated solvents, the organic compounds often of concern in at hazardous waste sites. Greene-Kelly (1955) measured a basal spacing of 12.5 Å for Na-montmorillonite in contact with chlorobenzene; similarly, Berkheiser and Mortland (1975) reported that the basal spacing for Ca-montmorillonite and Na-montmorillonite contacted dry with 1,2-dichloroethane was 14.7 Å and 12.6-13.0 Å, respectively, and Griffin et al. (1984) reported a value of 13.8 Å for carbon tetrachloride. Thus, these organic liquids did not appear to increase the basal spacing above that with air.

Although the literature concerning the basal spacing for initially air-dry montmorillonite clays contacted with organic liquids provides some insight, in the context of the field, it is more important to understand basal structure changes that may occur when the clay is already saturated with water since chlorinated DNAPL wastes pool on top of water-saturated clay layers and lenses in the subsurface. It appears that there is only a single reported measurement of a water-saturated smectitic clay in contact with a chlorinated organic liquid: Griffin et al. (1984) obtained a value of 20.5 Å for the basal spacing of water-saturated bentonite in contact with carbon tetrachloride, similar to the value of 20.1 Å reported in the same study for contact with water. This measurement suggests that the pure solvent was not able to displace water and cause a contraction of the basal spacing in cases where the clay was already saturated with water.

In addition to the paucity of basal spacing measurements of water saturated clays with pure chlorinated organic liquids, there are no reported measurements with actual chlorinated solvent wastes or mixtures simulating such wastes. Solvents found at hazardous waste sites are not pure. Surfactants are a critical component of the waste because they can change not only the wettability of mineral surfaces, but also the structure of clay. For example, contacting a Na-smectite with an aqueous solution of hexadecyltriammonium bromide increased the basal spacing from about 20 Å to as high as 40 Å (Lee and Kim, 2002), with the organic cations serving as "pillars" in the interlayer spacing. It may be thought that only cationic surfactants may sorb and expand the interlayer spacing, due to the predominantly negative charge of clay surfaces, but Shen (2001) showed that nonionic linear alcohol ethoxylates could also sorb and increase the basal spacing of dry bentonite from 11 Å up to 17 Å.

The significance of the modification in the structure of clays is that such changes have been linked to increases in transport. Laboratory measurements have shown increases in hydraulic conductivity of two to three (Anderson et al., 1985), three to four (Li et al., 1996) and

one to five orders of magnitude (Brown and Thomas, 1984) depending on the organic liquid, clay type and percent clay. The increase is attributed to the formation of cracks or channels due to the contraction of the clay structure resulting from the contact with organic solvents. Cracks observed during the permeation of organic solvents in clay soils were reported to be around 0.5 cm (McCaulou and Huling, 1999) and 1 cm (Abdul et al., 1989). However, such studies generally use substantial hydraulic gradients (up to 360 m/m [Anderson et al., 1985]) to drive the organic liquids through the low permeability materials. These gradients far exceed those which are generated by pools of DNAPL on top of low permeability layers; for example, Oolman et al. (1995) reported a depth of DNAPL of two meters at Hill AFB, UT, and typical pool depths are probably considerably less. If the forcing of the DNAPL into these geologic materials under a substantial gradient resulted in the cracking, then the ensuing changes in hydraulic conductivity may not reflect field processes.

Although cracking of clay soils due to contact with organic solvents under low hydraulic heads is still speculative, cracking induced by desiccation and its impact on hydraulic conductivity is well-documented. Numerous studies have focused on the characterization and quantification of dessication cracks, analyzing the number of intersections, number of segments, and area of cracks per unit surface area (Table 3.1). The investigations reveal that cracks form quadrangles with "T" or "+" shape intersection (Tang et al., 2012), squares (Tang et al., 2011), orthogonal squares (Velde, 1999) or pentagons and quadrangles (Li and Zhang, 2010). Velde (1999) studied more than 22 soils samples with clay contents of 17-100% and found that the segment to intersection ratio was in a range of 1.5 to 2 where 1.5 represents intersecting hexagons and 2 represents intersecting squares. Tang et al. (2012) stated when the segment to intersection ratio increased from 1.5 to 2, "T"-shaped intersections turned to "+"-shapes intersections. Desiccation cracks may be less than 2-3 mm wide (Table 3.1), whereas aperture sizes greater than 10 mm extending through an entire clay layer with a thickness of 6 m were also reported (Morris et al., 1992). Increases in hydraulic conductivity as a result of desiccation cracks ranged from 12-34 times (Rayhani et al., 2007) up to 100-1000 times (Omidi et al., 1996).

Table 3.1. Parameters and Properties of Desiccation Cracks Summarized From the Literature

Segment / Intersection Ratio	Crack area / Surface Area (%)	# Polygon / Area (cm^{-2})	Aperture Width (mm)	Aperture Length (mm)	Reference
1.49 – 1.61	9.3 – 24.2	-	-	-	Tang et al. (2008)
-	-	0.075 (max)	0.49 (average)	31.6 (average)	Li and Zhang, (2010)
-	14 (max)	-	2 (max)	-	Tang et al. (2011)
1.9*	19.3	0.53	2.2	17	Tang et al. (2012)

*Calculated from data provided in Tang et al. 2012. Dashes indicate no data.

This task aimed to evaluate the changes in clay structure by investigating the basal spacing of clay minerals saturated with water and contacted with pure organic solvents, and chlorinated solvent wastes from the field. Furthermore, changes at the macroscale were

observed and crack properties quantified such as length, aperture size, number of intersections and segments per unit area.

3.2.   Materials and Methods

Basal spacing measurements were made for three smectitic clays: two montmorillonites, one with Na as the major cation (SWy-2), and the other with Ca as the major cation (STx-1), obtained from the Clay Minerals Society Source Clays Repository (Chantilly, VA). Information about the cation exchange capacity of these clay minerals is given in Table 3.2. These clays were used as received. The third was a commercial Wyoming Na-bentonite (Southwestern Materials, Austin, TX), processed by grinding with a mortar and pestle, and then sieving using a 106 μm sieve. Hydrometer test indicated 96% of the material was < 2 μm, and mineralogical analysis showed Na-montmorillonite to be the primary mineral (> 90%).

Table 3.2. Cation Exchange Capacity of the Pure Clays Used in This Study

Clay	CEC (meq/ 100g)
Sodium montmorillonite (SWy-1, major cations: Na and Ca)	76.4
Texas montmorillonite (STx-1, major cation: Ca)	84.4

Clays from Clay Minerals Source Clays Repository (Chantilly, VA).
Data from Van Olphen and Fripiat (1979).

Although the principal organic solvents of concern in this study were chlorinated solvents, additional organic solvents were included to obtain a range of chemical properties, in terms of both solubility and dielectric constant (Table 3.3). In addition, two DNAPL wastes were examined. Characteristics of these wastes are described in Hsu (2005) and are summarized in Table 2.5. One of these wastes was a dry cleaning PCE waste, obtained from a waste storage tank of a dry cleaner (Ann Arbor, MI). This liquid was still transparent, but less clear than and with a density slightly less than that of pure PCE. Its interfacial tension was markedly less than that for pure PCE: 2-3 dyn/cm, rather than 47.5 dyn/cm (Demond and Lindner, 1993). Based on the chemical analyses reported in Hsu (2005), it is believed that this waste contained anionic surfactants at a concentration below 1 mM, and that nonionic surfactants were the dominant surface-active species. The other DNAPL waste was a degreasing TCE waste obtained from Operable Unit 2 at Hill Air Force Base (UT). Its appearance was black and opaque, with a density of 1.3 g/mL. The interfacial tension of this waste was also about an order of magnitude less than its pure counterpart, but the reduction was attributed to the presence of anionic surfactants, predominantly (Hsu, 2005). Neither of these wastes caused quartz to become organic-wet in the presence of water at neutral pH; the measured contact angle (measured through water) was approximately 30°.

Table 3.3. Organic Solvents Used for Basal Spacing Measurements

Solvent	Chemical formula	Supplier	Purity	Solubility (mg/L)	Density (g/cm^3)	Dielectric constant
Acetone	$(CH_3)_2CO$	Sigma Aldrich	>99.9%	Infinitely	0.78	20.9
Aniline	$C_6H_5NH_2$	Sigma Aldrich	>99.5%	33800	1.02	6.71
Butanol	C_4H_9OH	Sigma Aldrich	>99%	74500	0.81	20.45
2-Chloroaniline	$ClC_6H_4NH_2$	Sigma Aldrich	>99.5%	8760	1.21	13.4
1,2-Dichlorobenzene	$C_6H_4Cl_2$	Sigma Aldrich	99%	156	1.3	9.9
Ethanol	C_2H_6O	Sigma Aldrich	>99%	Infinitely	0.79	24.55
Nitrobenzene	$C_6H_5NO_2$	Acros Organics	>99%	1900	1.2	34.8
1,1,2-Trichloroethane	$C_2H_3Cl_3$	Acros Organics	98%	4400	1.43	7.29
Tetrachloroethylene	C_2Cl_4	Sigma Aldrich	>99.9%	150	1.61	2.28
1,2,4-Trichlorobenzene	$C_6H_3Cl_3$	Sigma Aldrich	>99%	-	1.45	-
Trichloroethylene	C_2HCl_3	Fisher Scientific	>99.5%	1370	1.45	3.42

Data from Riddick et al. (1986).

Four sets of measurements were performed using air-dry clays (i.e., exposed to air at 30% relative humidity at room temperature, 20 - 25°C) involving the addition of water (i.e., a 0.005 M CaSO$_4$ solution), the addition of pure organic liquids, and the addition of field wastes. For the wet specimens, oriented samples were prepared by a smear mount method, as suggested in the literature (Moore and Reynolds, 1997; Brown and Brindley, 1980). The samples were prepared by packing 0.2 g of air-dry clay in a 0.5-mm deep glass sample holder (Rigaku, The Woodlands, TX). The surface was then smoothed by passing the edge of a glass slide over it. Water-wetted samples were prepared by packing 0.2 g of air-dry clay onto the glass slide and then storing the glass slide in a plastic container in contact with a 0.005 M CaSO$_4$ solution for one day. The next day, the surface of the wet sample was smoothed using a glass slide.

The analysis of the solvent-wetted samples required an airtight sample holder due to the volatile nature of the solvents. Therefore, a special airtight sample holder made out of aluminum was used (Rigaku, The Woodlands, TX). Originally, the sample holder was covered with a beryllium membrane. A beryllium membrane is reported to have no peaks under 38° (Lexa, 1998) so it was not expected to interfere with the clay's diffraction peaks that are reported at 2θ angles lower than 20° (Brown and Brindley, 1980). On the contrary, Lerz and Kraemer (1966) found interference at smaller 2θ angles. The issue encountered here with the beryllium membrane was that the characteristic peak was not observed in the diffraction patterns, so it was unclear whether it was presenting an interference or not. This phenomenon might have arisen due to an unavoidable air gap between the membrane and sample surface during sample

preparation. Thus, Kapton® film was used instead which is compatible with chlorinated solvents and does not create any peak interference. It is also transparent so it permits the observation of any air gaps between the sample surface and the film.

The organic liquid-saturated samples were prepared by packing air-dry clay into the aluminum sample holder, followed by the addition of the solvent to the clay and then covered with a Kapton® film placed in the cover of the sample holder. To assess whether the variation in sample holders and covers caused any differences in the XRD measurements, some measurements of air-dry and water-saturated clays were also made using the aluminum sample holder and Kapton® film, and no appreciable differences were observed. For the samples that were scanned covered by Kapton® film, the film was scanned under the same conditions as the sample so that the resulting pattern could be categorized as part of the background. The standard equilibration time for measurements with air-dry clays was fifteen minutes. Some additional samples were run at extended times (up to one month) and no differences were observed in the basal spacing measurements. The lack of dependence on time is consistent with the observation of Amarasinghe et al. (2009) who found that organic solvents can enter the interlayer space of air-dry Na-montmorillonite almost immediately.

Changes in the basal spacing were measured using an x-ray diffractometer (XRD) (Rigaku, The Woodlands, TX), equipped with a rotary anode source (Cu) with a 12 kW X-ray generator and graphite monochromator and two wide angle horizontal goniometers (2°-138°). Initially, the samples were scanned at an incident angle range of 2-65° with a step size of 0.02^o and a counting time of 2 seconds. After the location of the (001) peak was determined, samples were scanned in a continuous mode within the 2-10° 2θ range at a speed of 2° per minute. JADE (Version 10; Materials Data, Livermore, CA) was used for the data analysis. A background curve was fitted automatically by the software. After determining the portion of the profile attributable to background, the PseudoVoigt profile function was then used to fit the profiles to determine the location of the peaks.

In addition, water-saturated clays were placed in both vials and in beakers in order to observe structural changes at the macroscale. Two vials were prepared by placing 0.5 to 1.0 grams of montmorillonite in 20-mL glass vials. Then about 10 mL of a 0.005 M $CaSO_4$ solution were added; the vials were then shaken and allowed to equilibrate for two days. After equilibration with water, about 10 mL of pure TCE was added to one of the vials, and 10 mL of PCE-based DNAPL waste added to the other one. The vials were rotated for seven days and then left to sit for another 49 days. Photographs were taken over time to record visual changes; samples were also taken at 18 days and 180 days and analyzed by XRD.

To investigate the impact of extended periods of equilibration under conditions that more closely simulate the subsurface, layered systems were constructed in 1-liter borosilicate glass beakers (Figure 3.1). These systems consisted of a saturated layer of sand about 3 cm thick, a saturated layer of clay about 0.5 cm thick on top of the sand, and a layer of organic liquid about 2.5 cm thick on top of the clay. The method used to pack the sand layer was similar to the one developed by Oliveira et al. (1996) involving sprinkling sand into ponded water, followed by

compaction. The clay layer was constructed from the commercial Na-bentonite clay. To pack the clay into a layer, an optimum consistency needed to be achieved. For this clay, it appeared that a ratio of 5 mL of 0.005 M $CaSO_4$ solution to 10 g of clay (close to the plastic limit of 52 wt%) gave a consistency that allowed the clay to be packed. Following packing, 100 mL of 0.005 M $CaSO_4$ solution were ponded on top of the clay and the system was left sitting for two weeks to saturate the clay; this time frame was consistent with the observed termination of expansion and the saturation times used in other studies (Nowak, 1984; Miyahara et al., 1991). As the clay layer absorbed water, it expanded to about three times its original height; consequently some of the clay was removed in order to readjust its thickness to about 0.5 cm. Then, a 2.5-cm layer of either pure PCE, TCE-based DNAPL waste or PCE-based DNAPL waste was ponded on top of the clay layer in each beaker. The beakers were covered to minimize evaporation and left to sit at ambient conditions for up to 300 days or more. Photographs were taken over time and analyzed using the image analysis software, ImageJ. Clay samples were removed and the basal spacing analyzed using XRD.
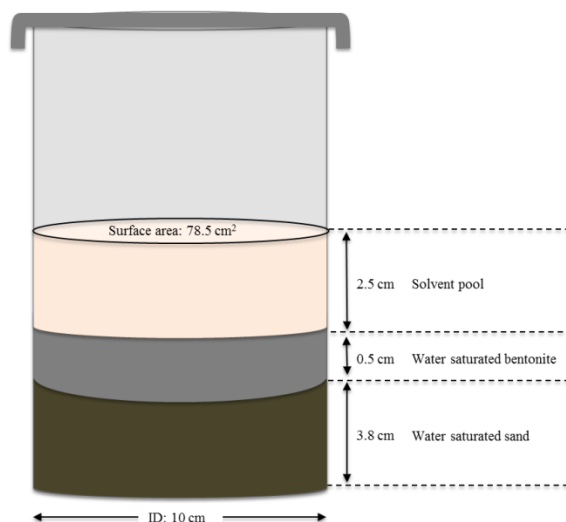
Figure 3.1. Diagram of layered clay and sand systems prepared in beakers.

3.3.   Results and Discussion

Figure 3.2 shows the measured basal spacings of air-dry (30% relative humidity) Ca- and Na-montmorillonite contacted with water or contacted with pure organic liquids. Contact of the air-dry samples with water increased their basal spacing, with the basal spacings reported here consistent with values reported in the literature (Barshad, 1952; Brindley et al., 1969; Brown and Brindley, 1980; Brown and Thomas, 1987; Li et al., 1996). For air-dry Ca and Na-montmorillonite contacted with organic liquids, the data show that the basal spacings are generally closer to those for an air-dry state than to those for a water-saturated state. The measurements reported here for the chlorinated solvents show that the basal spacings in contact with such compounds are consistent with those for nonchlorinated organic solvents with similar dielectric constants. Greater basal spacings were measured for acetone and ethanol. However, the difference does not seem to be a function of the dielectric constant, as nitrobenzene has a larger dielectric constant than acetone and ethanol, but yields a smaller basal spacing.
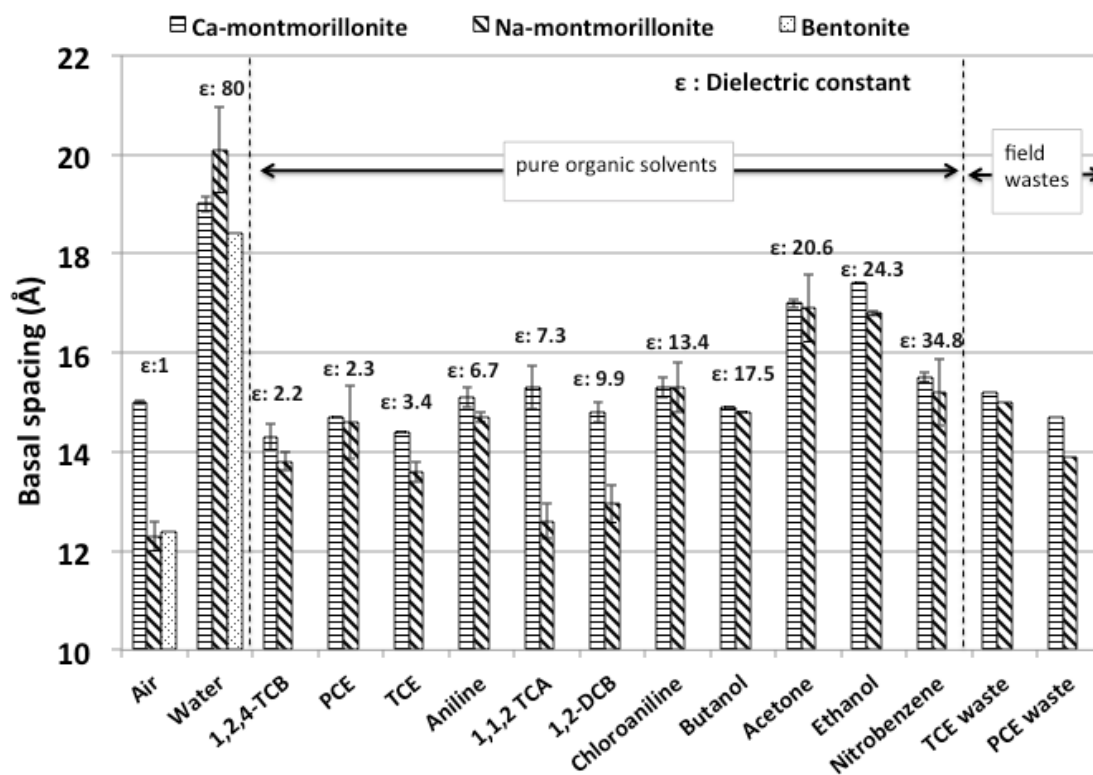
Figure 3.2. Basal spacing of smectites in contact with air, pure organic liquids and field wastes. Error bars represent the standard deviations. Water is 0.005 M CaSO$_4$ solution. Air dry is at room relative humidity (30%). Characteristics of the organic liquids and field wastes are given in Tables 3.3 and 2.5, respectively.

Figure 3.3 compares the results from this study with basal spacing measurements for organic liquids reported in the literature (MacEwan, 1948; Greene-Kelly, 1955; Berkheiser and Mortland, 1975; Griffin et al., 1984). The data presented in this figure corroborate the observation based on the data from this study, that basal spacings obtained with chlorinated compounds are consistent with those for nonchlorinated compounds with similar dielectric constants. Furthermore, it suggests that the impact of organic compounds on basal spacing may be more directly correlated with solubility, as those compounds that are completely miscible in water caused some expansion of the clay structure relative to the air-dry state, regardless of the dielectric constant. The relative impact of the parameters of solubility versus dielectric constant can be seen in particular in the case of pyridine versus nitrobenzene: pyridine is miscible in water and has a dielectric constant of 12.91 and the basal spacing of Ca-montmorillonite in contact with pyridine is 20.3 Å (Berkheiser and Mortland, 1975), whereas nitrobenzene has a solubility of 1900 mg/L and a dielectric constant of 34.78, and the basal spacing of Ca-montmorillonite in contact with nitrobenzene is 15.0 Å (Berkheiser and Mortland, 1975).
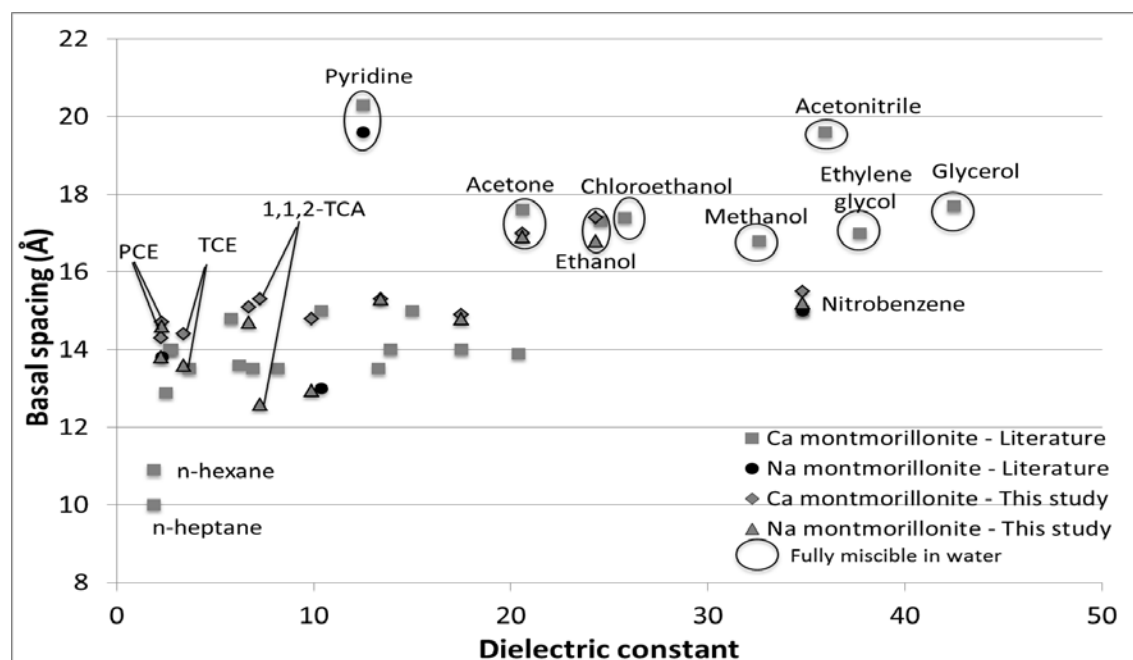
Figure 3.3. Comparison of basal spacings for air-dry montmorillonite contacted with pure organic liquids measured in this study with those reported in the literature (MacEwan, 1948; Greene-Kelly, 1955; Berkheiser and Mortland, 1975; Griffin et al., 1984).

The basal spacings for air-dry Ca-montmorillonite in contact with the TCE-based waste and the PCE-based waste were 15.2 ± 0.01 Å and 14.7 ± 0.7 Å, respectively, similar to those for the clays in contact with their pure solvent counterparts of 14.4 Å and 14.7 Å (Figure 3.2). Analogous behavior was observed for Na-montmorillonite: the basal spacing for Na-montmorillonite was 15.0 Å and 13.9 Å in contact with the TCE- and PCE-based DNAPLs,

respectively, whereas the basal spacing of Na-montmorillonite in contact with pure TCE and PCE was 13.6 ± 0.2 and 14.6 ± 0.7 Å respectively. Thus, it appears that the DNAPL wastes have an impact on the basal spacing of air-dry clays similar to that of their pure solvent counterparts.

At contaminated sites, however, waste DNAPLs contact water-saturated clays. To investigate whether contact with chlorinated organic liquids can cause a change in the basal spacing of water-saturated clays, additional XRD measurements were conducted with clay samples taken from the vials and beakers in which the clays were saturated with a 0.005 M $CaSO_4$ aqueous solution and then contacted with pure chlorinated solvents or DNAPL wastes. The basal spacings for these systems are shown in Table 3.4. The basal spacings for water-saturated clay in contact with pure TCE for 56 days in a vial were 17.9 Å and 18.8 Å, respectively for Ca- and Na-montmorillonite, similar to the measured basal spacings in contact with just water (Figure 3.2). The bentonite sample extracted from the layered beaker system in contact with pure PCE for 319 days had a basal spacing of 19.5 Å. Thus, if the clays were initially saturated with water, even extended contact with pure chlorinated solvents did not appear to alter the clays' basal spacing appreciably from the values obtained from contact with just water.

Table 3.4 also presents the basal spacing measurements for water-saturated montmorillonites in contact with the PCE-based DNAPL waste in a vial at 18 and 180 days. These measurements show that at even 18 days, the interlayer structure of Na-montmorillonite has started changing, yielding two peaks in the XRD profile (Figure 3.4.a). The peak with the higher intensity represents regions with a basal spacing of 20.9 Å, indicating that the interlayer space is still fully hydrated. However, the other peak indicates the existence of regions whose basal spacing has contracted to 14.0 Å. Figures 3.4.b and 3.4.c show XRD profiles obtained from samples of Na-bentonite taken from a beaker in which water-saturated bentonite was in contact with the TCE-based DNAPL waste for 105 days. These profiles show a shift in the basal spacing of the clay, with a greater shift occurring in the surficial sample (Figure 3.4.b) than in the one from below the surface (Figure 3.4.c). Therefore, these profiles suggest that the structure of water-saturated sodium smectites can contract due to contact with DNAPL wastes, shifting from a basal spacing indicative of contact with water to one indicative of contact with a low-solubility organic liquid.

Decreases in the basal spacing of the sodium smectites caused by the contact with DNAPL wastes were accompanied by cracking. Cracking of the center of the surface of the clay layer in the beakers started after about ten days of contact (Figure 3.5.a). At 40 days of contact, the length and number of cracks had grown considerably, forming polygonal patterns on the surface of the clay. Fourteen days later, new cracks were still forming and the existing cracks were growing both in length and aperture (Figure 3.5.b). After 175 days of contact, the pattern of the cracks had essentially stabilized; only one additional crack seemed to have formed (Figure 3.5.c). Although no changes had occurred in the pattern of the clay between days 175 and 251 (Figure 3.5.d), the aperture of the cracks continued to grow. Therefore, it seems that within

approximately the first fifty days, the general pattern of cracking was established and, as time proceeds, the pattern did not change, but the aperture of the cracks continued to grow, albeit at a reduced rate.

The lengths and apertures of the cracks were determined from the photographs shown in Figures 3.5.c and 3.5.d using ImageJ and are summarized in Table 3.5. Figure 3.6 shows an example crack map. The average crack length at 251 days was 6.3 mm and the median aperture size was 0.68 mm. Based on the aperture size and length, the fraction of crack area per unit surface area was found to be almost 5% after 251 days of contact. Although the total crack length and the aperture percentage between 400 and 1000 μm were almost the same at 175 and 251 days, the aperture percentage over 800 μm had increased three-fold. Fifteen segments were formed with 18 intersections, resulting in a segment per intersection value of 0.83. Four out of five segments in the middle of the surface were polygons with more than five sides. Compared to cracks resulting from desiccation, the number of segments per intersection was lower here than the reported range for dessication cracks of 1.5-2 (Velde, 1999), and the more common square or quadrangle shape segments (Tang et al., 2011; Tang et al., 2012) were not observed.

Table 3.4. Basal Spacings of Water-Saturated Smectites Contacted with Pure Chlorinated Solvents or DNAPL Waste

Vials (Contact time)	Basal spacing of Ca-montmorillonite* (Å)	Basal spacing of Na-montmorillonite (Å)	
		From 1st peak	From 2nd peak
TCE (56 days)	17.9	18.8	NP
PCE waste (18 days)	17.7	20.9	14.0
PCE waste (180 days)	18.5	19.4	13.0

Beakers (Contact time)	Basal spacing of Na-bentonite (Å)	
	From 1st peak	From 2nd peak
PCE (319 days)	19.5	NP
TCE waste (105 days) (sample from the surface)	18.3	14.5
TCE waste (105 days) (sample from below the surface)	19.4	15.7

*For Ca-montmorillonite samples, only a single peak was found. NP indicates that a second peak was not present.
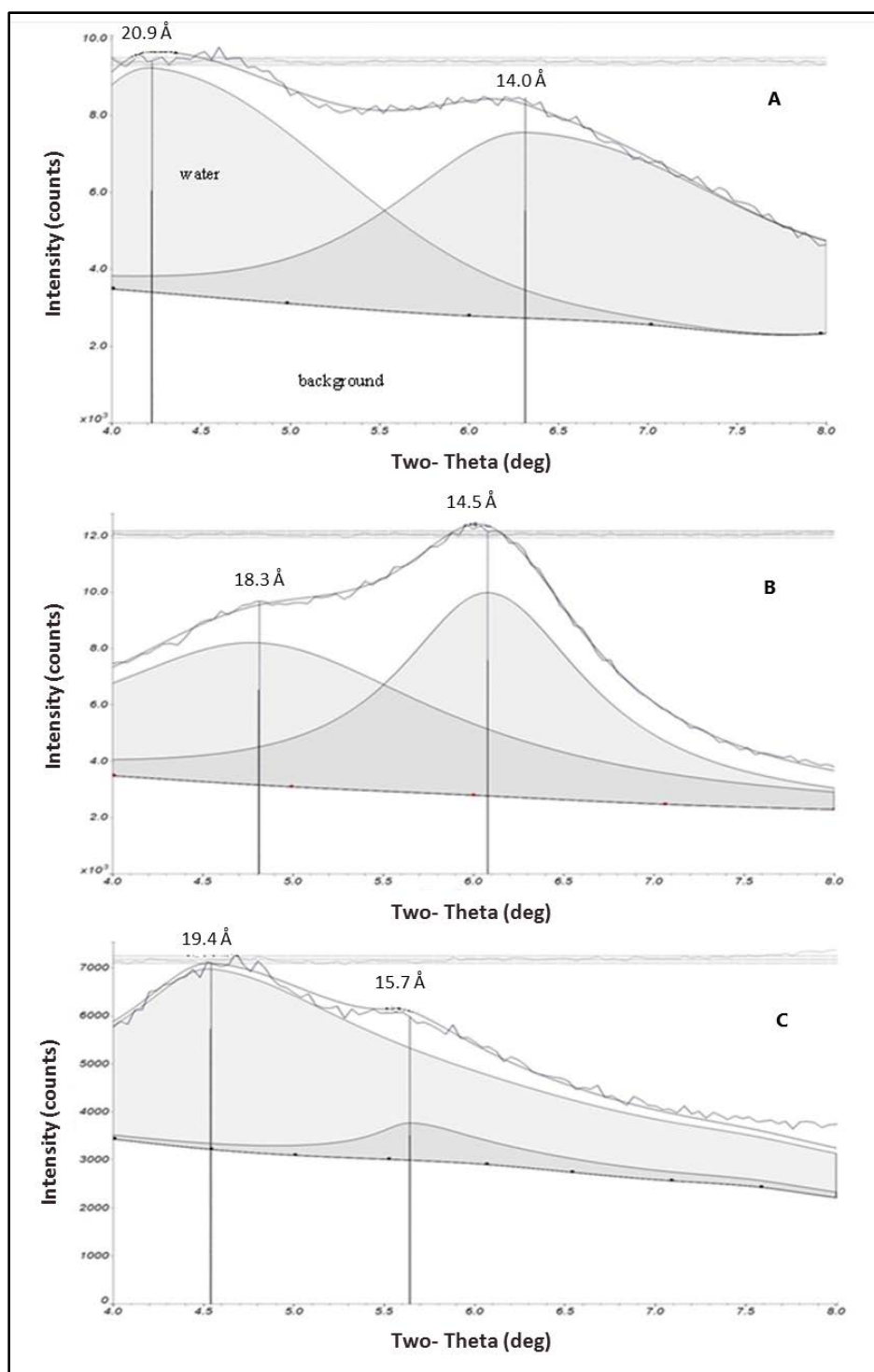
Figure 3.4. XRD profiles for A) water-saturated Na-montmorillonite in contact with PCE-based DNAPL waste for 18 days, B) Na-bentonite taken from the clay layer surface from a beaker containing TCE-based DNAPL waste ponded on top of the water-saturated clay for 105 days; and C) Na-bentonite taken from beneath the clay layer surface from a beaker containing TCE-based DNAPL waste ponded on top of the water-saturated clay layer for 105 days.
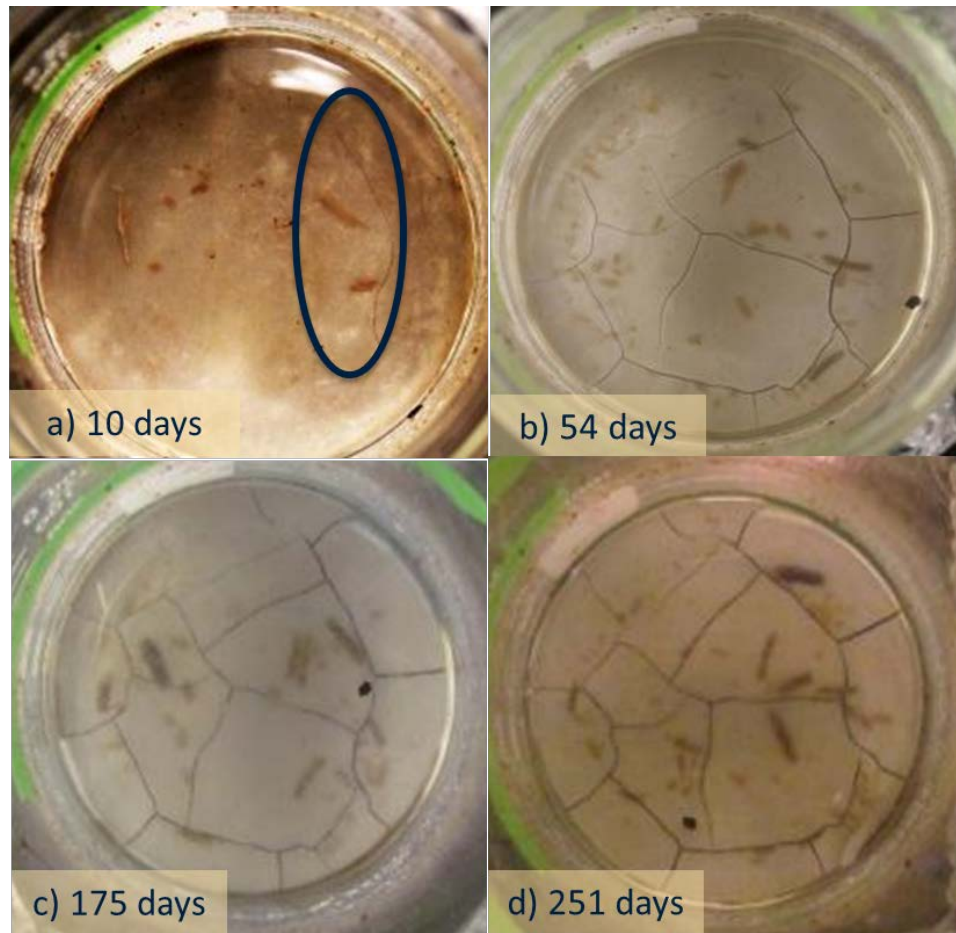
Figure 3.5. Photographs showing the cracking of Na-bentonite in contact with PCE-based DNAPL waste over time a) 10 days, b) 54 days, c) 175 days, and d) 251 days.
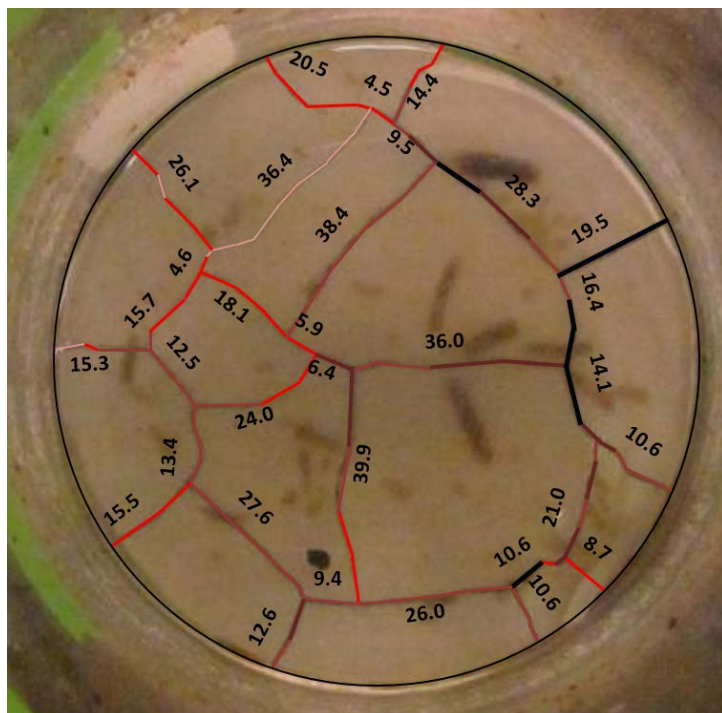
Color scale	Crack aperture (μm)	% of total length
	< 200	0
	200-400	9.8
	400-600	24.7
	600-800	41.4
	800-1,000	14.2
	1,000 <	9.9

Figure 3.6. Crack map of Na-bentonite in contact with PCE-based DNAPL waste at 251 days (Figure 3.5.d).

Table 3.5. Crack Apertures in Water-Saturated Na-montmorillonite in Contact with PCE-Based DNAPL Waste at 175 and 251 Days of Contact (Figures 3.5.c and 3.5.d)

Aperture (μm)	Percent of total length at 175 days*	Percent of total length at 251 days*
200-400	14.6	9.8
400-600	36.6	24.7
600-800	39.9	41.4
800-1,000	5.4	14.2
>1000	3.3	9.9

*Total crack length is 56.7 cm and 57.3 cm at 175 and 251 days, respectively, on a surface of 78.5 cm^2.

Figure 3.7.a shows cracks in Na-montmorillonite in a vial containing PCE waste at 18 days, and Figure 3.7.b shows the side of the beaker at 146 days of contact with PCE waste. The latter figure shows that some of the cracks have extended through the clay layer to the sand beneath and are beginning to serve as a conduit for the DNAPL to migrate into the sand layer below. Figure 3.7.c shows cracks in Na-montmorillonite in the beaker containing TCE waste at 105 days. Thus, cracks formed in contact with both wastes in a short time relative to the age of hazardous waste sites. On the other hand, water-saturated bentonite in contact with pure PCE did not show cracking in the center of the surface even after 319 days (Figure 3.7.d), consistent with the lack of change in the basal spacing measurements (Table 3.4). This observation is in contrast with that by McCaulou and Huling (1999) who reported cracking of bentonite in contact with pure TCE. It should be noted that in the experimental observations reported here, the applied hydraulic head was minimal (only 2.5 cm of organic solvent was ponded on top of the saturated clay), whereas in the case of the experiments of McCaulou and Huling (1999), a hydraulic head of up to 7 m was applied, which may have precipitated the cracking.
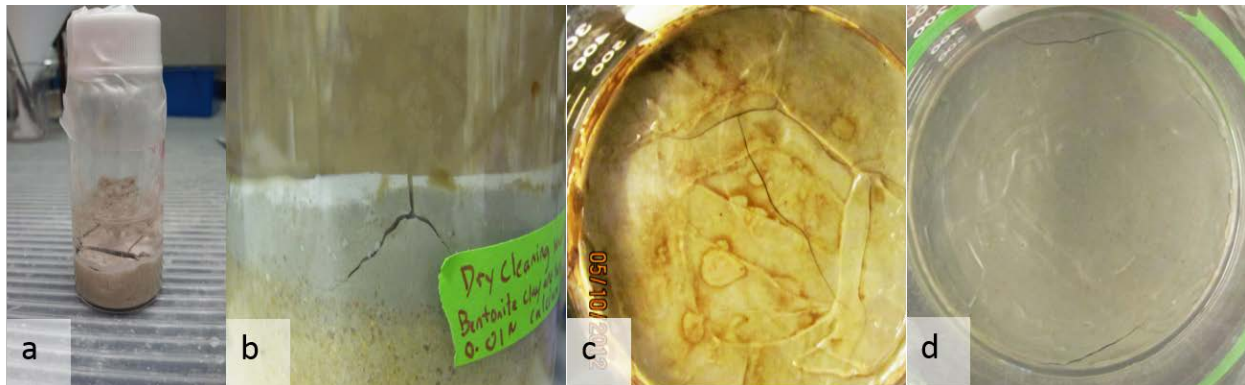
Figure 3.7. Photographs (from left to right) a) water-saturated Na-montmorillonite in contact with PCE-based DNAPL waste for 18 days in a vial; b) water-saturated Na-bentonite in contact with PCE-based DNAPL waste for 146 days: side view of beaker; c) water-saturated Na-bentonite in contact with TCE-based DNAPL waste for 105 days: top view of beaker; d) water-saturated Na-bentonite in contact with pure PCE for 319 days: top view of beaker.

3.4.   Conclusions

The basal spacing of air-dry Na-montmorillonite clay contacted with chlorinated solvents is similar to the basal spacing in contact with air, and is consistent with the basal spacing of such materials in contact with low-miscibility nonchlorinated solvents. Contact of water-saturated clays with pure chlorinated solvents did not lead to basal spacing changes, even after extended contact (up to 319 days). Similarly, contact of water-saturated Ca-montmorillonite with DNAPL wastes did not result in basal spacing changes. However, contact of water-saturated Na-smectites with DNAPL wastes led to basal spacing changes and significant cracking over the time frame of weeks to months. This finding suggests that passive contact with chlorinated DNAPLs over the time frame associated with hazardous waste sites may lead to basal spacing changes in the sodium smectite clay minerals in the clay layers at these sites. The shrinkage of the basal spacing may result in cracking, allowing enhanced transport into the clay layers.

3.5.   Implications

Data presented in Chapter 2 indicated that the measured effective diffusion coefficient of TCE was five times to two orders of magnitude lower than that deduced from field measurements. Calculations of mass accumulation reported in Section 2.5 suggested that the discrepancy in diffusion coefficients could result in a 2-17 fold overestimate of the mass storage in an aquitard over a 30-year time period attributed to diffusion. The research presented in this chapter suggests that clay layers in contact with DNAPL waste might crack in a relatively short time period. These cracks could enhance the transport of solutes into the aquitard, or alternatively, permit the entrance of free phase DNAPL directly into the aquitard.

The total mass of TCE accumulating over 30 years in a unit area model aquitard (Figure 2.11) was calculated to be 4 - 29 g (Table 2.17) when the diffusion of TCE into the aquitard was modeled as diffusion into a competent clay layer. To assess the impact of cracks, it was assumed that the crack length per unit surface area was the same as that reported in Table 3.5, or 0.73 m/m^2, giving a length of 7.3 x 10^3 cm on the 10^4 cm^2 surface of the model aquitard (Figure 3.8). The cracks were also assumed to form circles of a uniform diameter packed openly, rather than polygons of varying diameters. Based on these assumptions, the number of crack circles on the surface of the 1 m^2 model aquitard was calculated as 540, and the diameter of one circle was 4.3 cm. Information was not collected on the depth of the cracks; however, the photograph in Figure 3.7.b showed that the crack extended almost through the entire clay layer in the beaker after only 146 days. Based on this, the cracks were taken as 1 cm in depth. Two different scenarios were then considered: first, it was assumed that DNAPL did not enter into cracks directly; rather, the cracking resulted in advective transport of TCE as a solute into the cracks. In this scenario, the mass accumulated in the aquitard would have three different components: that due to diffusion into a plane sheet, that due to advection into the cracks, and that due to diffusion from the cracks into the cylinders representing the uncracked clay matrix (Figure 3.8). The mass per unit area due to diffusion into a plane sheet was calculated in the same manner as in Section 2.5,

neglecting the horizontal surface area of the cracks. The mass storage due to advection into the cracks was calculated by assuming that at t = 30 years, the distance travelled by the advective front was at least 1 cm. Thus, this was computed using the dissolved TCE concentration of 100 mg/L and the volume of the cracks. The volume was calculated as 50 cm^3, based on a length = 7.3 x 10^3 cm, a depth = 1 cm, and a median aperture of the cracks = 6.8 x 10^{-3} cm (Figure 3.9).

At small times, the mass per unit area entering a soil cylinder diffusively can be calculated as (Crank, 1975):

$$\frac{M_t}{M_\infty} = \frac{4}{\pi^{1/2}} \left(\frac{D_e t}{r^2}\right)^{1/2} - \frac{D_e t}{r^2} - \frac{1}{3\pi^{\frac{1}{2}}} \left(\frac{D_e t}{r^2}\right)^{\frac{3}{2}} + \cdots \tag{3.1}$$

where M_t is the total amount of diffusing substance per unit area which enters the cylinder in time t; r is the radius of the cylinder; and M_∞, the maximum mass per surface area, is given by:

$$M_\infty = r\left\{\frac{1}{2}C_s\right\} \tag{3.2}$$

where C_s is the uniform concentration at the surface of the cylinder.
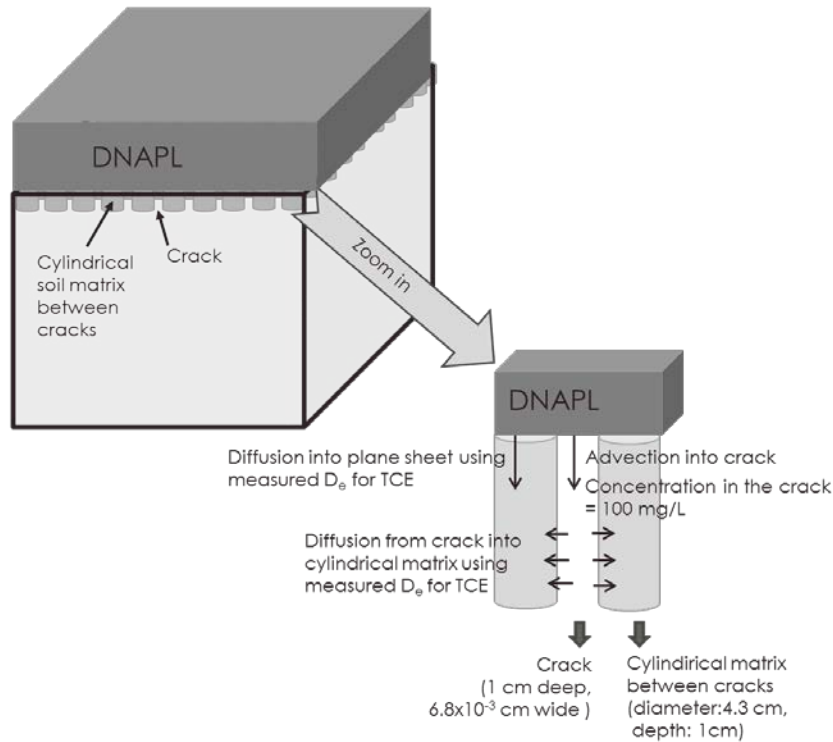
Figure 3.8. Scenario where DNAPL does not occupy the cracks but the moves advectively into the cracks as a solute.
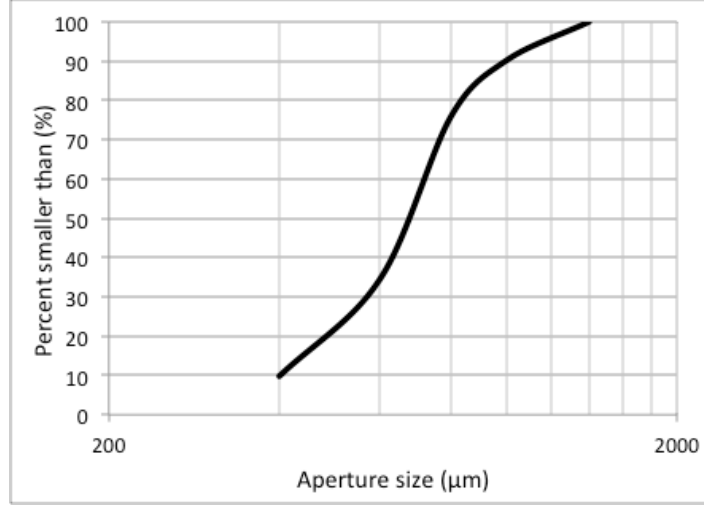
Figure 3.9. Distribution of crack apertures on the bentonite surface after 251 days of contact with PCE-based DNAPL waste (data from Table 3.5).

In the scenario modeled here with cylinders of a diameter = 4.3 cm and C_s = 100 mg/L, $M_t = M_\infty$ would be achieved in less than a year. As the mass storage calculations were based on 30-year time frame, M_∞ was used as the accumulated mass per surface area in one cylinder due to diffusion into the soil cylinders between the cracks. Thus, the total mass in the cylinders was calculated by multiplying M_∞ by the surface area of each cylinder and the total number of cylinders.

In this scenario then, the mass diffused into the aquitard from the top surface was 29 g, the mass transported through advection into the cracks was 0.005 g, and the mass diffused from the cracks into the cylindrical soil matrix was 0.8 g (Table 3.6). So, the overall mass (around 29.8 g) was only 3% higher than the mass attributed to diffusion into a plane sheet (Table 2.17). Thus advection into cracks and diffusion from the cracks into the clay matrix does not appear to explain the mass storage in the aquitard of 62.6 g calculated based on the diffusion coefficient reported by Johnson et al. (1989).

In the second scenario, it needs to be first assessed if DNAPL can overcome the entry pressure and enter into a crack which is water-wet and water-saturated. The height of the DNAPL pool required for a DNAPL to penetrate into a crack can be calculated from the Young-Laplace Equation (Kueper and McWhorter, 1991):

$$h = \frac{2\gamma cos\theta}{\Delta\rho gr}$$
(3.3)

where γ is the interfacial tension between the DNAPL and water, θ is the contact angle, $\Delta\rho$ is the density difference between water and the DNAPL, g is the gravitational acceleration constant and h is the depth of the DNAPL pool. The interfacial tension of the TCE-based field waste was 3 dyn/cm, the density was 1.30 g/cm^3, and the contact angle was 30° (Table 2.5) (Hsu, 2005). Using the median aperture size of 680 μm, determined from the crack aperture size distribution at day 251 (Figure 3.9), it was calculated that the depth of pooling necessary for free phase

51

DNAPL to enter a crack of this aperture is only 6 cm. As this pool height is well below the range observed in the field (Oolman et al., 1995; Parker et al., 2003; Parker et al., 2004), the entrance of DNAPL into such a crack is a distinct possibility.

Using the same crack characteristics as in the first scenario, the volume of the cracks was calculated to be 50 cm^3 for the 1 m x 1 m x 5 m domain shown in Figure 3.10. Based on the volume of the cracks and the density of the DNAPL waste, the additional mass accumulation due to the presence of free phase DNAPL in the cracks is 64.5 g (Table 3.6). Thus, the total mass stored in the aquitard increases to 94.3 g, which is substantial enough to explain the mass calculated from the diffusion coefficient observed in the field (Table 2.17). These results imply that the high observed "diffusion rates" observed in the field may be attributable to small-scale cracking in the clay lenses or aquitards. Because of the possible significant ramifications of such a finding, the mechanism of cracking needs to be elucidated. Thus, the following chapter summarizes the investigation into the mechanism by which the basal spacing is reduced when such clays are saturated with water.
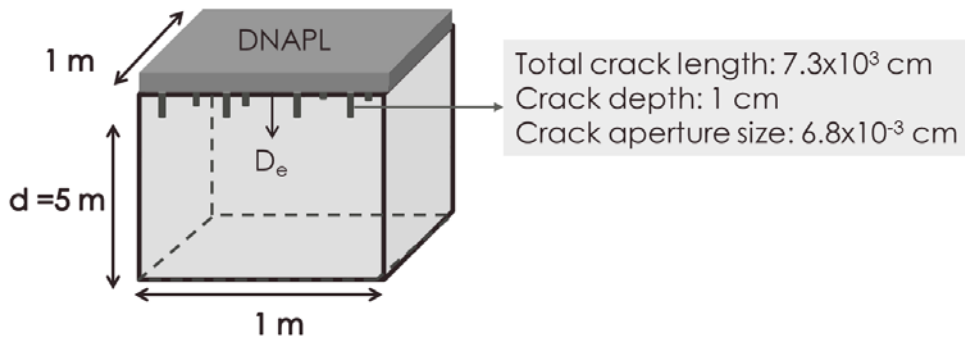
Figure 3.10. Scenario where DNAPL enters the cracks.

Table 3.6. Mass Storage in a Unit Area Model Aquitard After 30 Years

Scenario	Due to diffusion into domain from top surface (g)	Due to advection into the cracks (g)	Due to diffusion from the cracks (g)	Due to DNAPL presence in the cracks (g)	Total mass (g)
Advection into cracks	29.0	0.005	0.8	-	29.8
DNAPL present in cracks	29.0	-	0.8	64.5	94.3

4.0   Determination of Mechanism of Clay Structure Modification

4.1   Introduction

Work reported in Chapter 3 demonstrated that passive contact with pure chlorinated solvents cannot modify the basal spacing of water-saturated smectitic clays, whereas passive contact with DNAPL waste caused the cracking of water-saturated Na-montmorillonite in a time frame on the order of weeks, accompanied by a decrease in the basal spacing of the clay. This finding suggests a key role played by other components in DNAPL waste. The question now becomes what are the chemical components necessary for the contraction of the basal spacing of water-saturated montmorillonite in the presence of DNAPL waste, and how is the reduction accomplished.

To ascertain which components of the DNAPL waste may be important, screening experiments were designed utilizing different combinations of compounds, based on an understanding of what might be present in the DNAPL wastes utilized in this study. The mixture that caused cracking and basal spacing reductions in a time frame similar to the actual DNAPL wastes was utilized in XRD, sorption and Fourier Transform Infrared Spectroscopy (FTIR) experiments to elucidate a possible mechanism for basal spacing reduction.

The characteristics of the DNAPL wastes obtained from the field are presented in Table 2.5. One of the wastes comes from a dry cleaner, the other from an Air Force base and is a degreasing waste. PCE is rarely used in its pure form at dry cleaners. For example, the report by Linn and Stupak (2009) provides a list of dry cleaning cosolvents, including propanol and 2-butoxyethanol, among other glycol ethers. Moreover, it lists pre-cleaning agents such as potassium hydroxide and oxalic acid for water-based spotting agents, and amyl acetate and acetone as solvent-based spotting agents that may be applied prior to using PCE. In another report, prepared by Earnest et al. (1997), some additional spotting agents were given, with Pyratex among the most commonly used. Based on the Material Safety Data Sheet (MSDS) for Pyratex (http://www.autolaundrysystems.com/msds/Pyratex.pdf), this agent contains an aliphatic carboxylic ester (e.g., n-butyl acetate), a glycol ether (e.g., 2-butoyethanol), and an aliphatic ketone (e.g., methyl isobutyl ketone). Therefore, six groups of water-soluble compounds that may be present in the PCE waste were identified: inorganic compounds (e.g., potassium hydroxide), alcohols (e.g., propanol), aliphatic carboxylic esters (e.g., n-butyl acetate and amyl acetate), glycol ethers (e.g., 2-butoxyethanol), aliphatic ketones (e.g., methyl isobutyl ketone and acetone), and acids (e.g., oxalic acid).

One hypothesis as to how the basal spacing reduction and the ensuing cracking may occur in smectitic clays is that water-soluble organic compounds present in the waste dissolve in the water present in the interlayer spacing of the clay, enhancing the dissolution of the chlorinated solvent within the clay. Matthieu et al. (2013) cite evidence that the intercalation of TCE in sodium montmorillonite is possible. Furthermore, the ability of a cosolvent to increase the solubility of hydrophobic organic compounds is well documented (Schwarzenbach et al., 2003). The solubility of PCE can be increased by orders of magnitude by the presence of

alcohols, for example (Imhoff et al., 1995; Ladaa et al., 2001). Whether a chlorinated solvent and an alcohol mixture would result in a reduction of the basal spacing, however, is unclear. Contact of water-saturated bentonite with an aqueous solution of TCE at the solubility limig yielded a basal spacing similar to that in contact with water (18.2 Å [Matthieu et al., 2013] vs. 18.0 -18.2 Å [Brown and Thomas, 1987; Li et al. 1996]). But, aqueous mixtures containing on the order of 10% ethanol have been shown to expand the basal spacing beyond that in contact with water (Griffin et al., 1984; Brown and Thomas, 1987).

Other hypotheses may be based on surfactant content. An explanation based on altered wettability is not supported, however, as the DNAPL waste systems examined here are water-wet (Hsu, 2005), similar to the situation with the DNAPL waste recovered from the Savannah River site (Dou et al., 2008). Smectite surfaces are negatively charged and hydrophilic (Moore and Reynolds, 1997). As a consequence of the electrostatic attraction, cationic surfactants can readily sorb onto clay (Shen, 2001; Sanchez-Martin et al., 2008). Once the cationic surfactants have sorbed, they can enhance the sorption of nonpolar solvents, as increased sorption of organic compounds like aniline and benzene on smectite treated with cetyltrimethylammonium bromide (CTAB) has been reported (Zhu et al., 1998). Similarly, the sorption of chlorophenols on montmorillonite modified by nonionic surfactants was found to increase (Deng et al., 2003). However, the sorption of nonionics usually occurs through hydrogen bonding (Somasundaran and Krishnakumar, 1997; Zhang and Somasundaran, 2006), a weaker type of interaction than electrostatic interaction, resulting in less sorption of the surfactant (Somasundaran and Krishnakumar, 1997; Shen, 2001; Levitz, 2002; Deng et al., 2003; Sanchez-Martin et al., 2008). Due to the repulsion between the clay surface and the surfactant molecule's negatively-charged head group, anionic surfactants sorb considerably less, with sorption almost an order of magnitude lower than that of a nonionic surfactant (Del Hoyo et al., 2008; Sanchez-Martin et al., 2008).

The basal spacing of smectite minerals has been measured in complement to the measurements of surfactant sorption. In the case of cationic surfactants such as octadecyltrimethylammonium (ODTMA) or hexadecyltrimethylammonium (HDTMA) bromide, the basal spacing increased up to 19.5-21 Å (Lee et al., 2004, Lee et al., 2005, Sanchez-Martin et al., 2008). Even larger basal spacings were observed with the cationic surfactant cetyltrimethylammonium bromide (CTAB), ranging from 14.4 to 37.7 Å as the surfactant loading increased from 23% to 257% of Na-montmorillonite's cation exchange capacity (98 meq/100 g) (Hu et al., 2013). This expansion was interpreted as the intercalation of the cationic surfactant into the interlayer space of the smectite (Shen, 2001; Lee et al., 2004; Hu et al., 2013), with the conformation of the sorbed cationic surfactant molecules changing from a lateral monolayer to a lateral bilayer, a paraffin monolayer and a paraffin bilayer, leading to basal spacings even higher than that with water. Williams-Daryn and Thomas (2002) contacted vermiculite clays treated with alkyltrimethylammonium bromides with several organic compounds (toluene, hexane, cyclohexane, and ethanol) and measured the basal spacing. With exposure to these solvents, further increases in the basal spacing, up to 48 Å, were observed.

Nonionic surfactants caused an expansion of the lattice of smectite clay with the sample, with a dry basal spacing of up to around 17 Å. But, unlike the situation with cationic surfactants, a continuous expansion of the clay structure to spacings greater than that with water was not observed (Shen, 2001; Deng et al., 2003; Sonon and Thompson, 2005; Sanchez-Martin et al., 2008). Additionally, it was found that the intercalation of nonionic surfactants did not seem to enhance the interlayer sorption of cyclohexane, toluene, or octanol, as in the case with smectites treated with cationic surfactants (Deng et al., 2003). Based on this finding, it was proposed that the surfactants were sorbing at the margins of the interlayer space and the hydrophilicity of the interlayer space was not affected. With respect to anionic surfactants, the lack of any change in basal spacing has led researchers to surmise that anionic surfactants are excluded from the interlayer space montmorillonite (Sanchez-Martin et al., 2008), and any sorption that occurs is probably on the exterior of the clay particles.

The studies cited above considered the interaction of a single surfactant with clay. However, a DNAPL waste contains a surfactant mixture. The degree of sorption of an individual surfactant can be modified due to synergistic interaction among the different surfactant molecules, depending on the surface properties of the sorbent and sorbate as well as the concentration of the surfactants. For example, the sorption of an anionic surfactant onto kaolinite from a mixture of anionic-nonionic surfactants was greater than that in the presence of the anionic surfactant by itself, when the concentration was lower than the critical micelle concentration (CMC). However, the sorption of the anionic surfactant was less when the concentration was above CMC (Xu et al., 1991). The hydrophobic chain-chain interaction of the surfactants and the reduction of the repulsive forces between the negatively-charged heads of anionic surfactants by the nonionic surfactant were offered as possible explanations for such synergism (Xu et al., 1991; Zhang and Somasundaran, 2006). However, contradictory results suggest that there are other properties of the system playing a role: for instance, Somasundaran and Huang (2000) determined that the chain lengths of the nonionic and anionic surfactants influence the shielding of charge and, in turn, the degree of sorption. It should be noted that all the studies cited above examined surfactant sorption from aqueous solutions, and there are not comparable studies looking at sorption from nonpolar solvents. However, studies looking at surfactant behavior in nonpolar solvents show that surfactants can form reverse micelles (Fendler, 1976; Moulik, 1996), suggesting that interactions between anionic and nonionic surfactants in a DNAPL waste occur through their hydrophilic moieties. Furthermore, reverse micelles solubilize water in their core (Silber et al., 1999), a phenomenon that is exploited in the dry cleaning industry for the removal of water-based stains (Linn and Stupak, 2009).

To obtain greater detail of the interlayer space of clays during dehydration and surfactant sorption, FTIR spectroscopy has been used. The band at a wavenumber around 1635 cm^{-1} is assigned to the bending vibration of water (H-O-H) that is structurally bonded in the interlayer space (Madejová and Komadel, 2001). The location of this band is correlated with the water content of the clay, with a decrease in the wavenumber occurring as a result of dehydration (Russell and Farmer, 1964; Johnston et al., 1992). On the other hand, the sorption of surfactants

into the interlayer space of clay minerals may cause an increase, as, for instance, Ma et al. (2010) reported an increase from 1634 to 1649 cm^{-1} in the H-O-H bending band with increasing cationic surfactant loading. Similarly, it was observed that after being treated with nonionic surfactants, the location of H-O-H bending band of water in smectites shifted from a wavenumber of 1633 to 1645 cm^{-1} (Deng et al., 2003), and from 1636 to 1643 cm^{-1} (Del Hoyo et al., 2008). All of these studies attribute this increase in wavenumber to the partial displacement of water molecules from the interlayer space. Yet, again, these studies examined the changes in the H-O-H bending band in aqueous solutions, and complementary work in nonpolar solvent systems is not available.

In summary, the evidence reported in the literature suggests that aqueous solutions of water-miscible organic solvents and nonionic surfactants can increase the basal spacing of dry smectites up 16-17 Å (Shen, 2001; Deng et al., 2003; Sonon and Thompson, 2005; Sanchez-Martin et al., 2008). Aqueous solutions of anionic surfactants cause less swelling of dry smectites, up to a basal spacing of 14-15 Å (Del Hoyo et al., 2008; Sanchez-Martin et al., 2008). Since the clay minerals found in the aquitards are water-saturated, the impact of these components on the basal spacing of water-saturated smectites needs to be assessed. However, there appears to be little work examining the basal spacing of water-saturated smectites exposed to miscible organic solvents or surfactants; the presumption is if they are sufficiently small molecules, are water-miscible, and are not negatively-charged, they can enter the interlayer space of water saturated smectitic clay minerals. As a result of this entrance, a decrease in the basal spacing of water-saturated smectites from 18-19 Å to 16-17 Å may be postulated based on measurements with dry clay. Yet, the basal spacing for samples of bentonite that cracked in contact with TCE waste was around 15 Å (Table 3.4), implying that the presence of water-soluble organic compounds, surfactants, or chlorinated organic solvents fail to explain this observation if they are considered individually. Furthermore, the results presented in Chapter 3 suggest that non-polar low solubility chlorinated organic solvents do not have the ability to adjust the basal spacing if the interlayer space is already occupied by water. Consequently, it is hypothesized that the reduction in basal spacing is a synergistic phenomenon, with components of the DNAPL waste modifying the basal spacing of water-saturated smectites only when they are present together.

The first hypothesis as to how the basal spacing reduction might occur is that water-soluble organic compounds present in the waste dissolve into the water present in the interlayer spacing of clay, creating a solution with a reduced polarity. Acting as a co-solvent, they then facilitate the dissolution of high concentrations of a chlorinated compound into the interlayer spacing, with the net result of a reduction in the basal spacing. A similar hypothesis can be developed based on the surfactant content. Studies have shown that surfactants can sorb in the interlayer spacing and the sorption can lead to increased sorption of nonpolar organic compounds. Thus, if the surfactants present in the DNAPL waste sorb in the interlayer space, they provide an organic-rich site for the nonpolar chlorinated compounds in the interlayer space, leading to a reduction in the basal spacing. Although neither of these hypotheses was definitively supported by previous studies, they served as a starting point.

With these hypotheses in mind, screening experiments were performed to ascertain which components of DNAPL needed to be present to cause cracking and a decrease in basal spacing. Sorption experiments were also performed to determine the degree of sorption of the various components. Lastly, FTIR measurements were made to determine whether water molecules were displaced from the interlayer space. Based on these experimental results, a mechanism was proposed to explain how a decrease in basal spacing in water-saturated Na-montmorillonite may occur due to contact with DNAPL waste.

4.2.   Materials and Methods

4.2.1. Screening Experiments

To ascertain which components of DNAPL waste were responsible for the reduction in the basal spacing of Na-smectites, a series of experiments were performed. To determine whether water soluble organic components in the DNAPL wastes were enhancing the solubility of the chlorinated organics, the dry cleaning PCE waste and the degreasing TCE waste were contacted with water at a volume ratio of 4:1 (waste:water) for 56 days. After this period of equilibration, the aqueous phase was extracted with toluene at a 5:1 volume ratio (toluene:water). The toluene phase was then analyzed for concentrations of PCE and TCE by the method described in Section 2.2. In addition, a suite of 18 vials was set up. About one gram of bentonite was put into each 20-mL glass vial and contacted with 10 mL of a 0.005 M $CaSO_4$ solution to saturate it. After two weeks, the surficial excess water was removed. The solutions summarized in Table 4.1 were prepared containing water-soluble compounds at the concentrations given in Table 4.2 and surfactants, whose structures are shown in Figure 4.1, at the concentrations given in Table 4.. Then, 15 mL of one of these solutions was added on top of the clay. The vials were capped, stored at room temperature and observed over 90 days. Pictures were taken periodically to record visual changes such as the relative degrees of horizontal and vertical cracking as well as changes in clay color over time.

4.2.2. Basal Spacing Measurements

Bentonite was contacted with water in glass vials as in the screening experiments. After two weeks, the surficial excess water was removed and the clay paste was mixed. Two grams of the clay paste were then transferred into a 30-mL centrifuge tube (Nalgene, Rochester, NY). 20 mL of a solution containing combinations of TritonX-100, AOT and $C_{12}E_6$ as solutes, dissolved in either water or PCE, were added into the tubes. The first set of tubes was rotated for at least four days followed by passive contact of at least one week; the second set of tubes was rotated for three weeks. The clay-solution mixture was centrifuged at 600xg relative centrifugal force (RCF) for 20 minutes and the solid phase was analyzed by XRD.

Table 4.1. Composition of Mixtures for Screening Experiments

Vial	Surfactant			Alcohol	Aliphatic ketone	Glycol ether	Aliphatic carboxylic ester	Solvent
	Triton X-100	$C_{12}E_6$	AOT					
1				✓	✓	✓	✓	Water
2	✓							Water
3	✓	✓	✓	✓	✓	✓	✓	Water
4	✓							PCE
5	✓						✓	PCE
6	✓			✓	✓		✓	PCE
7		✓	✓					PCE
8		✓	✓	✓	✓	✓	✓	PCE
9	✓	✓	✓					PCE
10	✓	✓	✓	✓	✓			PCE
11	✓	✓	✓	✓	✓	✓		PCE
12	✓	✓	✓	✓	✓	✓	✓	PCE
13	✓	✓	✓				✓	PCE
14	✓	✓	✓	✓	✓		✓	PCE
15				✓				PCE
16					✓			PCE
17						✓		PCE
18				✓	✓	✓	✓	PCE

Table 4.2. Concentrations of Organic Solutes in Screening Experiment Mixtures

Chemical group	Compound	Concentration (mg/L)
Alcohol	Propanol	50
Aliphatic ketone	Acetone	10
	Methyl isobutyl ketone	2550
Aliphatic carboxylic esters	Amyl acetate	525
	n-Butyl acetate	528
Glycol ethers	2-Butoxyethanol	8992

All chemicals were laboratory grade from Fisher Scientific.

Table 4.3. Surfactants Used in Screening Experiments

	AOT	TritonX-100	$C_{12}E_6$
Chemical formula	$C_{20}H_{37}NaO_7S$ (anhydrous)	$C_{14}H_{22}O(C_2H_4O)_n$ (n = 9-10)	$C_{24}H_{50}O_7$
Concentration (mM)	3.3	3.3	6.7
Molecular weight (g/mol)	456	625	451
Critical micelle concentration in water (mM)	1.56[§]	0.22[†]	0.071[§]
Source	Fisher Scientific	ICN Biomedicals	Sigma Aldrich

[§]Hsu (2005); [†]Cuypers et al. (2002).
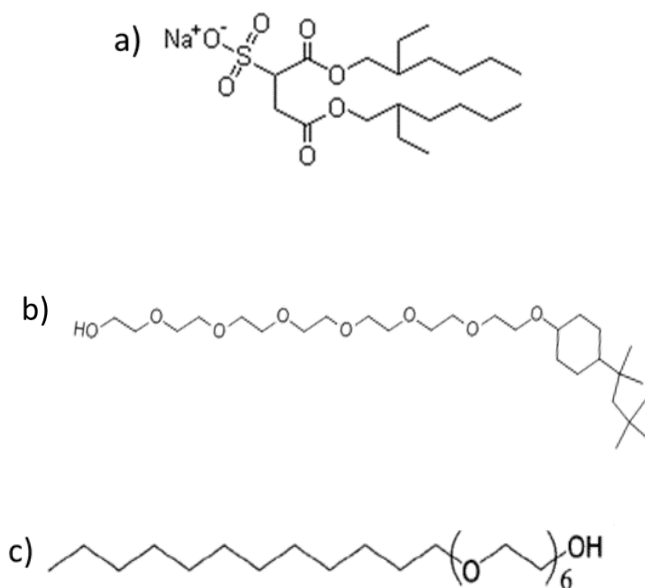
Figure 4.1. Molecular structure of a) AOT, b) TritonX-100, and c) $C_{12}E_6$.

4.2.3. Fourier Transform Infrared (FTIR) Spectroscopy Measurements

After XRD analysis, the samples were placed back into the centrifuge tubes. The samples were then analyzed using FTIR spectroscopy (Spectrum BX, Perkin Elmer, Boston, MA) with a MIRacle attenuated total reflectance (ATR) accessory. First, the background was scanned in a range of 650 cm^{-1} to 4000 cm^{-1} at a resolution of 4 cm^{-1}. Then, the sample was placed on the ATR crystal, and the data was collected in the transmission mode. The spectra were corrected using the background scan and the peaks on each spectrum greater than the threshold (5% of transmission) were labeled. Similar to the procedure with the basal spacing measurements, two sets of experiments with different rotation and contact times were used. In the first set, bentonite clay samples were rotated for at least four days and then were left sitting for almost 6 months in contact with either an aqueous surfactant solution or a PCE-based surfactant solution. In the second set of experiments, the samples were rotated for three weeks

with no additional passive contact. For comparison, scans were also made for dry and wet clay, and for solvents and solutions in the absence of clay; the total matrix of FTIR measurements is shown in Table 4.4.

Table 4.4. Experimental Matrix for FTIR Spectroscopy Measurements

Solvents and Solutions[§]	
Solute	**Solvent**
-	Water
TritonX-100	Water
AOT	Water
TritonX-100 and AOT	Water
-	PCE
TritonX-100	PCE
AOT	PCE
TritonX-100 and AOT	PCE
Air-Dry Bentonite	
Solute	**Solvent**
-	-
-	Water
-	PCE
Water-Saturated Bentonite Contacted with Solutions[§]	
Solute	**Solvent**
TritonX-100	Water
AOT	Water
TritonX-100 and AOT	Water
TritonX-100	PCE
AOT	PCE
TritonX-100 and AOT	PCE

[§]Surfactant concentrations are given in Table 4.3.

4.2.4. Sorption Experiments

One gram of Na-montmorillonite clay was saturated with 10 mL of Milli-Q water for two weeks. Similar to the protocol in the basal spacing measurements, surficial excess water was removed and the clay paste was mixed. Then, two or four grams of the clay were transferred to a 30-mL centrifuge tube. Surfactant solutions containing the same concentrations as in the screening and FTIR experiments (Table 4.3) were prepared in 50 mL volumetric flasks, and in the case of the surfactant solutions prepared in PCE, 0.06 mL ^{13}C-labeled TCE (Cambridge Isotope Laboratory, MA, >98%) was also injected into the volumetric flasks. 20 mL of the surfactant solutions were added into the centrifuge tubes. Following one week of rotation, the tubes were centrifuged at 600xg RCF for 20 minutes. The supernatant phase was sampled to determine the concentration of surfactant and ^{13}C-labeled TCE left in the solution from which the sorption of surfactant on the Na-montmorillonite was calculated by mass balance.

The AOT concentrations in both the aqueous phase and in PCE were determined by the same method described in Section 2.2. For analysis in the aqueous phase, calibration standards were prepared in the range of 20-67.5 mg/L and samples were diluted in the range of 28 to 40

60

times using Milli-Q water. For analysis in PCE, a calibration curve was determined over the range of 20-65 mg/L and the samples were diluted 20-40 times using PCE. TritonX-100 concentrations in the aqueous phase were analyzed using a HPLC (Hewlett-Packard HP 1090, Palo Alto, CA) instrument with a Sedere Sedex 75 ELSD (Richard Scientific, Novato, CA) detector. A Hypersil ODS C18 security guard (ID: 2 mm, L: 4 mm) was used to separate the compound. The range for the calibration standards was 20-65 mg/L. Samples taken from the supernatant in the centrifuge tubes were diluted 25 to 40 times using Milli-Q water. The TritonX-100 concentration in PCE was measured using the HPLC equipped with a Hypersil Gold column (1.9 μm, ID: 2.1 mm, L: 50 mm). A calibration curve was obtained over the range of 20-60 mg/L and samples were diluted 5-40 times using PCE. The concentration of ^{13}C-labeled TCE was analyzed using the same method described in Section 2.2.

4.3.   Results and Discussion

4.3.1. Screening Experiments

The PCE concentration in the aqueous phase contacted with dry cleaning PCE waste was measured to be 9500 mg/L, with no measurable concentrations of TCE. The concentrations in the aqueous phase contacted with the degreasing TCE waste were 125 mg/L and 500 mg/L for PCE and TCE respectively. The aqueous solubilities of PCE and TCE at 25°C are 150 mg/L and 1370 mg/L, respectively (Riddick et al., 1986). Thus, the components in the dry cleaning PCE-based waste increased the aqueous solubility of PCE significantly, but the components in the TCE-based waste reduced somewhat the aqueous phase solubility of TCE and PCE. Since both the PCE and TCE wastes cracked the clay, but the aqueous solubility increased only in the case of the PCE waste, it does not appear that enhanced solubility of the chlorinated compounds in the interlayer water is the primary mechanism by which basal spacing reduction occurs.

The main goal of other set of screening experiments was to determine the components of DNAPL waste that cause cracking. The results are summarized in Table 4.5. When only one of the water-soluble organic solutes listed in Table 4.2 was dissolved in the chlorinated solvent (PCE), no cracking was observed. Moreover, combinations of these compounds dissolved in PCE did not induce cracking, either (Figure 4.2). In addition, vials containing only a single surfactant dissolved in PCE did not cause cracking (Figures 4.3.a and 4.3.b, respectively). On the other hand, cracking of the water-saturated bentonite occurred in less than two weeks in the vial containing nonionic and anionic surfactants dissolved in PCE (Figure 4.4.a). Therefore, it was concluded that a surfactant combination was vital to the cracking process. As the same surfactants dissolved in water did not cause cracking (Figure 4.4.b), the implication was that the chlorinated solvent is also an indispensable constituent.

Table 4.5. Results of Screening Experiments Comparing the Time Frame and Relative Severity of Horizontal Cracking

Vial	Time Frame for Appearance of Horizontal Cracks						Cracked within 2 weeks
	0-7 days	7-14 days	14-25 days	25-50 days	50-75 days	>75 days	
1							✗
2	*	*		***			✗
3							✗
4							✗
5							✗
6							✗
7							✗
8				*****	*****		✗
9		*****			****	****	✔
10		**					✔
11							✗
12		***			***	****	✔
13		***		****			✔
14		***		***			✔
15							✗
16							✗
17							✗
18				*****	*****		✗

Number of stars indicates the relative severity of the cracking.

Figure 4.2. A mixture of propanol, acetone, methyl isobutyl ketone, 2-butoxyethanol, amyl acetate, and n-butyl acetate dissolved in PCE ponded on water-saturated bentonite for 42 days. No cracking was observed.
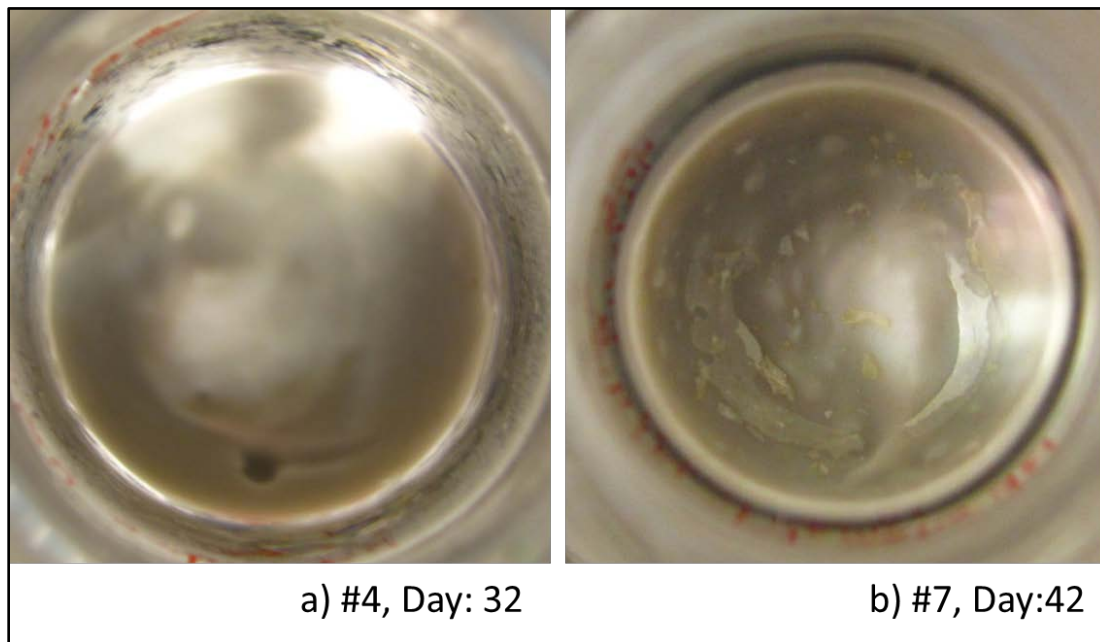
Figure 4.3. a) TritonX-100 dissolved in PCE, and b) AOT and $C_{12}E_6$ dissolved in PCE, ponded on water-saturated bentonite for 32 and 42 days, respectively. No cracking was observed.
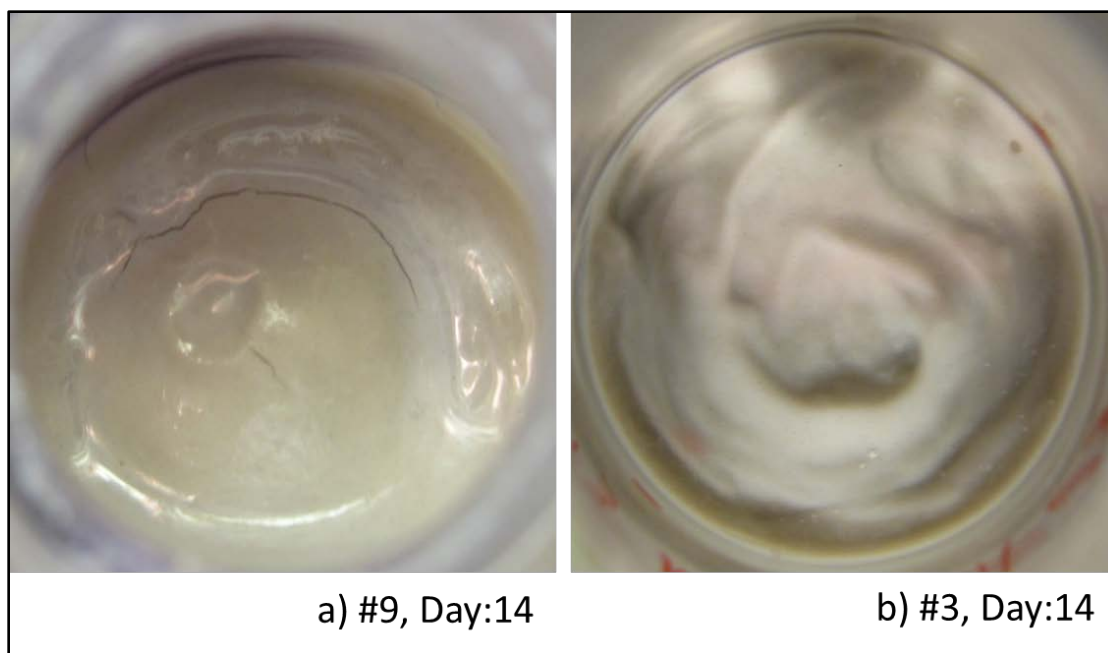
Figure 4.4. a) TritonX-100, AOT, $C_{12}E_6$ dissolved in PCE. Cracking was observed. b) TritonX-100, AOT, $C_{12}E_6$, propanol, acetone, methyl isobutyl ketone, 2-butoxyethanol, amyl acetate, and n-butyl acetate dissolved in water, ponded on water-saturated bentonite for 14 days. No cracking was observed.

4.3.2. Basal Spacing Measurements

The vial screening experiments showed that a mixture of anionic and nonionic surfactants dissolved in a chlorinated solvent was necessary in order to observe a magnitude and rate of cracking comparable to the DNAPL wastes. The beaker experiments described in Chapter 3 showed that a basal spacing decrease was always observed in the case of cracking. To corroborate this result with respect to the screening experiments reported in this chapter, the basal spacing of bentonite samples in contact with surfactant mixtures was measured.

The XRD results showed that an aqueous solution of TritonX-100 reduced the basal spacing of water-saturated bentonite from 19 Å to 17.5 Å; the combination of TritonX-100 and AOT had the same impact on basal spacing, as well (Table 4.6). On the other hand, when the three surfactants (TritonX-100, AOT, and $C_{12}E_6$) were present together in water, the basal spacing increased to 20 Å. In contrast, bentonite in contact with the same surfactant mixture (TritonX-100, AOT, and $C_{12}E_6$) in PCE showed a reduction in the basal spacing to 15.8 Å, similar to that observed when water-saturated bentonite was contacted with DNAPL waste. Similarly, the basal spacing of water-saturated bentonite in contact with a PCE solution of TritonX-100 and AOT decreased to 15.4 Å, suggesting that the second nonionic surfactant $C_{12}E_6$ was not necessary. The basal spacing of water-saturated bentonite in contact with PCE containing these surfactants decreased even further to 12.7 Å after three weeks of rotation, most likely due to the more rigorous interaction between the clay and solution for an extended time

frame. These results suggested that the minimum mixture needed for clay behavior similar to that observed with DNAPL waste was a combination of TritonX-100, AOT, and PCE.

Table 4.6. Basal Spacing of Water-Saturated Bentonite in Contact with Various Surfactant Solutions

Surfactant	Basal spacing (Å) (4 days of rotation and one week passive contact)		Basal spacing (Å) (3 weeks of rotation)	
	Dissolved in water	Dissolved in PCE	Dissolved in water	Dissolved in PCE
No surfactant	19.0	19.0	NM	NM
TritonX-100 (3.3 mM)	17.5	17.5	17.4	15.6
TritonX-100 (3.3 mM) and AOT (3.3 mM)	17.9	15.4	17.1	12.7
TritonX-100 (3.3 mM) and $C_{12}E_6$ (6.7 mM)	NM	18.8	NM	NM
TritonX-100 (3.3 mM), AOT (3.3 mM) and $C_{12}E_6$ (6.7 mM)	20.2	15.8	NM	NM

NM: not measured.

Figure 4.5 shows the XRD pattern of water-saturated bentonite contacted with the mixture of AOT and TritonX-100 dissolved in PCE for one week following four days of rotation. The broad peak suggests that not all of the interlayer space had contracted to the same degree. The XRD pattern appeared to be comprised of three overlapping peaks: one corresponding to a basal spacing of 18.9 Å (25% of total area as calculated by the profile fitting software), another one corresponding to 15.5 Å (50% of total area), and the third one corresponding to 11.5 Å (25% of total area). The magnitudes of the basal spacing suggest that about 25% of the interlayer space was still fully hydrated, 50% of the interlayer space was partially hydrated and 25% of the interlayer space of bentonite was dehydrated up to air-dry conditions, as 11.5 Å is the basal spacing of air-dry bentonite (Brown and Brindley, 1980; Moore and Reynolds, 1997). Sheng and Boyd (1998) and Lee et al. (2004) observed a similarly broadened peak in the case of naphthalene sorption onto smectite treated with a cationic surfactant. They attributed this to the collapse of some of the interlayer space due to the removal of water molecules as a result of naphthalene sorption.

4.3.3. Fourier Transform Infrared (FTIR) Spectroscopy Measurements

The question that was addressed with the FTIR measurements was whether the decrease in basal spacing occurred through the displacement of water molecules from the interlayer space. In order to evaluate this, the location of the H-O-H bending band of water in the interlayer space was observed for the systems in Table 4.4. Also, any sign of an interaction between the clay
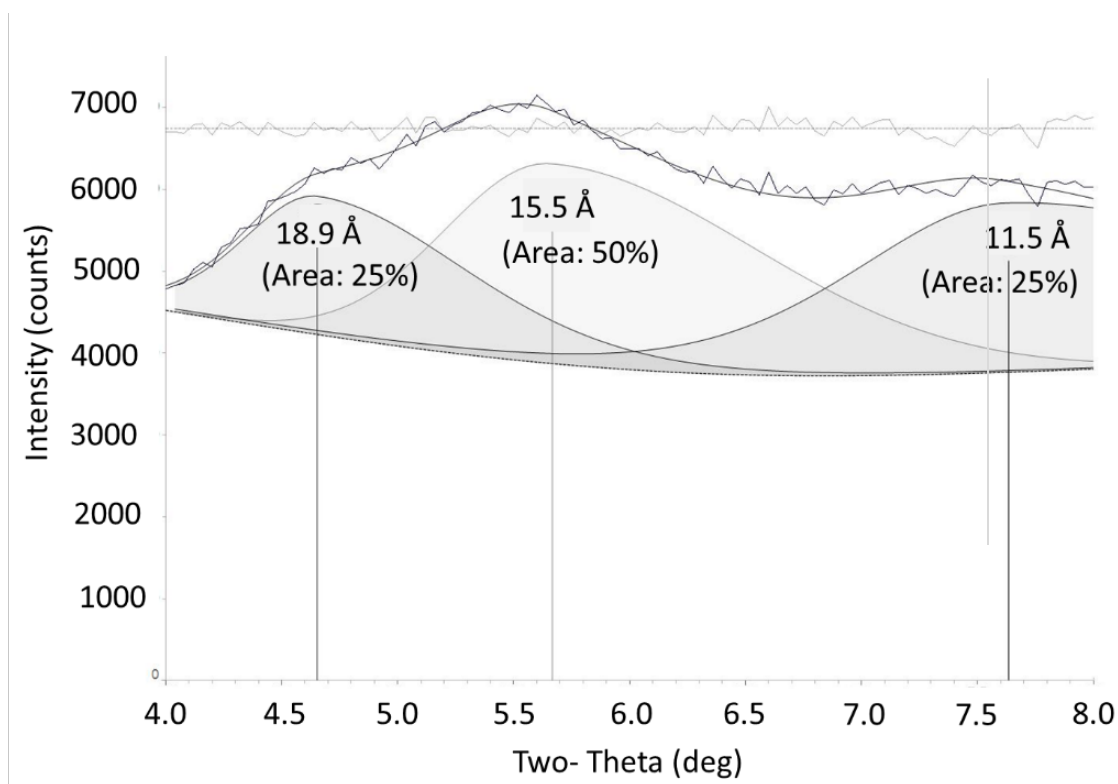
Figure 4.5. XRD pattern of water-saturated bentonite contacted with PCE containing 3.3 mM AOT and 3.3 mM TritonX-100.

surface, PCE and the surfactants was sought. The H-O-H bending band of water (Madejova and Komadel, 2001) is located at 1652 cm^{-1} for air-dry clay and at 1636 cm^{-1} for water-saturated bentonite, as shown here in Figure 4.6. This figure also shows that six months of contact with a TritonX-100 solution in PCE did not change the location of the H-O-H bending band relative to that for water-saturated clay, suggesting that the interlayer water was not impacted by the presence of the nonionic surfactant and chlorinated solvent. This observation agrees with the results of the screening experiments and basal spacing measurements since neither cracking nor a reduction in the basal spacing was observed for that system. However, after six months of contact with a mixture of TritonX-100, AOT and PCE, the wavenumber of the bending band of interlayer water increased to 1652 cm^{-1}, similar to the location in air-dry clay. This shift in wavenumber towards that for air-dry clay suggests a displacement of water molecules from the interlayer space, similar to the process of dessication. The shift in the wavenumber for the water-bending band was only from 1636 to 1639 cm^{-1} for the samples that were only aged for three weeks (Figure 4.7). This less pronounced change in the location of water bending band at shorter contact times implies that displacement of water molecules from the interlayer space of clay minerals may be a time-dependent process, with progressively more water being displaced over time.

66
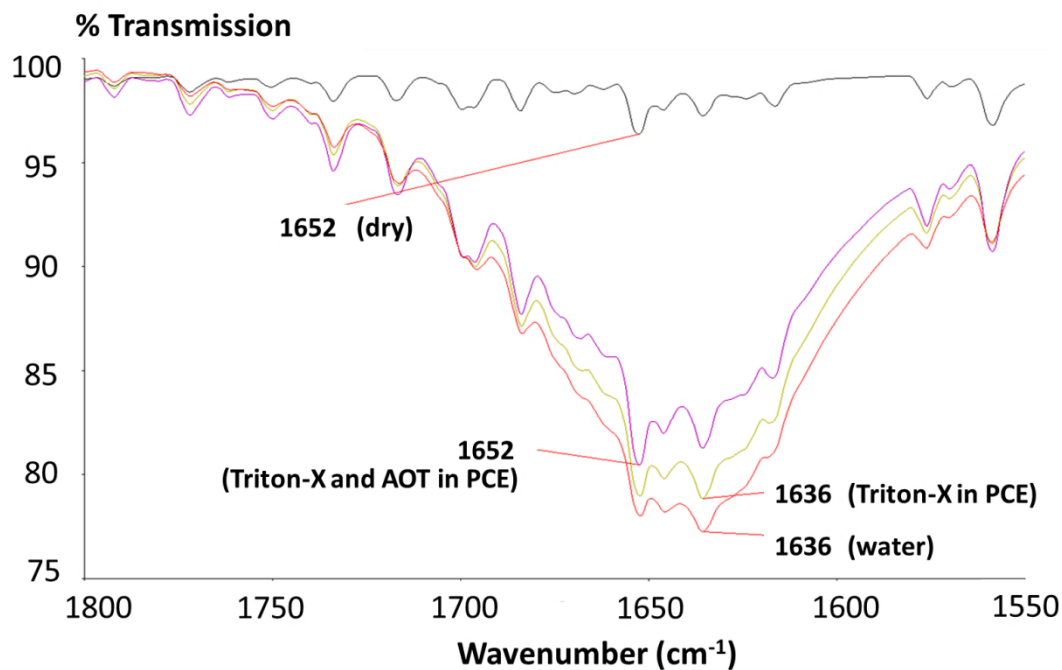
Figure 4.6. **FTIR spectra of water-saturated bentonite in contact with different fluids for six months in comparison with the spectrum of air-dry bentonite**.
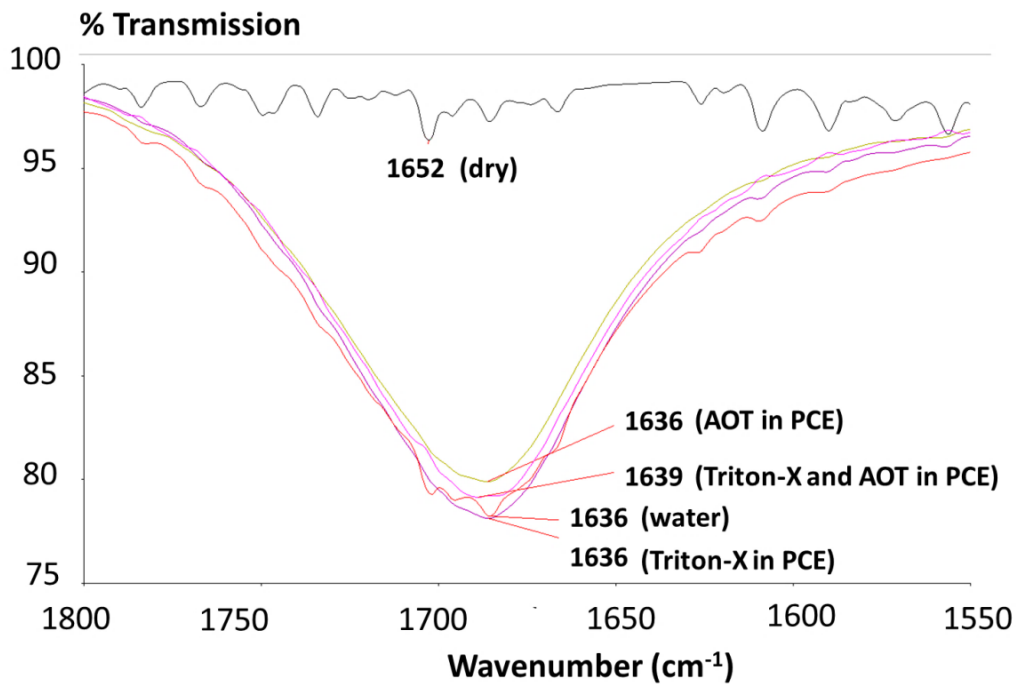
Figure 4.7. **FTIR spectra of water-saturated bentonite in contact with different fluids for three weeks in comparison with the spectrum of air-dry bentonite.**

67

Although some evidence was found suggesting an interruption of the hydration layers in clay, surfactant specific bands were not detected. In previous studies using FTIR to examine surfactants in clays, the clays were exposed to high concentration surfactant solutions and then dried. Here, the clays were exposed to relatively dilute concentrations of surfactants and were analyzed wet. Because of these differences in measurement conditions, changes in surfactant specific bands such as reported by Del Hoyo et al. (2008) could not be observed.

4.3.4. Sorption Experiments

The screening experiments and XRD measurements suggested that both an anionic and a nonionic surfactant needed to be present to decrease the basal spacing of water-saturated smectitic clay. The FTIR measurements suggested water displacement only in the case of contact with two surfactants and PCE. As synergistic activity of surfactants has been reported in the literature, it was thought that enhanced sorption may also occur with this mixture. To investigate this hypothesis, batch experiments were conducted, and the sorption of TritonX-100 and AOT on water-saturated Na-montmorillonite was measured. The results are summarized in Table 4.7 and in Figures 4.8 and 4.9. They show that 65% of TritonX-100 was sorbed from an aqueous solution of TritonX-100, versus 57% if the aqueous solution contained AOT also (Table 4.7; Figure 4.8). On the other hand, the degree of AOT sorption increased from 7% to 14% if both AOT and TritonX-100 were present (Table 4.7; Figure 4.9). Thus, the presence of TritonX-100 increased the sorption of AOT two fold, giving a sorbed molar ratio of TritonX-100:AOT of around 5:1 from the aqueous solution. Similar experiments were conducted with the surfactants dissolved in PCE. The results showed that the degree of TritonX-100 sorption increased slightly, from 72% to 85%, in the presence of AOT (Table 4.7; Figure 4.8). On the other hand, the degree of AOT sorption increased almost eight fold in the presence of TritonX-100 (Table 4.7; Figure 4.9). In the case of sorption from PCE, the sorbed molar ratio of TritonX-100:AOT was 3:2. Although AOT is an anionic surfactant, its sorption increased considerably through its association with a chlorinated solvent and a nonionic surfactant.

Table 4.7. Sorption of TritonX-100 and AOT from Aqueous and PCE Solutions onto Na-montmorillonite

Solvent	Solute (Initial concentration)	Mass of wet soil (g)	Sorption of	C_{sorbed} (mmol/ g wet clay)	Percent sorption (%)
Water	TritonX-100 (3.3 mM)	2	TritonX-100	0.0242	64.9
	TritonX-100 (3.3 mM) **&** AOT (3.3 mM)	2		0.0238	57.1
	AOT (3.3 mM)	2	AOT	0.0022	6.5
	TritonX-100 (3.3 mM) **&** AOT (3.3 mM)	2		0.0050	14.3
PCE	TritonX-100 (3.3 mM)	4	TritonX-100	0.0120	72.4
	TritonX-100 (3.3 mM) **&** AOT (3.3 mM)	4		0.0126	84.9
	AOT (3.3 mM)	4	AOT	0.0011	7.3
	TritonX-100 (3.3 mM) **&** AOT (3.3 mM)	4		0.0082	57.8
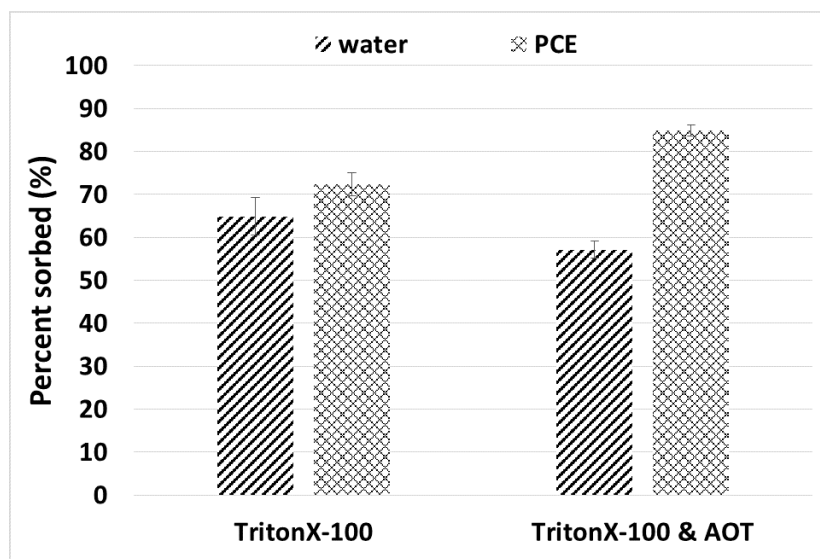
Figure 4.8. Percent sorption of TritonX-100 from aqueous and PCE solutions onto Na-montmorillonite.
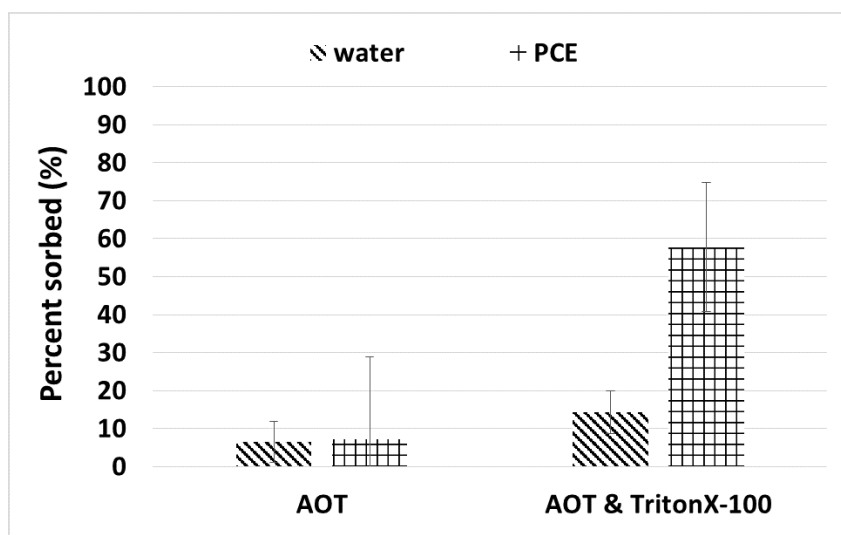
Figure 4.9. Percent sorption of AOT from aqueous and PCE solutions onto Na-montmorillonite.

The XRD results presented in Chapter 3 showed that the basal spacing of water-saturated Na-montmorillonite contacted with DNAPL waste decreased to that of air-dry clay, so it was speculated that the surfactants penetrated into the interlayer space of water-saturated smectite, allowing the chlorinated solvent to then enter. To investigate the possibility of an increased uptake of the chlorinated compound by the clay in the presence of surfactants, measurements of the sorption of ^{13}C-labeled TCE were performed in the presence and absence of surfactants. Table 4.8 shows the results of those measurements. These data show that the quantity of TCE

sorbed is higher (33%) in the case where AOT and TritonX-100 were dissolved in PCE. Therefore, it appears that presence of the surfactant mixture enhanced the sorption of the chlorinated solvent somewhat but considerably less than the increase observed for the sorption of AOT (around 800%). This result suggests that an explanation based solely on increased quantities of TCE in the interlayer space of water-saturated smectitic clays is not reasonable as this quantity of sorption could occur on the outer edges of the clay minerals. The fundamental difference noted in the presence of the chlorinated solvent is an increased sorption of the surfactants, in particular, the anionic surfactant AOT.

Table 4.8. Sorption of ^{13}C-labeled TCE From PCE Containing TritonX-100 and AOT onto Na-montmorillonite

Solution	C_{sorbed} (mmol/g wet clay)	% sorbed
AOT in PCE	0.006 (0.007)	7 (7)
AOT &TritonX-100 in PCE	0.008 (0.008)	33 (23)
TritonX-100 in PCE	0.003 (0.003)	5 (4)
No surfactant in PCE	ND*	ND*

*Below the limit of instrument error.
Numbers in parentheses are standard deviations.

4.4.   Proposed Mechanism for Basal Spacing Decrease

The screening experiments suggested that a mixture of anionic and nonionic surfactants and chlorinated solvent caused a decrease in basal spacing and the formation of cracks, similar to a DNAPL waste. The sorption results suggested that there was increased sorption in the presence of PCE, with about 85% of the nonionic surfactant, TritonX-100, and nearly 60% the anionic surfactant, AOT, sorbed onto water-saturated Na-montmorillonite, giving a sorption ratio of 3:2. The location and orientation of the molecules relative to the clay surface of the interlayer space will depend, in part, on the size of the molecules. The basal spacing is the sum of the tetrahedral-octahedral-tetrahedal (TOT) layer and the interlayer space (Figure 4.10). The TOT structure of smectite clay minerals has a thickness of around 9.6 Å (Moore and Reynolds, 1997); thus, the interlayer space will have a thickness of around 5.5 Å, if the basal spacing is 15 Å. TritonX-100 can conceivably penetrate and sorb into the water-filled interlayer space since it is miscible in water, nonionic and has a width of 3 Å (based on the diameter of a phenyl group). However, due to its length (around 48 Å, Table 4.9), it cannot be aligned vertically in the interlayer space. So, TritonX-100 is thought to lie generally parallel to the interlayer surfaces, as also hypothesized by Deng et al. (2003). However, AOT is unlikely to enter into the interlayer space because it has a negatively-charged head, whose diameter is 5 Å. AOT's enhanced sorption in the presence of TritonX-100, suggests that AOT interacts with TritonX-100, most likely through their hydrophilic moieties because of the nonpolar nature of the surrounding solvent (Moulik, 1996). Furthermore, if there is water retained on the exterior surfaces, it is anticipated that AOT can partition into that region, as AOT shows preferential partitioning into water over PCE ($K_{PCE,water}$ = 0.001) (Hsu, 2005). Assuming interactions between TritonX-100

and AOT through their hydrophilic moieties, a 3:2 ratio of sorption, that TritonX-100 can penetrate into the interlayer space, but AOT cannot, a schematic may be developed as in Figure 4.11.

With the sorption of TritonX-100, some of the water molecules at the margins of the interlayer space of the clay particle may be displaced. In addition to this displacement of water by TritonX-100, it is speculated that the association of the AOT molecules in close proximity with the interlayer space stimulates further reductions in the quantity of the interlayer water. AOT is known to spontaneously form thermodynamically stable premicellar aggregates and reverse micelles in nonpolar solvents, with water being an essential component in their formation. These aggregates can solubilize substantial amounts of water, reaching molar ratios of water to micellized surfactant of up to 40-60, depending on the temperature and the nature of the nonpolar solvent (Silber et al., 1999). Thus, AOT's association with TritonX-100 may facilitate its attraction of water from the interlayer structure to fulfill its need for aqueous solvation.
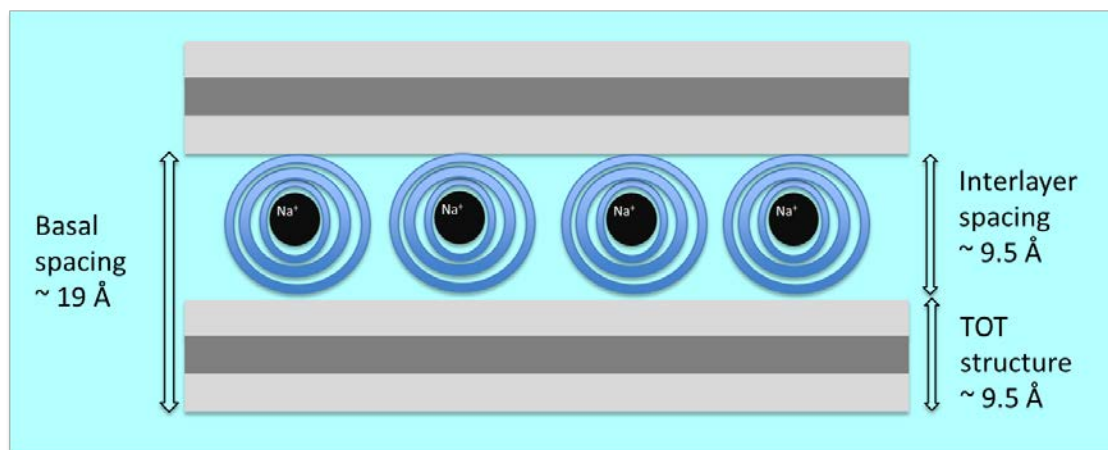
Figure 4.10. Diagram illustrating interlayer space of water-saturated Na-montmorillonite. Rings around the sodium cations represent the presence of three layers of water in the interlayer space of water-saturated Na-montmorillonite (Brown and Brindley, 1980; Moore and Reynolds, 1997).

Table 4.9. Dimensions of Molecules in Model DNAPL Waste System

Head diameter of AOT (Å) (Moulik and Mukherjee, 1996)	5.0
Tail length of AOT (Å) (Moulik and Mukherjee, 1996)	12.6
Diameter of phenyl group (Å)	3
Total length of TritonX-100 (Å) (Paradies, 1980)	48
Width of PCE molecule (Å) (Zhou, 1994)	3.6
Width of water molecule (Å) (Cheng et al., 2001)	2.8
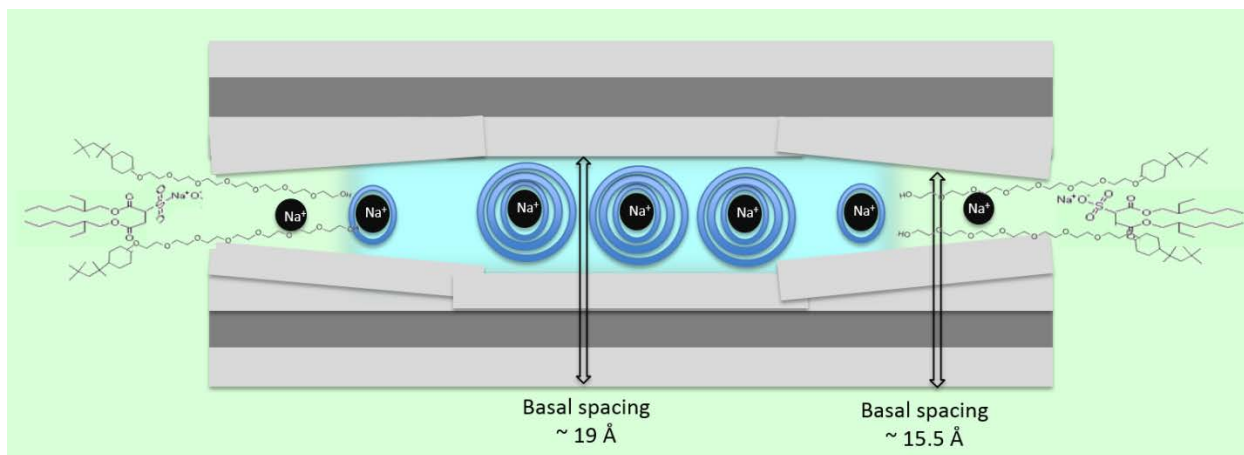
Figure 4.11. Diagram illustrating the partially collapsed interlayer space of water-saturated Na-montmorillonite in contact with PCE containing AOT and TritonX-100. (Green represents PCE and blue represents water.)

4.5. Conclusions

DNAPL waste is a mixture of many different compounds. Traditionally, the focus of research has been on the solvent matrix of the waste, with the contribution of the other components receiving less attention. However, the work presented in Chapter 3 showed that PCE or TCE by itself does not cause a collapse of the clay structure as do PCE-based or TCE-based field wastes. Screening experiments were performed to determine the critical components of the field wastes. The modified structure of Na-montmorillonite clays was observed at two different scales: basal spacing was measured at the microscale and the formation of cracks was monitored at the macroscale. These experiments showed that the minimum mixture required to match the behavior of DNAPL wastes was comprised of an anionic and nonionic surfactant, specifically AOT and TritonX-100, dissolved in a chlorinated solvent, PCE. With passive contact with this mixture, the basal spacing decreased from around 19 Å to 15 Å, and the water-saturated clay cracked within about a two-week time period.

Since all three components must be present for cracking to occur and none caused cracking individually, possible synergistic interactions were investigated. It was found that, in the presence of PCE, the nonionic surfactant, TritonX-100, sorbed onto water saturated Na-montmorillonite in greater quantities than from water and, in addition, the sorption of the anionic surfactant, AOT significantly increased. Thus, the presence of PCE and TritonX-100 allowed the sorption of AOT, which, generally, does not sorb onto clay surfaces due to the repulsion between the negatively-charged clay surface and the negative charge of the surfactant. Furthermore, the presence of the surfactants increased the sorption of TCE, although to a considerably lesser extent. Thus, it appears that the primary role of the chlorinated solvent is to increase the sorption of the surfactants, particularly AOT. FTIR data suggested a partial displacement of water molecules as a result of contact with the PCE, anionic and nonionic surfactant mixture. When this information is considered in concert with the sorption data, it was

72

concluded that the surfactants sorbed on the water-saturated Na-smectite, displacing some water molecules. Because of its length, TritonX-100 is hypothesized to lie horizontally relative to the interlayer surface. Since the sorption of AOT increased in the presence of TritonX-100, it is speculated that it interacts with TritonX-100 through their hydrophilic moieties due to surrounding nonpolar solvent. However, the AOT lies external to the clay particle, due to the size of its head and the repulsion between the negatively-charged clay surface and the negatively-charged head group. AOT is known to spontaneously form thermodynamically stable premicellar aggregates and reverse micelles in nonpolar solvents, with water being an essential component in their formation. Thus, AOT's association with TritonX-100 may facilitate its attraction of water from the interlayer structure to fulfill its need for aqueous solvation.

As the displacement of water molecules from the interlayer space is not uniform, there is a range of basal spacings; this is reflected in the XRD pattern as a very broad peak which actually represents overlapping peaks, with each peak indicating interlayer space with different thicknesses. This shrinkage of the lattice structure is accompanied by cracking. The evidence presented here supports a mechanism of syneresis, involving the extraction of water from the interlayer space by the synergistic sorption of nonionic and anionic surfactants. Burst (1965) documented the cracking of clay layers containing as little as 10% bentonite due to syneresis, driven by increases in salinity in the surrounding aqueous solution. The evidence presented in this study suggests that cracking may be similarly precipitated by the solvation of the clay's interlayer water in surfactant aggregates.

5.0   Modeling the Impact of Enhanced Transport on the Longevity of the Dissolved Phase Plume

5.1.   Introduction

The transport of dissolved contaminant into and out of low permeability zones is conventionally modeled assuming that the transport occurs through Fickian diffusion in a competent, homogeneous, soil matrix (Parker et al., 1994). It is generally thought that the diffusional mass transfer into the low permeability layers occurs due to the relatively high concentrations of the dissolved chlorinated compound found around pooled and residual DNAPL in the high permeability zones and the lower concentrations in the low permeability zones, leading to an accumulation in the latter over time. After the removal of the DNAPL pools, the contaminant diffuses out of the low permeability layers into the adjacent high permeability regions, acting as a secondary source to the high permeability regions. Due to the lower concentration gradients driving the diffusion out of the low permeability zones, as well as the continuing diffusion of the contaminant farther into these zones, back diffusion is much slower and longer lasting than the diffusion process that originally drove the contaminant therein (Sale et al., 2008a). Although back diffusion is slow, it can contribute enough mass to the flowing groundwater to propagate plumes in excess of regulatory maximum concentration levels (MCLs) for decades. Parker et al. (2008) modeled a small number of low permeability clay layers in a predominantly high permeability sand aquifer and concluded that back diffusion can cause down gradient concentrations to remain above MCLs for many years after the remediation of the original source.

The conventional approach to modeling the impact of back diffusion is to assume diffusion into and out of a competent low permeability zone. However, cracks can occur naturally in clay layers as the result of fluctuations in pressure due to erosion or excavations, changes in water table levels (McKay et al., 1993a) or changes in salinity in the surrounding solution (Burst, 1965). Table 5.1 summarizes some of the literature that quantifies the extent of cracking observed in geologic strata in the field. It may also be hypothesized that the presence of pooled DNAPL atop of clay may result in cracking as observed in laboratory experiments reported in Chapter 3 and summarized in Ayral et al. (2014). While the application of diffusion-based models to field sites has been successful in some cases, other attempts to fit a diffusion-based model to cracked clay, for example landfill liners, have failed to produce satisfactory results (Goodall and Quigley 1977; Crooks and Quigley 1984).

The presence of cracks, whether due to natural processes or to the interaction of a DNAPL mixture with clay-containing zones, may result in enhanced transport of the contaminant into (and out of) the zones due to a number of factors. For example, a cracked low permeability layer will have a higher hydraulic conductivity than a competent layer, due to the existence of the cracks. Increases in hydraulic conductivity of two to three orders of magnitude (Anderson et al., 1985), three to four orders of magnitude (Li et al., 1996), and one to five orders

of magnitude (Brown and Thomas, 1984) have been reported depending on the organic liquid, clay type and percent clay.

In addition to the possible enhancement of solute transport within the low permeability zones due to the existence of cracks, the contaminant may accumulate as an organic liquid phase in the cracks. Kueper and McWhorter (1991) examined the height of the DNAPL pool necessary for entry into fractures, using Eqn. 3.3. Using a similar approach, the DNAPL pool height needed to overcome the entry pressure of cracks summarized in Table 5.1 was calculated, assuming that the DNAPL was either pure TCE or a TCE-based field waste. The pool height estimates presented in Table 5.1 are conservative as they assume a contact angle of 0° and there is evidence of less hydrophilic conditions *in situ* (e.g., Dwarakanath et al., 2002). Given the pool heights that have been observed in the field (for example, 3.0 to 7.3 m at Hill AFB [Oolman et al., 1995]), DNAPL pools may have a sufficient height to exceed the entry pressure of naturally occurring cracks. Furthermore, as noted in Section 3.5, the cracks observed forming in the laboratory are also of a sufficient magnitude (median aperture = 680 µm), that DNAPL may enter them.

Parker et al. (1994) developed an analytical solution to calculate the time required for DNAPL residing in a fracture to completely dissolve into the surrounding geologic matrix. Their solution assumed Fickian diffusion from a single fracture into immobile water present in a geologic matrix, comprised either of clay (relatively high porosity and effective diffusion coefficient) or sandstone/shale (relatively low porosity and effective diffusion coefficient). The current study moves beyond the analytic modeling presented by Parker et al. (1994) to investigate how the presence of cracks in low permeability media in a DNAPL source zone affects the evolution and persistence of down gradient plumes in the surrounding aquifer. Since the concern at hazardous waste sites is meeting the MCL in aquifers (high permeability layers) down gradient, the current study addresses the goal of remediation. It uses a numerical model which allows for advective transport into the low permeability media, in addition to purely diffusive transport. The numerical model also allows for the quantification of the dissolved plume concentrations over space and time in the surrounding aquifer, as well as the dissolved concentrations in the water in the low permeability zone. Thus, the analysis of the model results described in this chapter provides an increased understanding of the relationship between cracking, mass storage, and plume behavior. As contamination by compounds which can exist in the subsurface as DNAPLs is extremely common at DoD installations, the enhanced understanding gained through this modeling can help guide DoD remedial project managers as they make management decisions at their contaminated sites.

5.2.   Modeling Approach

5.2.1. Constant Rate of DNAPL Dissolution

In this study, a numerical flow and transport model was employed to investigate the impact of cracking in low permeability zones on the evolution and persistence of groundwater contamination down gradient of a DNAPL pool, using TCE as the model DNAPL. The

numerical model was used to compare plume evolution in the situation of an aquifer (high permeability sand layer) underlain by a low permeability layer (clay) that is (1) competent, with transport of TCE as a solute into the low permeability layer due to diffusion, (2) cracked, allowing an enhanced advective transport of TCE as a solute into the low permeability layer followed by diffusion within the clay layer, and (3) cracked, with separate phase DNAPL movement into the cracks followed by dissolution and subsequent diffusion into the surrounding clay matrix. In all simulations, the degradation and sorption of TCE in both the clay and sand materials were assumed to be insignificant.

Table 5.1. Pool Heights of TCE Necessary for Entry into Naturally Occurring Cracks

Crack Characteristics				Calculated Pool Height§ (m)	
Depth (m)	Spacing (m)	Aperture (μm)	Reference	Pure TCE[†]	Waste TCE[¶]
<4	0.04-0.1	26-32	D'Astous et al. (1989)	0.97	0.06
<18	0.05-0.15	1-14	Day (1977)	2.22	0.15
<7	0.04	4	Grisak and Pickens (1980)	7.76	0.51
<16	0.4	50	Hendry et al. (1986)	0.62	0.04
2-2.5	-	1-120	Hinsby et al. (1996)	0.26	0.02
12-18	<.15	11	Keller et al. (1986)	2.82	0.19
1.7-3.2	0.04-0.13	9-43	McKay et al. (1993b)	0.72	0.05
<5	0.02-1.0	<43	McKay et al. (1993a)	0.72	0.05
<4	0.03	150	Pankow et al. (1986)	0.21	0.01
3.7-4.2	-	5-17	O'Hara et al. (2000)	1.82	0.12
<20	1.5	30	Rudolph et al. (1991)	1.03	0.07
4-5	-	1-5	Sims et al. (1996)	6.20	0.41
40-50	1.2-5	140-210	Thompson (1990)	0.15	0.01

§Calculated using Eqn. 3.3 assuming that the contact angle is 0°.
[†]Assumes that TCE has a density of 1.46 g·cm^{-3} and an interfacial tension of 35 dyne·cm^{-1} (Demond and Lindner, 1993).
[¶]Assumes that the TCE is a field waste and has a density of 1.30 g·cm^{-3} and an interfacial tension of 2-3 dyne·cm^{-1}, as measured by Hsu (2005).

In the first scenario (Scenario 1), the advection-dispersion equation for the transport of a non-sorbing, conservative solute in the sand layer, was coupled with Fick's Second Law of diffusion (Eqn. 2.4) to describe transport into the competent clay. The transport mechanisms in the sand comprised advection, dispersion and molecular diffusion, while the dominant transport mechanism in the competent clay was diffusion. During the initial ten years of the simulation, the presence of a DNAPL pool as a source was modeled by setting the concentration of cells in the high permeability layer directly above the clay layer at 10% of TCE's solubility (110 mg L^{-1}) to account for mass transfer limitations. The removal of the DNAPL pool was assumed to occur at ten years and was simulated by eliminating the constant concentration cells at the interface

between the sand and clay. Thus, after ten years, the concentration gradient was reversed, resulting in back diffusion from the clay layer to the overlying sand layer.

In the second scenario (Scenario 2), the clay beneath the DNAPL pool was considered to be cracked. To simulate the influence of the cracks on transport, the vertical conductivity was increased by two orders of magnitude. This level of increase was based on a study that analyzed the relationship between hydraulic conductivity and cracking (McKay et al., 1993a). Thus, this scenario considered enhanced advective transport, in addition to diffusive transport within the clay.

In the third scenario (Scenario 3), the clay beneath the DNAPL pool was considered to be cracked; in addition, the depth of the pool of DNAPL was considered to be large enough that TCE was resident in the cracks at the beginning of the simulation. To calculate the volume of DNAPL residing in the cracks, it was assumed that the cracks extended to a depth of 4 m, had a diameter of 150 μm, and were 0.03 m apart (Pankow et al., 1986) and contained a residual water saturation of 10%, giving a total of 6.62 x 10^{-5} DNAPL m^3 per m^3 of cracked clay. As the cracks were not explicitly modeled, the assumption is that this volume of DNAPL was initially uniformly distributed throughout the cracked clay zone. During the first ten years of the simulation, the DNAPL mass was reduced due to diffusion into the clay matrix. This mass was not continually replenished, due to limitations of the model. However, to simulate the replenishment from the overlying DNAPL pool that might actually occur in the field, the cracks were refilled with DNAPL at ten years, the time of source removal.

To migrate out of the cracks, the DNAPL had to first dissolve. Eqn. 5.1 models the dissolution of the DNAPL as a first-order process, with the parameter F "turning off" the DNAPL dissolution the DNAPL was fully dissolved:

$$\rho_{NAPL} \frac{\partial S_{NAPL}}{\partial t} = k_{eff}(C - F) \tag{5.1}$$

$$F = \begin{cases} C_S & S_{NAPL} > 0 \\ C & S_{NAPL} = 0 \end{cases}$$

where ρ_{NAPL} is the DNAPL density (1460 kg·m^{-3} for pure TCE), S_{NAPL} is the DNAPL saturation, C_S is the effective DNAPL solubility in water (taken as 10% TCE solubility or 110 mg-L^{-1}), k_{eff} is the first-order mass transfer coefficient between the DNAPL and the surrounding water, and C is the concentration of the dissolved DNAPL. k_{eff} was modeled as a function of DNAPL mass using the following relationship (Christ et al., 2006):

$$k_{eff} = K_0' \left(\frac{M(t)}{M_0}\right)^\beta \tag{5.2}$$

where K_0' is a fitting parameter, $M(t)$ is the DNAPL mass as a function of time, M_0 is the DNAPL mass at time t = 0, and β is a fitting parameter. Values of 8.2 x 10^{-3} d^{-1} and 0.85 were used for K_0' and β, respectively, derived from numerical analyses of various source zone scenarios presented in Christ et al. (2006). Assuming that $\frac{M(t)}{M_0} = 0.5$, k_{eff} was approximated as a

constant equal to 4.55 x 10^{-3} d^{-1}. In essence, this approximation is equivalent to assuming that the DNAPL architecture is relatively homogenous over time.

Figure 5.1 depicts the domains. A three-dimensional grid was created with a length of 100 m, a width of 70 m, and a total depth of 14 m. Each cell in the grid was 1 m x 1 m x 1 m. A 6-m thick sand layer was located on top of a 6-m thick clay layer, with another 2-m thick sand layer below the clay. For Scenarios 2 and 3, a 192 m^2 area by 4 m deep cracked zone was emplaced in the clay layer. A nest of three observation wells was placed 50 m down gradient from the source screened in the upper sand layer, at the interface between the sand and the clay, and in the clay layer, respectively.

The simulations were performed using the Ground Water Modeling System (GMS) (Owen et al., 1996). Within GMS, MODFLOW (McDonald and Harbaugh, 2003) was used to compute the steady-state heads and groundwater velocities for each of the three scenarios based on the hydraulic parameters in Table 5.2. Then, the steady-state flow solution of MODFLOW was input into RT3D (Clement et al., 1998) for the simulation of contaminant transport. Since RT3D does not have the capability to describe dissolution from a separate organic liquid phase, followed by diffusion into the clay matrix, a user-defined transport routine was developed to simulate this process. Transport parameters such as the longitudinal dispersivity and effective diffusion coefficient were assigned to the sand, clay, and cracked clay as shown in Table 5.2.

A sensitivity analysis was also conducted to determine which parameters most significantly affect the dissolved plume's down gradient behavior and mass storage in the low permeability layer. Scenario 3 was used as the baseline scenario for this analysis; the parameters examined were the first-order DNAPL dissolution mass transfer rate constant (k_{eff}) and the vertical hydraulic conductivity (K_v) of the cracked clay directly below the source. The dissolution mass transfer rate constant (k_{eff}) was varied by four orders of magnitude, from two orders below its baseline value of 4.55 x 10^{-3} d^{-1}, to two orders of magnitude above. Similarly, the vertical hydraulic conductivity (K_v) of the cracked clay directly below the source was varied by four orders of magnitude, from two orders below its baseline value of 4.32 x 10^{-4} m·d^{-1}, to two orders of magnitude above.

The aquifer was assumed to be unconfined, and a horizontal hydraulic gradient of 1 m/100 m was established by setting the head at the left and right side upper boundaries of the domain at 14.5 m (0, 0 < y <70, 0) and 13.5m (100, 0 < y <70, 0), respectively. A vertical hydraulic gradient of 0.5 m/14 m was established by setting the heads at the left and right lower boundaries at 14.0 m (0, 0 < y <70, 14) and 13.0 m (100, 0 < y <70, 14), respectively. Figure 5.2 shows the resulting head distribution in the model domain. The model was used for two types of analyses: (1) to simulate concentration versus time plots, or breakthrough curves, at the nest of observation wells located 50 meters downgradient, and to quantify DNAPL mass and dissolved mass in the low permeability zone as a function of time.

Table 5.2. Groundwater Flow and Transport Parameter Values for Simulations

Parameter	Sand	Clay	Cracked Clay
Horizontal hydraulic conductivity (m/d)	17.28	4.32×10^{-5}	4.32×10^{-5}
Vertical hydraulic conductivity (m/d)	1.728	4.32×10^{-6}	$4.32 \times 10^{-4\S}$
Longitudinal dispersivity (m)	1.0	1.0×10^{-4}*	1.0×10^{-4}*
Porosity (-)	0.35	0.43*	0.487*
Effective diffusion coefficient ($cm^2 \cdot s^{-1}$)	NA	$8.64 \times 10^{-6\dagger}$	$8.64 \times 10^{-6\dagger}$

Parameter values are from Chapman and Parker (2005) except as noted.

§Based on McKay et al. (1993a).

*Miniter (2011). Porosities based on range reported in Domenico and Schwartz (1997).

†The effective diffusion coefficient for TCE in the clay was calculated as the diffusion coefficient of TCE in water, 1.05×10^{-5} $cm^2 \cdot s^{-1}$ (Schwarzenbach et al., 2003), multiplied by a relative diffusivity of 0.82 (Bear 1972).

NA: not applicable as the dispersivity is sufficiently large that dispersion is >> diffusion.
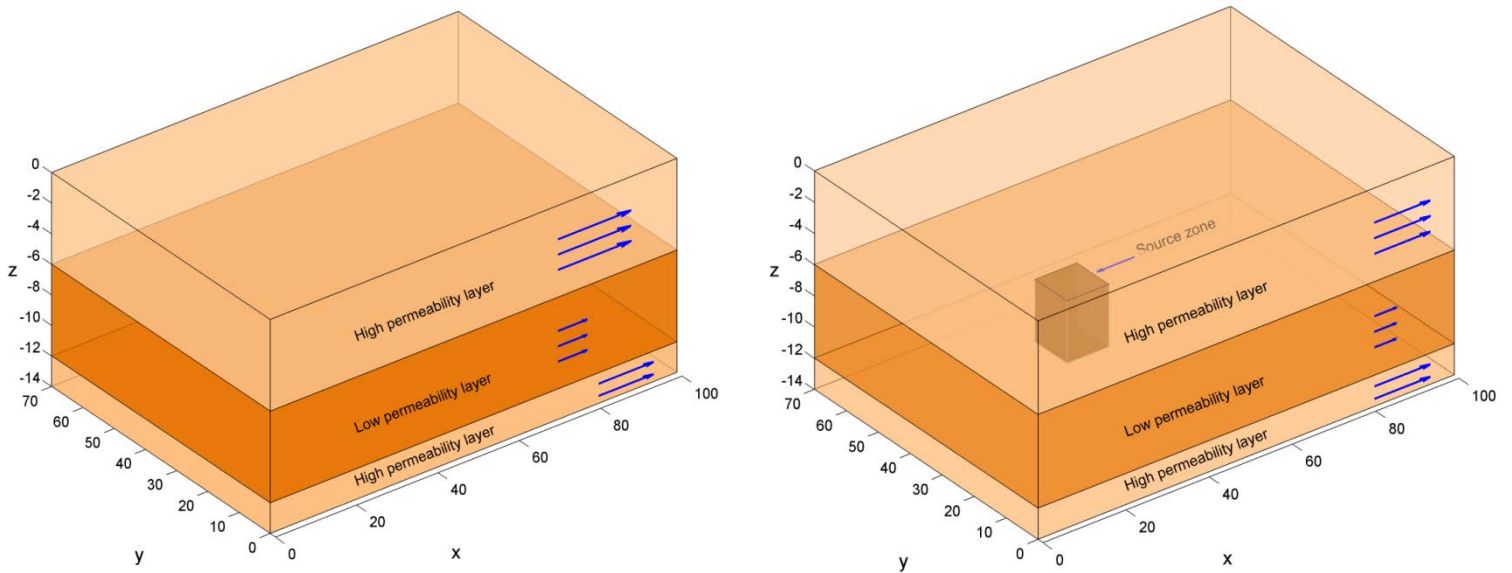
Figure 5.1. Domain used for (left) Scenario 1 involving no cracking of the clay layer, and (right) Scenarios 2 and 3 involving cracking (darkened area shows the location of the cracks).
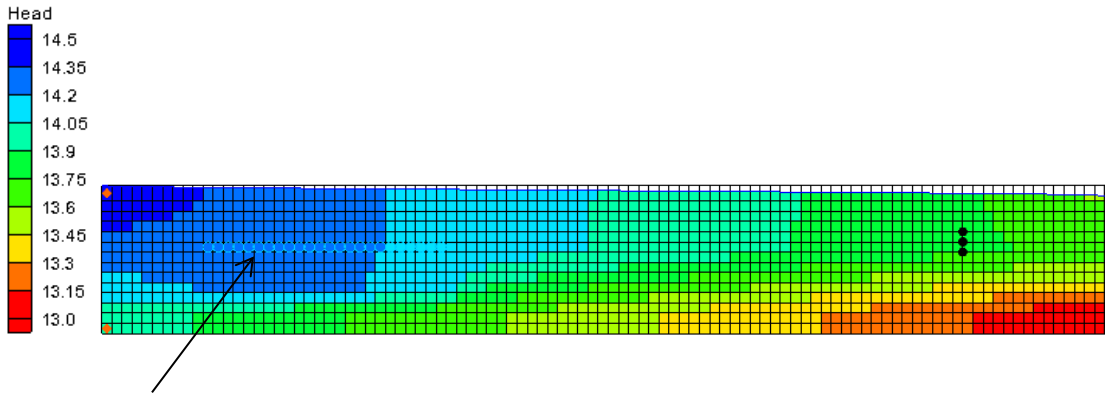
Figure 5.2. MODFLOW output showing distribution of hydraulic heads along a longitudinal cross section for simulations assuming a constant rate of dissolution. Each cell is 1 m x 1m x 1m. The black dots represent the location of the nest of observation wells down gradient. The red dots in the corners designate the constant head boundaries. The blue dots (see arrow) represent the source cells.

5.2.2. Variable Rate of DNAPL Dissolution

The work described in this section is an extension of the work described above. The model outlined above assumed that the rate of mass dissolution from the DNAPL source was constant. However, it is thought that, in reality, the rate of dissolution declines with the degree of saturation (Eqn. 5.2), as at early times, the rate of dissolution may be controlled by DNAPL in the smaller cracks, with a high surface area to volume ratio, compared to later times, at which point the DNAPL in the smaller cracks has totally dissolved. Christ et al. (2006) developed a mass transfer model, using parameters based on a contaminated site at Bachman Road in Michigan, to examine DNAPL dissolution kinetics. This model was incorporated into the GMS for these simulations.

In addition, a new domain was developed based on the characteristics of the Bachman Road Site (Abriola et al., 2005). The domain had a length of 70 meters (m), a width of 70 m, and a depth of 14 m, 30 meters shorter than the previous domain, but with the same width and depth. Each cell in the grid was a cube with sides of 1 m. The high permeability sand layer was 8 m thick atop a 6-m thick low permeability clay layer. The clay layer overlaid a 2-m thick permeability sand layer to avoid having a no-flow boundary condition at the bottom of the clay layer. A 4 x 4 x 4 m cracked clay zone was placed in the low permeability layer, as shown in Figure 5.3, overlaid by a source. A nest of three observation wells was placed 50 m down gradient from the source (Figures 5.3 and 5.4).
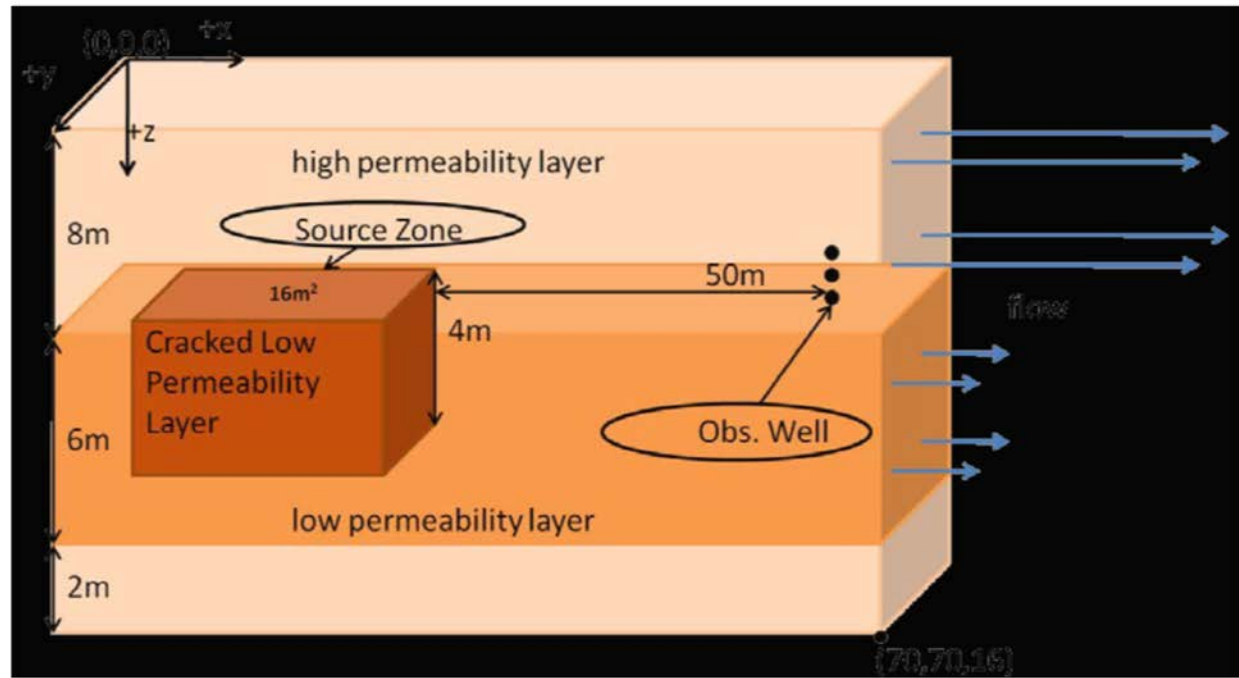
Figure 5.3. Conceptual model of contaminated aquifer for the variable dissolution rate simulations.
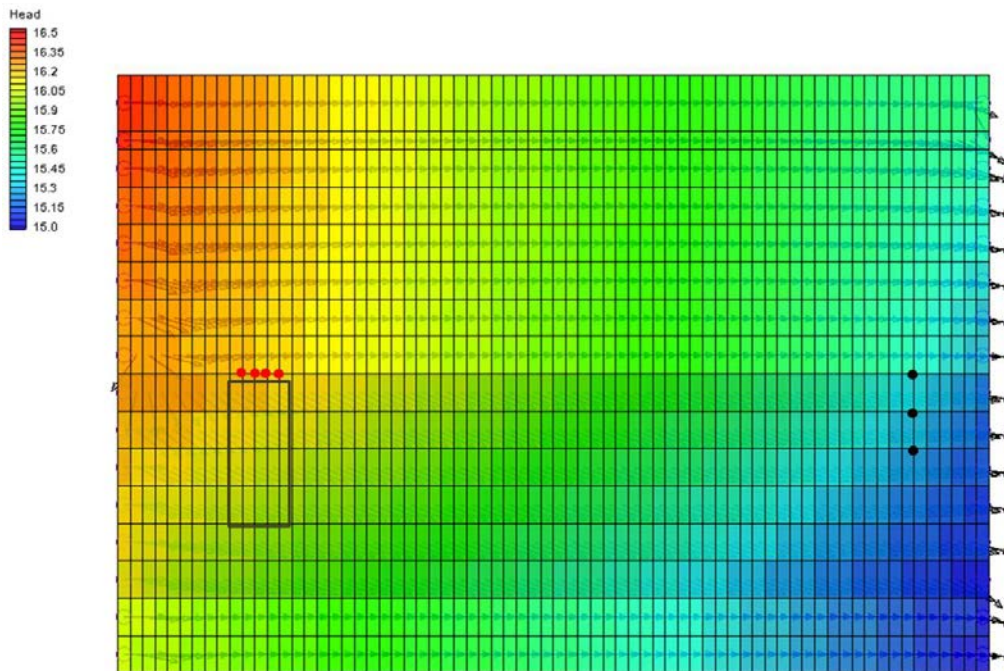
Figure 5.4. MODFLOW output showing distribution of hydraulic heads along a longitudinal cross section for simulations assuming a variable rate of dissolution. Each cell is 1 m x 1m x 1m. The black dots represent the location of the nest of observation wells down gradient. The red dots represent the source. The rectangle represents the cracked clay.

The aquifer was assumed to be unconfined, and a horizontal hydraulic gradient of 1 m/70 m was established by setting the heads at the left and right boundaries of the domain at 16.5 m and 15.5 m, respectively. A vertical hydraulic gradient of 0.5 m/16 m was established by setting the bottom heads at the left and right hand boundaries to 16 m and 15 m, respectively. Figure 5.4 shows the resulting steady-state distribution of hydraulic heads based on these boundary conditions, as calculated by MODFLOW. MODFLOW also computed the groundwater velocities based on the hydraulic parameters in Table 5.2. These flow velocities were then used as input by the RT3D code, which then simulated the contaminant transport. The same parameter values were used as for the simulations assuming a constant rate of dissolution (Table 5.2). The source again was simulated by setting a constant concentration of 110 mg/L at the top of the clay layer. After the first 10 years, the source was assumed to be remediated, and the constant concentration boundary condition was removed.

The DNAPL saturation was again set to 6.62×10^{-5} at times 0 and 10 years. However, in this series of simulations, a submodel to simulate DNAPL dissolution kinetics was incorporated into the RT3D code based on the kinetic dissolution model presented in Christ et al. (2006). Since RT3D tracks NAPL saturation, rather than mass, the first-order mass transfer coefficient was related to NAPL saturation as follows:

$$k_{eff} = K_0' \left(\frac{M(t)}{M_0}\right)^{\beta} = K_0' \left(\frac{V\rho_{NAPL}S_{NAPL})}{V\rho_{NAPL}S_0)}\right)^{\beta} \tag{5.3}$$

where V is the volume of DNAPL, and S_0 is the initial saturation of DNAPL. Rewriting Eqn. 5.3 yields:

$$k_{eff} = K_0' \left(\frac{S_{NAPL}}{S_0}\right)^{\beta} = \frac{K_0'}{S_0{}^{\beta}} (S_{NAPL})^{\beta} \tag{5.4}$$

Alternatively, Eqn. 5.4 can be rewritten as:

$$k_{eff} = K_0' \left(\frac{S_{NAPL}}{S_0}\right)^{\beta} = k_{dis}(S_{NAPL})^{\beta} \tag{5.5}$$

where the dissolution rate parameter, $k_{dis} = \frac{K_0'}{S_0^{\beta}}$. For the values of β and K_0' used by Christ et al. (2006) to simulate dissolution at the Bachman Site, 8.5×10^{-1} and 8.2×10^{-3} day^{-1}, respectively, and an initial DNAPL saturation in the cracks of 0.9, the resulting value of k_{dis} is 8.97×10^{-3} day^{-1}. Coupling Eqn. 5.5 with Eqn. 5.1 allows the rate of mass dissolution to be calculated. This model was used for similar analyses as those for the constant rate of dissolution: to simulate breakthrough curves 50 m down gradient of the source and to quantify DNAPL mass and dissolved mass in the clay layer as a function of time. Sensitivity analyses were performed for two parameters that describe the dissolution rate: β and k_{dis}. These parameters were varied as shown in Table 5.3.

Table 5.3. Values for Mass Dissolution Rate Parameters

Parameter	Lower Value	Baseline Value	Upper Value
β [−]	8.5×10^{-5}	8.5×10^{-3}	8.5×10^{-1}
k_{dis} [day^{-1}]	8.97×10^{-3}	8.97×10^{-1}	89.7

5.3.   Results and Discussion

5.3.1.   Constant Rate of DNAPL Dissolution

Figure 5.5 shows breakthrough curves for the three scenarios outlined in Section 5.2.1 for the total simulation period of 50 years at an observation point 50 m down gradient at the clay-sand interface, with the MCL of TCE of 5 µg/L shown for comparison. These curves show that the concentration rises quickly when the source is present. When the source is removed, the concentration decreases rapidly, with back diffusion out of the clay responsible for the extended tailing. At this observation point, the concentration remains above the MCL for over forty years due to back diffusion. Similar modeling results have been obtained for back diffusion from competent clay (Chapman and Parker 2005). This figure also shows the impact of cracks. If the clay cracks contain DNAPL, the time that it takes for concentrations to drop below the MCL increases by a decade (Figure 5.5.b).

The mass storage of TCE in the clay layer was quantified at three points in time: at the start of the simulation (0 years), immediately following source removal (10 years), and at the end of the simulation (50 years). Table 5.4 shows the calculated TCE masses in the entire 100 m x 70 m x 6 m clay layer at these times for the three scenarios. The dissolved TCE mass at both 10 and 50 years is somewhat larger in Scenario 3 than in Scenarios 1 and 2 due to the dissolution of the DNAPL and the subsequent diffusion into the clay. While the difference in dissolved mass is not particularly large, it may explain the more extensive tailing seen for Scenario 3 in Figure 5.5.b. A key observation is that only a relatively small fraction of mass is removed from the clay layer over a 50-year period for all three scenarios; in fact, in Scenario 3, the fraction is only 1.1% (Table 5.4). Thus, although the dissolved down gradient concentration may be low, the DNAPL mass remaining in the subsurface is relatively large. These observations are consistent with the results presented in Parker et al. (1994) who showed that for the same parameters as those used in the current study, DNAPL would be present in the cracks for approximately 500 years.
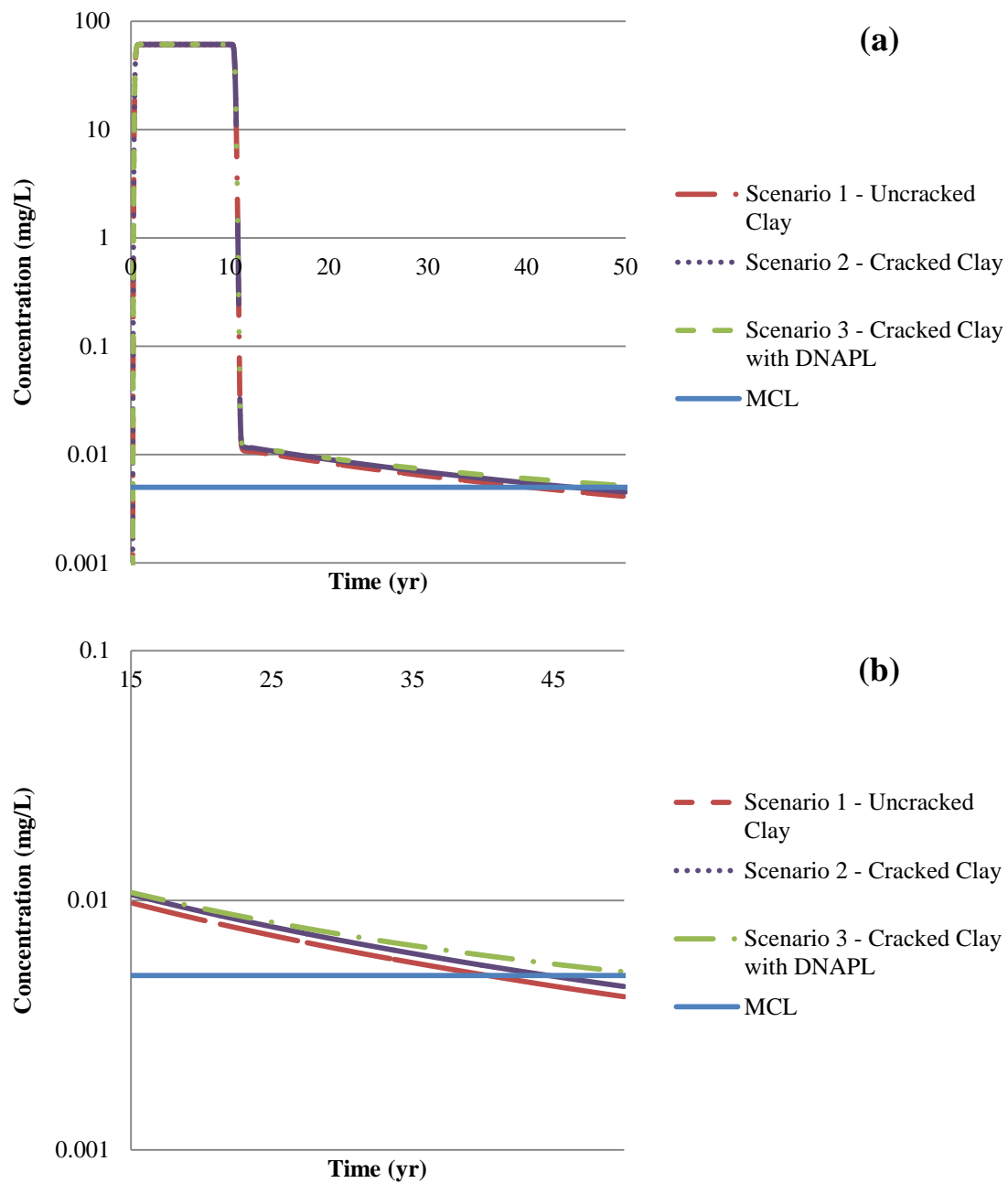
Figure 5.5. Simulated breakthrough curves for the three scenarios 50 m down-gradient of the source at the interface between the upper sand and clay layers for (a) 0-50 years, (b) 15-50 years, assuming a constant rate of dissolution.

Table 5.4. Mass of TCE in Clay Layer for Three Scenarios Assuming a Constant Rate of Dissolution

Time	Scenario 1			Scenario 2			Scenario 3[§]		
	0 yrs	10 yrs	50 yrs	0 yrs	10 yrs	50 yrs	0 yrs	10 yrs	50 yrs
Dissolved TCE (kg)	0.0	8.19	6.23	0.0	8.29	6.36	0.0	8.38	6.89
DNAPL TCE (kg)	0.0	0.0	0.0	0.0	0.0	0.0	36.1	36.1	35.7
Total TCE (kg)	0.0	8.2	6.2	0.0	8.3	6.4	36.1	44.4	42.6

[§]In Scenario 3, the mass of DNAPL in the cracks was set at the beginning of the simulation (t = 0 yrs) and reset to the same value at t = 10 yrs when the source was removed.

A sensitivity analysis was performed to assess the impact of the mass transfer rate coefficient k_{eff} and the vertical hydraulic conductivity K_v on the dissolved plume breakthrough behavior and mass storage in the low permeability layer, using Scenario 3 as the base case. Figure 5.6 shows the breakthrough curves for this analysis and Table 5.5 summarizes the quantity of mass stored in the clay layer. k_{eff} was varied by two orders of magnitude above and below its baseline value in the sensitivity analysis. When k_{eff} was increased, there was a large increase in tailing, coupled with a second concentration peak (Figures 5.6.a and 5.6.b). The second peak can be attributed to the rapid dissolution of the DNAPL. The observed rebound is similar to concentrations observed down gradient of a TCE and PCE source area that was treated using *in situ* chemical oxidation (Mundle et al., 2007). Once the source was removed, a large difference between the concentrations in the low permeability layer and in the clean sand layer developed, resulting in rapid contaminant transport into the sand layer. Figure 5.6.b shows that, due to the high value of the mass transfer coefficient, down gradient concentrations remain above the MCL for centuries. This result is of particular interest, as Table 5.5 shows that when the mass transfer coefficient is high, over 99% of the DNAPL (as a separate liquid phase) is no longer present in the clay layer after only 50 years. However, the results in Table 5.5 also indicate that, after 50 years, much of the contaminant mass still remains in the clay layer, but as a solute. Thus, with a high dissolution rate, the DNAPL in the clay layer dissolves and is transported deeper into the clay matrix as a solute. It is the back diffusion of this dissolved mass that results in down gradient concentrations exceeding the MCL for over 800 years. On the other hand, Figure 5.6.a and Table 5.5 indicate that decreasing k_{eff} by two orders of magnitude from its baseline value had little effect on either the down gradient concentration or the mass distribution in the clay layer. This result suggests that the value used for k_{eff} in the baseline scenario represents a low rate of DNAPL mass dissolution in comparison to the mass transfer rates of other processes (e.g., advection). Furthermore, this analysis suggests that the diffusional process within (not just into or out of) the clay layer is of significance. Since this sensitivity analysis showed substantive differences in the outcome with increased values of k_{eff}, this parameter merited additional investigation.
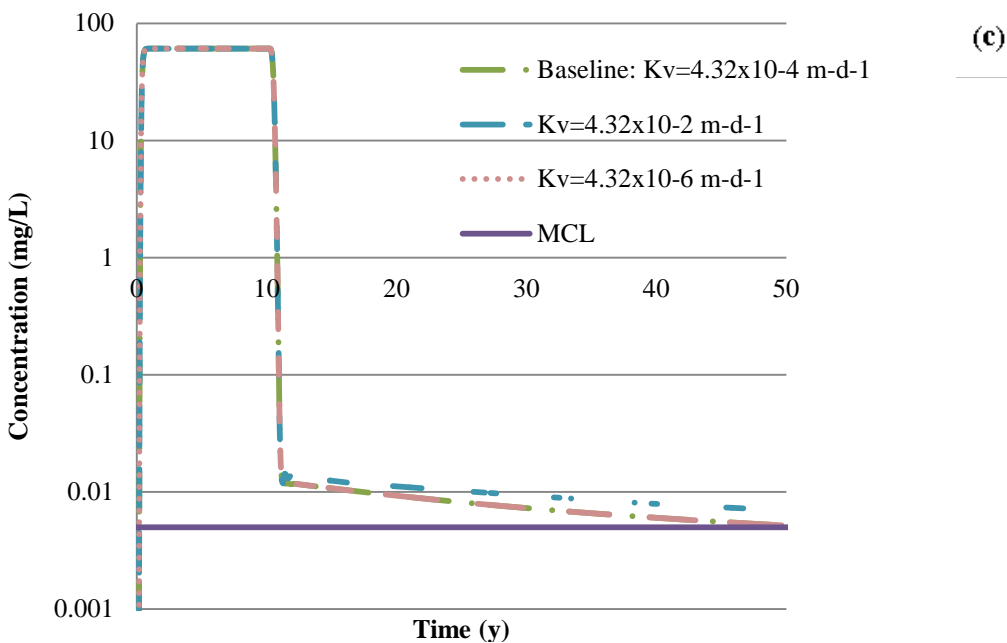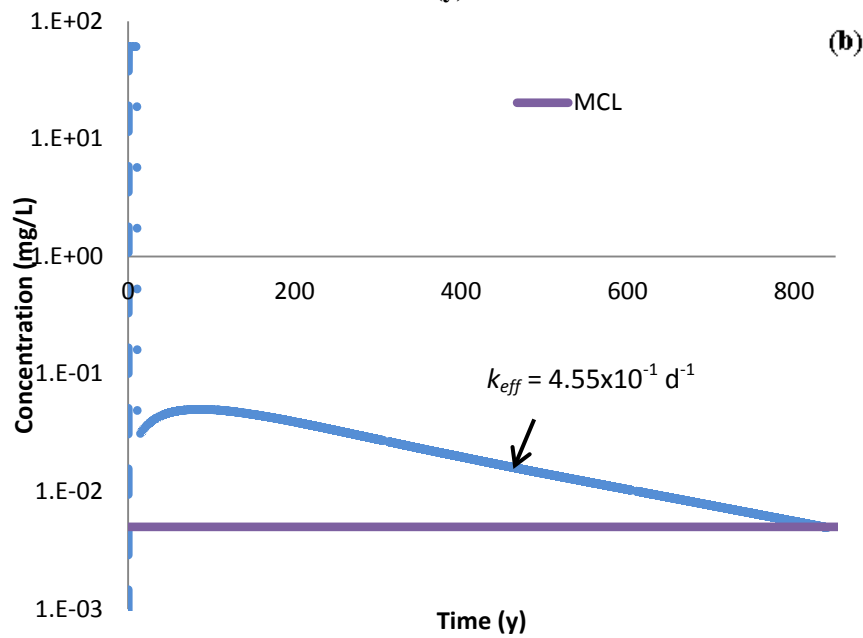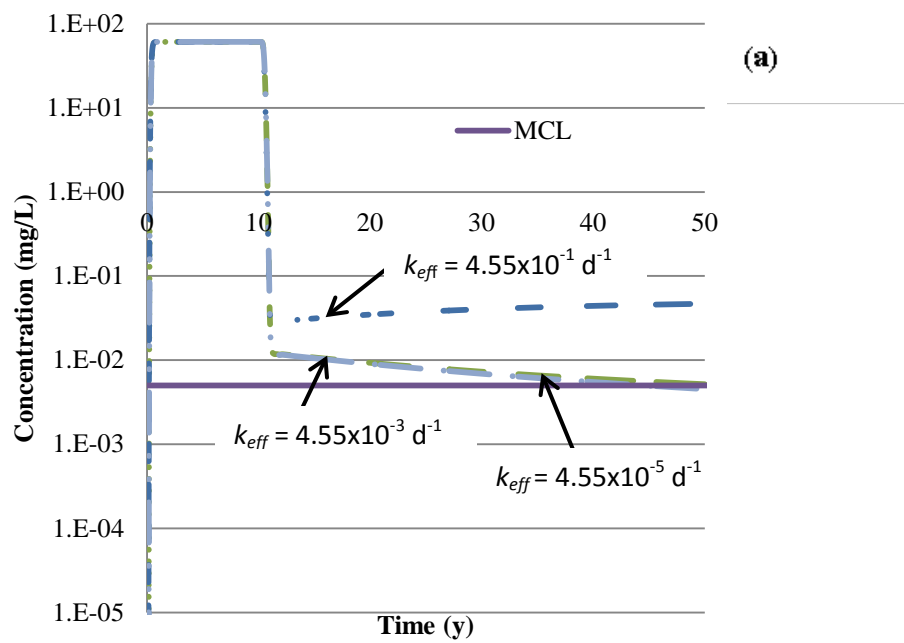
Figure 5.6. Simulated breakthrough curves 50 m down-gradient of the source at the interface between the upper sand and clay layers for Scenario 3 showing the effect of (a) varying the DNAPL mass transfer coefficient (k_{eff}), (b) a high mass transfer coefficient (k_{eff}) on long-term concentrations, and (c) varying the vertical hydraulic conductivity (K_v).

Table 5.5. Mass of TCE in Clay Layer as a Function of (a) Mass Transfer Rate Coefficient and (b) Vertical Hydraulic Conductivity

(a) k_{eff} (d^{-1})	4.55 x 10^{-5}			4.55 x 10^{-3} (baseline)			4.55 x 10^{-1}		
Time	0 yrs	10 yrs	50 yrs	0 yrs	10 yrs	50 yrs	0 yrs	10 yrs	50 yrs
Dissolved TCE (kg)	0.0	8.3	6.5	0.0	8.38	6.89	0.0	15.6	29.4
DNAPL TCE (kg)	36.1	36.1	36.1	36.1	36.1	35.7	36.1	36.1	0.1
Total TCE (kg)	36.1	44.3	42.6	36.1	44.4	42.6	36.1	44.3	29.5
(b) K_v (m·d^{-1})	4.32 x 10^{-6}			4.52 x 10^{-4} (baseline)			4.32 x 10^{-2}		
Time	0 yrs	10 yrs	50 yrs	0 yrs	10 yrs	50 yrs	0 yrs	10 yrs	50 yrs
Dissolved TCE (kg)	0.0	8.2	6.7	0.0	8.4	6.9	0.0	8.6	7.1
DNAPL TCE (kg)	36.1	36.1	35.8	36.1	36.1	35.7	36.1	36.1	35.8
Total TCE (kg)	36.1	44.3	42.5	36.1	44.5	42.6	36.1	44.7	42.9

In this research, the effect of cracking in the clay layer on vertical advective transport was modeled as an increase in the vertical hydraulic conductivity. When the vertical conductivity increased by two orders of magnitude, tailing also increased (Figure 5.6.c). Table 5.5 shows that the dissolved contaminant mass within the clay layer was somewhat greater with increases in vertical hydraulic conductivity. These observations stem from the fact that the increased conductivity allowed more contaminant to be transported by advection into the clay layer from the DNAPL pool. However, the impact of this parameter on tailing and mass storage was considerably less than the impact of the dissolution rate.

5.3.2. Variable Rate of DNAPL Dissolution

Since the time that the down gradient concentrations remained above the MCL depended significantly on the rate of DNAPL dissolution, this process was explored in more detail. In this study, the rate of DNAPL dissolution was described by Eqns. 5.1 and 5.5. Thus, the parameters β and k_{dis} determined the rate of dissolution. The concentrations over a 50-year period at an observation point 50-m down gradient in the sand were simulated for three values of β: 8.5 x 10^{-1} (based on the work of Christ et al. (2006) at the Bachman Road site), and then two and four orders of magnitude lower (Table 5.3).

The results of the simulations in which the parameter β was varied are shown in Figure 5.7. In all cases, the concentrations increased rather quickly and then rapidly decreased after the removal of the source, followed by tailing caused by back diffusion, similar to the behavior shown in Figure 5.5 for the constant rate of mass dissolution. The concentration profile generated with the highest value of β showed a longer persistence above the MCL. As β increased, the dissolution rate over time decreased, leading to more DNAPL mass remaining in the low permeability zone and more tailing. Table 5.6 shows the results of the computations of

the mass of TCE in the clay layer. As the value of β increased, the mass of TCE remaining as DNAPL increased and the mass of dissolved TCE decreased. In fact, at $\beta = 8.5$ x 10^{-5}, all of the DNAPL mass was predicted to be dissolved in 50 years. This result is in contrast to the prediction of more than half of the TCE mass remaining as DNAPL after 50 years at $\beta = 8.5$ x 10^{-1}. Thus, as β increased, the dissolution rate decreased over time, reducing the quantity of dissolved TCE and leaving more TCE as a separate phase liquid. Table 5.7 shows "half-lives," defined here as the time when the DNAPL is reduced to 50% of its mass at 10 years, the time of source removal. The DNAPL mass for $\beta = 8.5$ x 10^{-1} was reduced to roughly 50% 52 years later. In contrast, the DNAPL mass for $\beta = 8.5$ x 10^{-5} was reduced to 50% of the initial mass only two years later. Thus, the rate at which the DNAPL mass dissolves is critical to determining the remediation time frame.

The parameter k_{dis} also determines the rate of dissolution (Eqn. 5.5). To investigate its impact, simulations were performed varying this parameter over four orders of magnitude, from 8.97 x 10^{-3} to 8.97 x 10^{-1} day^{-1}. The breakthrough curves at the observation point in the sand 50 meters down gradient are shown in Figure 5.8, and the simulated masses of TCE in the clay layer are given in Table 5.6.
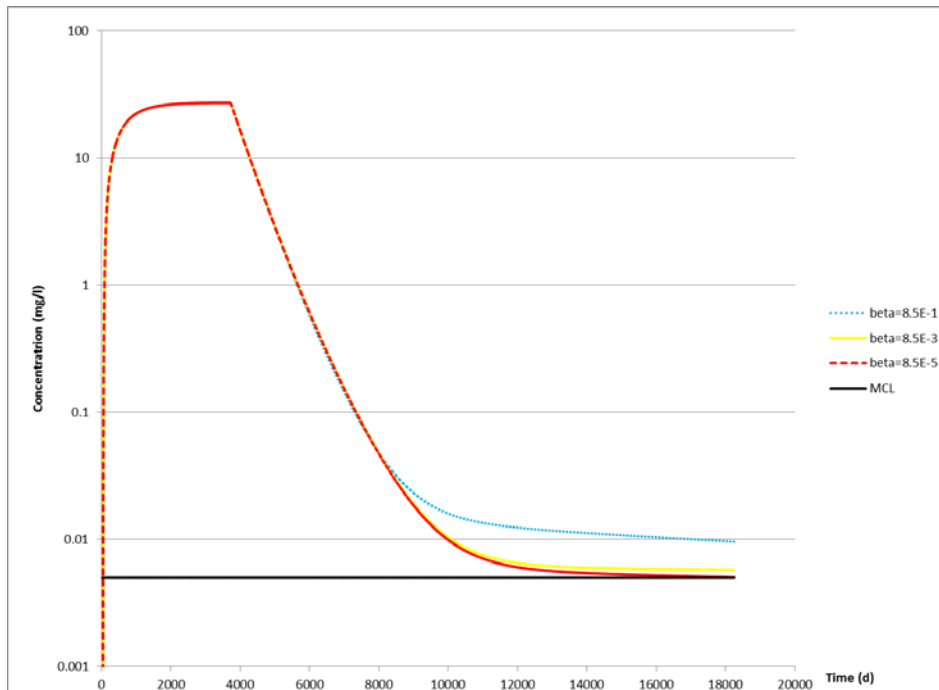
Figure 5.7. Breakthrough curves 50 m down-gradient of the source in the upper sand layer for various values of β, the mass transfer rate exponent (Eqn. 5.5).

Table 5.6. Mass of TCE in Clay Layer as a Function of Mass Dissolution Rate Parameters (Eqn. 5.5)

β (-)	8.5×10^{-5}			8.5×10^{-3}			8.5×10^{-1}		
Time	**0 yrs**	**10 yrs**	**50 yrs**	**0 yrs**	**10 yrs**	**50 yrs**	**0 yrs**	**10 yrs**	**50 yrs**
Dissolved TCE (kg)	0	20.4	1.65	0	20.3	1.35	0	20.1	1.30
DNAPL TCE (kg)	6.18	6.18	0	6.18	6.18	2.74	6.18	6.18	3.41
Total TCE (kg)	6.18	26.6	1.65	6.18	28.9	4.75	6.18	26.3	4.24

For all simulations, $k_{dis} = 8.97 \times 10^{-3}$ day^{-1}

k_{dis} (days^{-1})	8.97×10^{-5}			8.97×10^{-3}			8.97×10^{-1}		
Time	**0 yrs**	**10 yrs**	**50 yrs**	**0 yrs**	**10 yrs**	**50 yrs**	**0 yrs**	**10 yrs**	**50 yrs**
Dissolved TCE (kg)	0	22.0	1.28	0	20.1	1.30	0	22.7	2.3
DNAPL TCE (kg)	6.18	6.18	6.18	6.18	6.18	3.41	6.18	6.18	0
Total TCE (kg)	6.18	28.2	7.46	6.18	26.3	4.24	6.18	28.9	2.3

For all simulations, $\beta = 8.50 \times 10^{-1}$
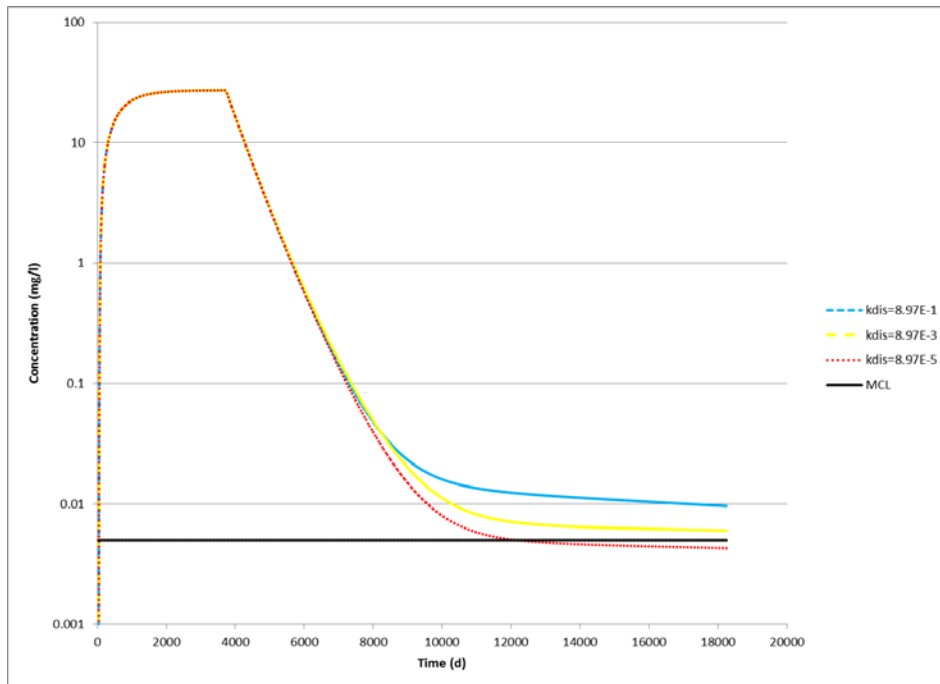
Figure 5.8. Breakthrough curves 50 m down-gradient of the source in the upper sand layer for various values of k_{dis}, the dissolution rate parameter (Eqn. 5.5).

Table 5.7. DNAPL Dissolution Half Lives

β [-][§]	Time (yrs)	$k_{dis}\ [days^{-1}]$[†]	Time (yrs)
8.50 x 10^{-5}	2	8.97 x 10^{-5}	90+
8.50 x 10^{-3}	21	8.97 x 10^{-3}	52
8.50 x 10^{-1}	52	8.97 x 10^{-1}	1

[§]k_{dis} = 8.97 x 10^{-3} day^{-1} for the simulations in which β was varied.
[†]β = 8.50 x 10^{-1} for all the simulations where k_{dis} was varied.

Figure 5.7 shows that as k_{dis}, increases, there is more extensive tailing, similar to the situation with increasing values of β (Figure 5.6). However, in examining the data in Tables 5.6 and 5.7, the difference in the effect of the two parameters becomes clearer. At low values of k_{dis}, there is essentially no dissolution, whereas at low values of β, all the DNAPL has dissolved within 50 years. At high values of k_{dis}, all the DNAPL has dissolved at 50 years, whereas at high values of β, the majority of TCE is still in the form of a separate organic liquid phase. Given the rapid dissolution of the DNAPL at high values of k_{dis}, the more extensive tailing shown in Figure 5.7 may be unanticipated. However, at longer times (about 95 years), the predicted concentrations do drop below those for the other values of k_{dis}. Table 5.7 shows that as β increased, the half-life increased, but as k_{dis} increased, the half-life decreased. After 90 years for the very low k_{dis} value of 8.97x 10^{-5} days^{-1}, only 10% of the initial DNAPL mass had dissolved, so it can be speculated that it would take several more decades for the DNAPL to be reduced by 50%, despite the low value of β.

5.4.   Conclusions

The simulations presented in this chapter show that cracks, either naturally present or induced by contact with DNAPL, have a substantive effect on down gradient concentrations. The increase in vertical hydraulic conductivity that may result from cracking did not impact the down gradient concentrations significantly; rather, the storage of the DNAPL in the cracks and the rate of dissolution were key. In particular, if DNAPL is present in the cracks, it is the process of DNAPL dissolution, which drives the contaminant farther into the clay matrix, is a key mechanism that impacts down gradient concentration rebound and tailing. Previous research has suggested that the dissolution rate of DNAPLs is time-dependent, with the rate decreasing as the DNAPL saturation decreases (Christ et al., 2006). The analysis of mass distribution and breakthrough curves presented here showed that when the dissolution rate depended on DNAPL saturation, the mass of DNAPL that persisted in the low permeability zone was greater. The persistence of the DNAPL mass resulted in a more persistent plume in an overlying high permeability zone, with a higher dissolved concentration. The assumption of a saturation-dependent dissolution rate is critical; if the dissolution rate was taken as a constant, the half-life of the DNAPL source decreased by several decades.

These results indicate that conventional remediation, even if effective in removing contaminant from high permeability areas, will fail to decrease contaminant concentrations below the MCL for decades, suggesting lengthy and costly cleanups for contaminated sites where the remedial objective is meeting the MCL. The EPA has been considering adopting a "…flexible approach to setting remedial objectives" (Inside EPA.com, 2013). One approach that has been proposed is to base site management decisions on flux or mass discharge measurements, rather than concentration measurements (ITRC, 2010). Given the fact that even small cracks in clay layers underlying an aquifer can result in prolonged tailing, this approach may be advisable. The model developed in this study could readily be adapted to simulate mass discharge and flux data for site management decisions.

6.0   Conclusions and Implications for Future Research/Implementation

6.1.   Conclusions

Chlorinated solvents are often disposed of in such a manner that they form pools on subsurface clay layers. There they slowly migrate into the clay layers, accumulating therein over time. Due to the low permeability of these layers, it is assumed that the migration occurs by dissolution and diffusion. However, field evidence suggests that more solvent may be stored in such layers than can be accounted for through these processes. Consistent with the SERDP Statement of Need of improving the understanding of how low permeability storage may occur, the overall objective of the research was to examine the validity of diffusion as the dominant mechanism of transport and to examine the possibility that cracks in low permeability clay layers contribute to the accumulation of contamination therein and the long remediation times associated with these sites.

Steady-state diffusion measurements were made using the time-lag method for a suite of systems containing silt and clay. The effective diffusion coefficient of TCE measured here was 1.30×10^{-6} cm^2/sec for an unconfined saturated silt-clay mixture (75% silt and 25% Na-montmorillonite clay) and 0.7×10^{-6} cm^2/sec for a confined saturated silt-clay mixture. These values are in agreement with those reported by Grathwohl (1998) and others (Khandelwal et al, 1998; Itakura et al., 2003). The diffusion coefficient for the expanded silt-clay sample contacted with field DNAPL waste was 1.14×10^{-8} cm^2/sec, which is considerably lower than previously reported values. The diffusion coefficients for TCE measured here are almost four times lower than the ones calculated from Parker et al. (1994)'s data, and five times lower than the observed diffusion coefficients reported in Johnson et al. (1989) of 3.25×10^{-6} cm^2/sec. As the diffusion coefficient of TCE observed in the field were reported as 1.7 times higher than the diffusion coefficient of TCE estimated based on the relative diffusivity of chloride (Johnson et al., 1989), the fact that the measured diffusion coefficients are all lower than the estimates magnifies the reported discrepancy between the field observed values and what can be attributed to diffusion.

In studies looking at the mass accumulation in aquitards, the effective diffusion coefficient is often estimated because there are very few measured values. The results reported here for TCE and iodide suggest that such methods grossly overestimate the diffusion coefficient, especially in soils with a clay content higher than 25%.   Similarly, it was found that the relative diffusivities of TCE based on field studies provide an overestimate of the values measured here.   Two novel estimation methods were explored: a log-linear relationship developed by regression using experimental data for the diffusion of tritiated water in clay soils and a theoretical relation by Bourg et al. (2006) developed for clay soils considering clay variables such as the fraction of interlayer space.   Both of these estimation methods performed better than conventional methods in estimating the relative diffusivities of TCE and iodide.   Thus, these methodologies are recommended for adoption for estimating the diffusion coefficient in low permeability soils, rather than those conventionally used.

To investigate the impact of DNAPL contact, the basal spacing of clays in contact with pure and waste DNAPLs was measured. The basal spacing of air-dry Na-montmorillonite clay contacted with chlorinated solvents was similar to the basal spacing in contact with air, and was consistent with the basal spacing of such materials in contact with low-miscibility nonchlorinated solvents. Contact of water-saturated clays with pure chlorinated solvents did not lead to basal spacing changes, even after extended contact (up to 319 days). Similarly, contact of water-saturated Ca-montmorillonite with DNAPL wastes did not result in basal spacing changes. However, contact of water-saturated Na-smectites with DNAPL wastes led to basal spacing changes and significant cracking over the time frame of weeks to months, with crack apertures as large as 1 mm and greater. This finding suggests that passive contact with chlorinated DNAPLs over the time frame associated with hazardous waste sites may lead to basal spacing changes in the sodium smectite clay minerals in the low permeability layers at these sites. The shrinkage of the basal spacing may result in cracking, allowing enhanced transport into the clay layers. Calculations showed that even minimal cracking could result in enough mass storage to explain field observations.

The basal spacing measurements showed that contact with neat PCE or TCE did not cause a collapse of the clay structure as did PCE-based or TCE-based field wastes. Screening experiments were performed to determine the critical components of the field wastes that result in crack formation when in contact with Na-smectitic clay. These experiments showed that the minimum mixture required to match the behavior of DNAPL wastes in cracking clay was comprised of an anionic and nonionic surfactant, specifically AOT and TritonX-100, dissolved in a chlorinated solvent, PCE. Since all three components had to be present for cracking to occur and none caused cracking individually, possible synergistic interactions were investigated. Sorption measurements suggested that the primary role of the chlorinated solvent is to increase the sorption of the surfactants, particularly AOT which, generally, shows minimal sorption on clays due to the repulsion between the negatively-charged clay surface and the negative charge of the surfactant. FTIR data suggested a partial displacement of water molecules as a result of contact with the PCE, anionic and nonionic surfactant mixture. When this information was considered in concert with the sorption data, it was concluded that the surfactants sorbed on the water-saturated clay, displacing some water molecules. Because of its length, TritonX-100 is hypothesized to lie horizontally relative to the interlayer surface; AOT sorbs to the TritonX-100 and lies external to the clay particle, due to the size and charge of its head. Interlayer water molecules move to solvate the micellar aggregates present at the margins of the interlayer space, thus causing an additional displacement of water. This dehydration of the interlayer space is accompanied by cracking, analogous to the situation observed by Burst (1965) in the presence of increased salinity. Thus, the cracking mechanism appears to be one of syneresis, driven primarily by the solvation of water in the sorbed surfactant aggregates.

Simulations were performed to evaluate the impact of cracks in low permeability layers. The results of these simulations showed that the presence of cracks, either naturally present or induced by contact with DNAPL, have a substantive effect on down gradient concentrations.

The increase in vertical hydraulic conductivity that may result from cracking did not impact the down gradient concentrations significantly; rather the storage of the DNAPL in the cracks and the rate of dissolution were critical. In particular, if DNAPL is present in the cracks, the process of DNAPL dissolution, which drives the contaminant farther into the clay matrix, is a key mechanism that impacts down gradient concentration rebound and tailing. These results suggest that conventional remediation, even if effective in removing contaminant from high permeability areas, will fail to decrease contaminant concentrations below the MCL for decades, suggesting lengthy and costly cleanups for contaminated sites where the remedial objective is meeting the MCL. The EPA has been considering adopting a "…flexible approach to setting remedial objectives" (Inside EPA.com, 2013). One approach that has been proposed is to base site management decisions on flux or mass discharge measurements, rather than concentration measurements (ITRC, 2010). Given the fact that even small cracks in clay layers underlying an aquifer can result in prolonged tailing, this approach may be advisable.

6.2. Implications for Future Research/Implementation

This study revealed that Na-smectite clays undergo lattice structure contraction and cracking due to contact with DNAPL waste. This modification of the structure may lead to high accumulations of the contaminants in clay layers, which conventionally have been viewed as barriers to contaminant movement.

This study demonstrated that the composition of waste plays a very important role as the field wastes caused cracking, but pure PCE and TCE did not. The field wastes examined here were a degreasing TCE-based waste from an Air Force Base (Hill Air Force Base, Ogden, UT) and a PCE-based waste from a dry cleaner (Ann Arbor, MI). It was demonstrated that a synthetic waste containing PCE, an anionic surfactant, AOT, and a nonionic surfactant, TritonX-100, could cause basal spacing reductions and cracking similar to the real wastes. Although the predominant component in a chlorinated DNAPL may be PCE or TCE, DNAPLs contain a range of solutes, added to enhance their performance (Jackson and Dwarakanath, 1999; Linn and Stupak, 2009), obtained through their use (Jackson and Dwarakanath, 1999) or acquired during their residence in the subsurface (Harrold et al., 2003). In fact, Jackson and Dwarakanath (1999) make the point that any chlorinated solvent in the subsurface will contain solutes that may significantly influence its behavior. Based on reports of the composition for DNAPLs at other DoD/DoE sites (U.S. DoE Savannah River Site [Dou et al., 2008]; Kelly Air Force Base, San Antonio, TX, and U.S. Marine Corp. Base, Camp Lejeune, NC [Dwarakanath et al., 2002]), it is anticipated that many DNAPLs contain surface-active constituents that may have a similar effect on clay structure. However, further research is necessary to generalize this research to other waste compositions and to understand the possible synergistic activity among chemicals in various types of waste and the resultant impact on low permeability layers.

This study examined the structure of pure smectites contacted with DNAPL wastes in a laboratory setting. Although the wastes were taken from the field, the clays were commercially purchased. It would be invaluable to assess whether the structural modifications observed in the

lab occur in the field. This verification might involve the isolation of clay from real waste sites and an analysis of the clay structure. Bentonite, which is primarily Na-montmorillonite, is frequently used in the construction of impermeable barriers at contaminated sites to prevent further migration of the contaminants. At some sites where bentonite slurry walls have been constructed around DNAPL pools, there is anecdotal evidence of leakage. It would be valuable to assess whether there is evidence of clay structure alteration due to contact with DNAPL waste at such sites.

This study focused on the changes in the structure of Na-montmorillonite clays since these clays are an important component of not only low permeability geologic strata but also containment structures such as landfill liners and slurry walls. However, an aquitard contains clay minerals other than just Na-smectites. There is some evidence that the structure of nonexpansive clay minerals, such as kaolinite, may also be affected by contact with DNAPL waste (Demond, 2012). The colloidal structure of nonexpansive clay minerals may be influenced by contact with waste, leading to greater flocculation. A more flocculated state can also lead to cracking and enhanced non-diffusive transport. Thus, additional research addressing the impact of DNAPL contact on clays like kaolinite is necessary to document the structural changes and to understand the mechanism by which these changes may occur.

This research found that, frequently, modeling studies use diffusion coefficients that are significantly in error for soils which contain greater than 25% clay. This work recommends using a log-linear relationship developed by fitting experimental data for the diffusion of tritiated water in clay soils (detailed in Chapter 2) or a theoretical relation by Bourg et al. (2006) developed for clay soils considering clay variables such as the fraction of interlayer space to estimate diffusion coefficients. The overly large diffusion coefficients used in some studies may be masking the accumulation of DNAPL in low permeability layers through the process of penetration into cracks, either naturally occurring or caused by contact with DNAPL waste. This study used DoD's Ground Water Modeling System (GMS) and developed a new sub-routine to account for the process of DNAPL dissolution from cracks. The results showed that if DNAPL is present in the cracks, the process of DNAPL dissolution, which drives the contaminant farther into the clay matrix, is a key mechanism that impacts down gradient concentration rebound and tailing. Failure to account for these processes may provide overly optimistic estimates of remediation time frames.

7.0   Literature Cited

Abdul, A. S., Gibson, T. L., and Rai, D. N. (1990). Laboratory studies of the flow of some organic solvents and their aqueous solutions through bentonite and kaolin clays. *Groundwater*, *28*(4), 524–533.

Abriola, L. M., Drummond, C. D., Hahn, E. J., Hayes, K. F., Kibbey, T. C. G., Lemke, L. D., Rathfelder, K. M. (2005). Pilot-scale demonstration of surfactant-enhanced PCE solubilization at the Bachman road site. 1. Site characterization and test design. *Environmental Science and Technology, 39*, 1778-1790.

Amarasinghe, P. M., Katti, K. S., and Katti, D. R. (2009). Nature of organic fluid-montmorillonite interactions:An FTIR spectroscopic study. *Journal of Colloid and Interface Science*, *337*(1), 97–105. doi:10.1016/j.jcis.2009.05.011

Anderson, D. C., Brown, K. W., and Thomas, J. C. (1985). Conductivity of compacted clay soils to water and organic liquids. *Waste Management and Research*, *3*(1), 339–349. doi:10.1177/0734242X8500300142

Archie, G. E. (1942). The electrical resistivity log as an aid in determining some reservoir characteristics. *J. Petroleum Technology*, *5*, 54–62.

ASTM International (2007a.) Standard Test Method for Particle-Size Analysis of Soils, ASTM D422-63(2007a)e2, ASTM International, West Conshohocken, PA.

ASTM International (2007b). Standard Test Method for Measurement of Hydraulic Conductivity of Porous Material Using a Rigid-Wall, Compaction-Mold Permeameter, ASTM D5856-95(2007b), ASTM International, West Conshohocken, PA.

Ayral D., and Demond, A.H. (2014). Estimation of Diffusion Coefficients for Organic Solutes of Environmental Concern in Saturated Clay-Silt Mixtures in *Clay and Clay Minerals: Geological Origin, Mechanical Properties and Industrial Application*s (L. Wesley, ed., Nova Science Publishers, Hauppauge, NY, pp. 45-66).

Ayral, D., Otero, M., Goltz, M. N., and Demond, A. H. (2014). Impact of DNAPL contact on the structure of smectitic clay materials. *Chemosphere*, *95*, 181-186.

Ball, W. P., Liu, C., Xia, G., and Young, D. F. (1997). A diffusion-based interpretation of tetrachloroethene and trichloroethene concentration profiles in a groundwater aquitard. *Water Resources Research*, *33*(12), 2741–2757. doi:10.1029/97WR02135.

Barone, F. S., Rowe, R. K., and Quigley, R. M. (1992). A laboratory estimation of diffusion and adsorption coefficients for several volatile organics in a natural clayey soil. *Journal of Contaminant Hydrology*, *10*(3), 225–250. doi:10.1016/0169-7722(92)90062-J

Barrer, R. M., and Rideal, E. K. (1939). Permeation, diffusion and solution of gases in organic polymers. *Transactions of the Faraday Society*, *35*, 628–643. doi:10.1039/tf9393500628.

Barshad, I. (1952). Factors affecting the interlayer expansion of vermiculite and montmorillonite with organic substances. *Soil Science Society of America Journal*, *16*(2), 176–182.

Bear, J. (1972). *Dynamics of Fluids in Porous Media*, Elsevier, New York.

Berkheiser, V., and Mortland M. M. (1975). Variability in exchange ion position in smectite: Dependence on interlayer solvent. *Clays and Clay Minerals*, *23*(5), 404–410.

Bourg, I. C., Sposito, G., and Bourg, A. C. M. (2006). Tracer diffusion in compacted, water-saturated bentonite. *Clays and Clay Minerals*, *54*(3), 363–374. doi:10.1346/CCMN.2006.0540307.

Boving, T. B., and Grathwohl, P. (2001). Tracer diffusion coefficients in sedimentary rocks: correlation to porosity and hydraulic conductivity. *Journal of Contaminant Hydrology*, *53*(1-2), 85–100. doi:10.1016/S0169-7722(01)00138-3.

Brindley, G. W., Wiewiora, K., and Wiewiora, A. (1969). Intracrystalline swelling of montmorillonite in some water-organic mixtures: Clay-organic studies-17. *American Mineralogist*, *54*(11), 1635–1644.

Brown, G., and Brindley, G. (1980). *Crystal Structures of Clay Minerals and their X-Ray Identification,* Mineralogical Society, London (pp. 361–410).

Brown, K. W., and Thomas, J. C. (1984). Conductivity of three commercially available clays to petroleum products and organic solvents. *Hazardous Waste*, *1*(4), 545–553.

Brown, K. W., and Thomas, J. C (1987). A mechanism by which organic liquids increase the hydraulic conductivity of compacted clay materials. *Soil Science Society of America Journal*, *51*(6), 1451–1459.

Burst, J. F. (1965). Subaqueously formed shrinkage cracks in clay. *Journal of Sedimetnary Petrology*, *35*(2), 348-353.

Chapman, S. W., and Parker, B. L. (2005). Plume persistence due to aquitard back diffusion following dense nonaqueous phase liquid source removal or isolation. *Water Resources Research*, *41*(12). doi:10.1029/2005WR004224.

Chapman, S. W. and Parker, B. L. (2011). High Resolution Field Characterization and Numerical Modeling for Analysis of Contaminant Storage and Release from Lower Permeability Zones, SERDP/ESTCP Partners in Environmental Technology Technical Symposium and Workshop, November 29 - December 1, 2011, Washington D.C.

Cheng, L., Fenter, P., Nagy, K. L., and Schlegel, M. L. (2001). Molecular-scale density oscillations in water adjacent to a mica surface. *Physical Review Letters*, *87*(15), 156103.

Christ, J.A., Ramsburg, C. A., Pennell, K. D., and Abriola, L. M. (2006). Estimating mass discharge from dense nonaqueous phase liquid source zones using upscaled mass transfer coefficients: An evaluation using multiphase numerical simulations. *Water Resources Research, 42*, 1-13.

Clement, T. P., Sun, Y., Hooker, B. S., and Petersen, J. N. (1998). Modeling multispecies reactive transport in groundwater. *Groundwater Monitoring & Remediation*, Spring (1998), 79-92.

Clement, T. P., T.R. Gautam, K.K. Lee, M.J. Truex, G.B. Davis (2004). Modeling of DNAPL-Dissolution, Rate-Limited Sorption and Biodegradation Reactions in Groundwater Systems. *Bioremediation Journal, 8,* 47-64.

Crank, J. (1975). *The Mathematics of Diffusion*, 2nd ed, Oxford University Press, London.

Crooks, V. E., and Quigley, R. M. (1984). Saline leachate migration through clay: a comparative laboratory and field investigation." *Canadian Geotechnical Journal* 21 (1984): 349-362.

Cuypers, C., Pancras, T., Grotenhuis, T., and Rulkens, W. (2002). The estimation of PAH bioavailability in contaminated sediments using hydroxypropyl-b-cyclodextrin and TritonX-100 extraction techniques. *Chemosphere*, *46*, 1235–1245.

D'Astous, A. Y., Ruland, W. W., Bruce, J. R. G., Cherry, J. A., and Gillham, R. W. (1989). Fracture effects in the shallow groundwater zone in weathered Sarnia-area clay. *Canadian Geotechnical Journal*, *26*(1), 43–56.

Day, M. J. (1977). *Analysis of Movement and Hydrochemistry of Groundwater in the Fractured Clay and Till Deposits of the Winnipeg Area, Manitoba,* M.Sc. thesis, Univ. of Waterloo,Waterloo, Ontario, Canada.

Del Hoyo, C., Dorado, C., Rodríguez-Cruz, M. S., and Sánchez-Martín, M. J. (2008). Physico-chemical study of selected surfactant-clay mineral systems. *Journal of Thermal Analysis and Calorimetry*, *94*(1), 227–234. doi:10.1007/s10973-007-8934-6

Demond, A. H. (2012). I*mpact of Clay-DNAPL Interactions on Transport and Storage of Chlorinated Solvents in Low Permeability Zones*, SERDP Project ER-1737, Interim Report, SERDP, Alexandria, VA. 37pp.

Demond, A., and Lindner, A. (1993). Estimation of interfacial tension between organic liquids and water. *Environmental Science and Technology*, *27*(12), 2318–2331.

Deng, Y., Dixon, J. B., and White, G. N. (2003). Intercalation and surface modification of smectite by two non-ionic surfactants. *Clays and Clay Minerals*, *51*(2), 150–161. doi:10.1346/CCMN.2003.0510204

Domenico, P. A., and Schwartz, F. W. (1998). *Physical and Chemical Hydrogeology*, 2nd ed. Wiley, New York.

Donahue, R. B., Barbour, S. L., and Headley, J. V. (1999). Diffusion and adsorption of benzene in Regina clay. *Canadian Geotechnical Journal*, *36*(3), 430–442. doi:10.1139/t99-017

Dou, W., Omran, K., Grimberg, S. J., Denham, M., and Powers, S. E. (2008). Characterization of DNAPL from the U.S. DOE Savannah River Site. *Journal of Contaminant Hydrology*, *97*(1-2), 75–86. doi:10.1016/j.jconhyd.2008.01.002

Dwarakanath, V., Jackson, R. E., and Pope, G. A. (2002). Influence of wettability on the recovery of NAPLs from alluvium. *Environmental Science and Technology*, *36*(2), 227–231.

Earnest, G. S., Beasley Spencer, A., Smith, S. S., Heitbrink, W. H., Mickelsen, R. L., McGothlin, J. D., Ewers, L. M. (1997). *Control of Health and Safety Hazards in Commercial Drycleaners: Chemical Exposures, Fire Hazards, and Ergonomic Risk Factors*, NIOSH Publication No. 97-150, U.S. Department of Health and Human Services, Public Health Service, Centers for Disease Control and Prevention, National Institute for Occupational Safety and Health, Atlanta, GA.

Fendler, J. H. (1976). Interactions and reactions in reversed micellar systems. *Accounts of Chemical Research*, *9*, 153-161.

García-Gutiérrez, M., Cormenzana, J.L., Missana, T., and Mingarro, M. (2004). Diffusion coefficients and accessible porosity for HTO and ^{36}Cl in compacted FEBEX bentonite. *Applied Clay Science*, *26*(1-4), 65–73. doi:10.1016/j.clay.2003.09.012

Goodall, D., and Quigley, R. (1977). Pollutant migration from two sanitary landfill sites near Sarnia, Ontario. *Canadian Geotechnical Journal*, *14*(2), 223–236.

Grathwohl, P. (1998). *Diffusion in Natural Porous Media: Contaminant Transport, Sorption/Desorption and Dissolution Kinetics.* Kluwer Academic Publishing, Boston.

Greene-Kelly, R. (1954). Sorption of aromatic organic compounds by montmorillonite. Part 1. Orientation studies. *Transactions of the Faraday Society*, *51*, 412–424.

Griffin, R. A., Hughes, R. E., Follmer, L. R., Stohr, C. J., Morse, W. J., Johnson, T. M., Bartz, J.K., Steele, J. D., Cartwright, K., Killey, M. M. and DuMontelle, P. B. (1984). Migration of industrial chemicals and soil-waste interactions at Wilsonville, Illinois in *Land Disposal of Hazardous Waste, Tenth Annual Research Symposium*, Fort Mitchell, KY, 61–77.

Grisak, G.E., and Pickens, J. F. (1980). Solute transport through fractured media, 1. The effect of matrix diffusion. *Water Resources Research, 16*, 719-730.

Harrold, G., Gooddy, D. C., Reid, S., Lerner, D. N., and Leharne, S. A. (2003). Changes in interfacial tension of chlorinated solvents following flow through U.K. soils and shallow aquifer materials. *Environmental Science and Technology*, *37*(9), 1919-1925.

Hayduk, W., and Laudie, H. (1974). Prediction of diffusion coefficients for nonelectrolytes in dilute aqueous solutions. *AIChE Journal*, *20*(3), 611–615.

Hayduk, W., and Minhas, B. (1982). Correlations for prediction of molecular diffusivities in liquids. *The Canadian Journal of Chemical Engineering*, *60*(2), 295–299.

Headley, J. V., Boldt-Leppin, B. E., Haug, M. D., and Peng, J. (2001). Determination of diffusion and adsorption coefficients for volatile organics in an organophilic clay-sand-bentonite liner. *Canadian Geotechnical Journal, 38*(4), 809–817.

Hendry, M. (1982). Hydraulic conductivity of a glacial till in Alberta. *Ground Water*, *20*(2), 162–169.

Hinsby, K., McKay, L. D., Jørgensen, P., Lenczewski, M., and Gerba, C. P. (1996). Fracture aperture measurements and migration of solutes, viruses, and immiscible creosote in a column of clay-rich till. *Ground Water*, *34*(6), 1065–1075.

Hsu, H.-L. (2005). *Determination of Interfacial Tension and Contact Angle of Dense Non-Aqueous Phase Liquid Waste Mixtures*, Ph.D. dissertation, University of Michigan, Ann Arbor, MI, USA.

Hu, Z., He, G., Liu, Y., Dong, C., Wu, X., and Zhao, W. (2013). Effects of surfactant concentration on alkyl chain arrangements in dry and swollen organic montmorillonite. *Applied Clay Science*, *75-76*, 134–140. doi:10.1016/j.clay. 2013.03.004

Imhoff, P. T., Gleyzer, S. N., McBride, J. F., Vancho, L. A., Okuda, I., and Miller, C. T. (1995). Cosolvent-enhanced remediation of residual dense nonaqueous phase liquids: Experimental investigation. *Environmental Science and Technology*, 29:1966-1976.

InsideEPA.com. (2013). EPA seeks to ease groundwater cleanup policy following NAS report. I*nside EPA Public Content*, *34*(38), 1-3 [online]. [Accessed 23 September 2013].

Itakura, T., Airey, D. W., and Leo, C. J. (2003). The diffusion and sorption of volatile organic compounds through kaolinitic clayey soils. *Journal of Contaminant Hydrology*, *65*(3-4), 219–43. doi:10.1016/S0169-7722(03)00002-0

ITRC (Interstate Technology & Regulatory Council) (2010). Use and measurement of mass flux and mass discharge, MASSFLUX-1. Interstate Technology & Regulatory Council, Integrated DNAPL Site Strategy Team, Washington, D.C.

Jackson, R. E., and Dwarakanath, V. (1999). Chlorinated degreasing solvents: Physical-chemical properties affecting aquifer contamination and remediation. *Ground Water Monitoring and Remediation*, *19*(4), 102-110.

Johnson, R. L., Cherry, J. A., and Pankow, J. F. (1989). Diffusive contaminant transport in natural clay: A field example and implications for clay-lined waste disposal sites. *Environmental Science and Technology*, *23*(3), 340–349.

Johnston, C. T., Sposito, G., and Erickson, C. (1992). Vibrational probe studies of water interactions with montmorillonite. *Clays and Clay Minerals*, *40*(6), 722–730.

Keller, C. K., Kamp, G. V. D., and Cherry, J. A. (1986). Fracture permeability and groundwater flow in clayey till near Saskatoon, Saskatchewan. *Canadian Geotechnical Journal*, *23*(2), 229–240.

Khandelwal, A., Rabideau, A. J., and Shen, P. (1998). Analysis of diffusion and sorption of organic solutes in soil-bentonite barrier materials. *Environmental Science and Technology*, *32*(9), 1333–1339.

Kueper, B.H. and McWhorter, D.B. (1991). The behavior of dense, nonaqueous phase liquids in fractured clay and rock. *Ground Water, 29* (1991), 716-728.

Ladaa, T. I., Lee, C. M., Coates, J. T. and Falta, R. W. (2001). Cosolvent effects of alcohols on the Henry's Law constant and aqueous solubility of tetrachloroethylene (PCE). *Chemosphere, 44*(5), 1137-1143.

Lee, S., and Kim, S. (2002). Expansion of smectite by hexadecyltrimethylammonium. *Clays and Clay Minerals*, *50*(4), 435–445.

Lee, S. Y., Kim, S. J., Chung, S. Y., and Jeong, C. H. (2004). Sorption of hydrophobic organic compounds onto organoclays. *Chemosphere*, *55*(5), 781–785. doi:10.1016/j.chemosphere.2003.11.007

Lee, S., Cho, W., Hahn, P., Lee, M., Lee, Y., and Kim, K. (2005). Microstructural changes of reference montmorillonites by cationic surfactants. *Applied Clay Science*, *30*(3-4), 174–180. doi:10.1016/j.clay.2005.03.009

Lerz, V. H., and Kraemer, V. (1966). Ein verfahren zur herstellung texturfreier rontgen-pulverpraeparate von tonmineralen fur zaehlrohrgoniometer mit senkrechter drehachse. *Neues Jahrb. Minerol, Monatsh*, 50-59.

Levitz, P. E. (2002). Adsorption of non ionic surfactants at the solid/water interface. *Colloids and Surfaces A: Physicochemical and Engineering Aspects*, *205*(1-2), 31–38. doi:10.1016/S0927-7757(01)01139-6

Lexa, D. (1998). Hermetic holder for x-ray powder diffraction of air-sensitive differential scanning calorimetry samples. *Review of Scientific Instruments*, *69*(12), 4249–4250.

Li, J. H., and Zhang, L. M. (2010). Geometric parameters and REV of a crack network in soil. *Computers and Geotechnics*, *37*(4), 466–475. doi:10.1016/j.compgeo.2010.01. 006

Li, J., Smith, J. A., and Winquist, A. S. (1996). Permeability of earthen liners containing organobentonite to water and two organic liquids. *Environmental Science and Technology*, *30*(10), 3089–3093.

Linn, B., and Stupak, S. (2009). *Chemicals Used in Dry Cleaning Operations*. Retrieved from http://www.drycleancoalition.org/chemicals/ChemicalsUsedInDrycleaning Operations.pdf

Ma, Y., Zhu, J., He, H., Yuan, P., Shen, W., and Liu, D. (2010). Infrared investigation of organo-montmorillonites prepared from different surfactants. *Spectrochimica Acta. Part A, Molecular and Biomolecular Spectroscopy*, *76*(2), 122–9. doi:10.1016/j.saa.2010.02.038

MacEwan, D. (1948). Complexes of clays with organic compounds. I. Complex formation between montmorillonite and halloysite and certain organic liquids. *Transactions of the Faraday Society*, *44*, 349–367.

Mackay, D., and Cherry, J. (1989). Groundwater contamination: Pump-and-treat remediation. *Environmental Science and Technology*, *23*(6), 630–636.

Madejová, J., and Komadel, P. (2001). Baseline studies of the Clay Minerals Society Source Clays: Infrared methods. *Clays and Clay Minerals*, *49*(5), 410–432.

Matthieu III, D. E., Brusseau, M. L., Johnson, G. R., Artiola, J. L., Bowden, M. L., and Curry, J. E. (2013). Intercalation of trichloroethene by sediment-associated clay minerals. *Chemosphere*, *90*(2), 459–463.

McCaulou, D. R., and Huling, S. G. (1999). Compatibility of bentonite and DNAPLs. *Groundwater Monitoring and Remediation*, *19*(2), 78–86.

McDonald, M. G., and Harbaugh, A. W. (2003). The history of MODFLOW. *Ground Water 41* (2003), 280-283.

McKay, L. D., Cherry, J. A., and Gillham, R. W. (1993a). Field experiments in a fractured clay till, 1. Hydraulic conductivity and fracture aperture. *Water Resources Research*, *29*(4), 1149–1162. doi:10.1029/92WR02592

McKay, L. D., Gillham, R. W., and Cherry, J. A. (1993b). Field experiments in a fractured clay till 2. Solute and colloid transport. *Water Resources Research, 29*, 3879-3890.

Michaels, A. S., and Bixler, H. J. (1961). Flow of gases through polyethylene. *Journal of Polymer Science*, *50*(154), 413–439. doi:10.1002/pol.1961.1205015412

Middleton, T. A., and Cherry, J. A. (1996). The effects of chlorinated solvents on the permeability of clay in *Dense Chlorinated Solvents and Other DNAPLS in Groundwater: History, Behavior, and Remediation*, Pankow, J.F., and Cherry, J.A., (Eds.), Waterloo Press, Portland, OR, 313-335.

Millington, R., and Quirk, J. (1960). Transport in porous media, in *Transactions of 7th International Congress of Soil Science*, Vol. 1, F. A. van Baren. (Ed.), 97–106.

Millington, R., and Quirk, J. (1961). Permeability of porous solids. *Transactions of the Faraday Society*, *57*, 1200–1207.

Miniter, J. M., *Modeling Enhanced Storage of Groundwater Contaminants Due to the Presence of Cracks in Low Permeability Zones Underlying Contaminant Source Areas*. M.S. thesis, AFIT/GES/ENV/11-M02. Graduate School of Engineering and Management, Air Force Institute of Technology (AU), Wright-Patterson AFB OH, March 2011.

Miyahara, K., Ashida, T., Kohara, Y., Yusa, Y., and Sasaki, N. (1991). Effect of bulk density on diffusion for cesium in compacted sodium bentonite. *Radiochimca Acta*, *52*(2), 293–298.

Montgomery, J. H. (2007). *Groundwater chemicals desk reference,* 4th ed, CRC Press, Boca Raton, Florida.

Moore, D. M., and Reynolds, R. C. (1989). *X-ray Diffraction and the Identification and Analysis of Clay Minerals,* Oxford University Press, Oxford.

Morris, P. H., Graham, J., and Williams, D. J. (1992). Cracking in drying soils. *Canadian Geotechnical Journal,* 29(2), 263-277.

Mott, H. V., and Weber, Jr., W. J. (1991). Factors influencing organic contaminant diffusivities in soil-bentonite cutoff barriers. *Environmental Science and Technology*, *25*(10), 1708–1715.

Moulik, S. P. (1996). Micelles: Self-organic surfactant assemblies. *Current Science*, *71*(5), 368-376.

Moulik, S. P., and Mukherjee, K. (1996). On the versatile surfactant Aerosol-OT (AOT): Its physicochemical and surface chemical behaviours and uses. *Proceedings-Indian National Science Academy, Part A, 62,* 215–236.

Mundle, K., Reynolds, D. A., West, M. R., and Kueper, B. H. (2007). Concentration rebound following in situ chemical oxidation in fractured clay. *Ground Water*, *2007*, 692-702.

Murray, R. S., and Quirk, J. P. (1982). The physical swelling of clays in solvents. *Soil Science Society of America Journal*, *46*(4), 856–868.

Muurinen, A. (1990). Diffusion of uranium in compacted sodium bentonite. *Engineering Geology*, *28*(3), 359–367.

Myrand, D., Gillham, R. W., Sudicky, E. A., O'Hannesin, S. F., and Johnson, R. L. (1992). Diffusion of volatile organic compounds in natural clay deposits : Laboratory tests. *Journal of Contaminant Hydrology*, *10*(2), 159–177.

Nowak, E. J. (1983). Diffusion of colloids and other waste species in brine–saturated backfill materials <u>in</u> *Symposium D–Scientific Basis for Nuclear Waste Management VII, Materials Research Society Proceedings*, Vol. 26, Cambridge University Press, Cambridge, UK, 59-68.

O'Hara, S. K., Parker, B. L., Jørgensen, P. R., and Cherry, J. A. (2000). Trichloroethene DNAPL flow and mass distribution in naturally fractured clay: Evidence of aperture variability. *Water Resources Research*, *36*(1), 135–147. doi:10.1029/1999WR900 212

Olejnik, S., Posner, A. M., and Quirk, J. P. (1974). Swelling of montmorillonite in polar organic liquids. *Clays and Clay Minerals*, *22*, 361–365.

Olesen, T., Moldrup, P., and Gamst, J. (1999). Solute diffusion and adsorption in six soils along a soil texture gradient. *Soil Science Society of America Journal*, *63*(3), 519–524.

Oliveira, I. B., Demond, A. H., and Salehzadeh, A. (1996). Packing of sands for the production of homogeneous porous media. *Soil Science Society of America Journal*, *60*(1), 49–53.

Omidi, G., Thomas, J., and Brown, K. (1996). Effect of desiccation cracking on the hydraulic conductivity of a compacted clay liner. *Water, Air, and Soil Pollution*, *89*(1-2), 91–103.

Oolman, T., Godard, S. T., Pope, G. A., Jin, M., and Kirchner, K. (1995). DNAPL flow behavior in a contaminated aquifer: Evaluation of field data. *Groundwater Monitoring and Remediation*, *15*(4), 125–137.

Oscarson, D. W., Hume, H. B., Sawatsky, N. G., and Cheung, S. C. H. (1992). Diffusion of iodide in compacted bentonite. *Soil Science Society of America Journal*, *56*(5), 1400–1406.

Oscarson, D. W. (1994). Diffusion coefficients for iodide in compacted clays. *Clay Minerals*, *29*, 145–151.

Owen, S. J., Jones, N. L., and Holland, J. P. (1996). A comprehensive modeling environment for the simulation of groundwater flow and transport. *Engineering with Computers, 12*, 235-242.

Pankow, J. F., Johnson, R. L., Hewetson, J. P., and Cherry, J. A. (1986). An evaluation of contaminant migration patterns at two waste disposal sites on fractured porous media in terms of the equivalent porous medium (EPM) model. *Journal of Contaminant Hydrology*, *1*, 65-76.

Paradies, H. H. (1980). Shape and size of a nonionic surfactant micelle: TritonX-100 in aqueous solution. *The Journal of Physical Chemistry*, *84*(6), 599–607.

Parker, B. L., Gillham, R. W., and Cherry, J. A. (1994). Diffusive disappearance of immiscible-phase organic liquids in fractured geologic media. *Ground Water*, *62*(5), 805–820.

Parker, B. L. (1996). *Effects of Molecular Diffusion on the Persistence of Dense, Immiscible Phase Organic Liquids in Fractured Porous Media,* Ph.D. dissertation, University of Waterloo, Waterloo, Ontario, Canada.

Parker, B. L., Cherry, J. A., Chapman, S. W., and Guilbeault, M. A. (2003). Review and analysis of chlorinated solvent dense nonaqueous phase liquid distributions in five sandy aquifers. *Vadose Zone Journal*, *2*(2), 116-137. doi:10.2136/vzj2003.0116

Parker, B. L., Cherry, J. A., and Chapman, S. W. (2004). Field study of TCE diffusion profiles below DNAPL to assess aquitard integrity. *Journal of Contaminant Hydrology*, *74*(1-4), 197–230. doi:10.1016/j.jconhyd.2004.02.011

Parker, B. L., Chapman, S. W., and Guilbeault, M. A. (2008). Plume persistence caused by back diffusion from thin clay layers in a sand aquifer following TCE source-zone hydraulic isolation. *Journal of Contaminant Hydrology*, *102*(1-2), 86–104. doi:10.1016/j.jconhyd.2008.07.003

Rayhani, M. H., Yanful, E. K., and Fakher, A. (2007). Desiccation-induced cracking and its effect on the hydraulic conductivity of clayey soils from Iran. *Canadian Geotechnical Journal*, *44*(3), 276–283. doi:10.1139/t06-125

Riddick, J., Bunger, W., and Sakano, T. (1986). *Organic Solvents: Physical Properties and Methods of Purification,* John Wiley, New York.

Robinson, R. A., and Stokes, R.H. (1959). *The Measurement and Interpretation of Conductance, Chemical Potential and Diffusion in Solutions of Simple Electrolytes,* 2nd ed, Butterworths, London.

Rudolph, D. L., Cherry, J. A. and Farvolden, R. N. (1991). Groundwater flow and solute transport in fractured lacustrine clay near Mexico City. *Water Resources Research*, *27*(9), 2187–2201.

Russell, J. D., and Farmer, V. C. (1964). Infrared spectroscopic study of the dehydration of montmorillonite and saponite. *Clay Minerals Bulletin*, *5*(32), 443–464.

Sale, T., Illangasekare, T., Zimbron, J., Rodriguez, D., Wilking, B., Marinelli, F. (2007). *AFCEE Source Zone Initiative.* Final Report. Submitted to Air Force Center for Engineering and the Environment, Brooks City-Base, TX.

Sale, T., Newell, C., Stroo, H., Hinchee, R., and Johnson, P. (2008a). *Frequently Asked Questions Regarding Management of Chlorinated Solvents in Soils and Groundwater.* Environmental Security Technology Certification Program, Arlington, VA.

Sale, T. C., Zimbron, J. A., and Dandy, D. S. (2008b). Effects of reduced contaminant loading on downgradient water quality in an idealized two-layer granular porous media. *Journal of Contaminant Hydrology, 102*, 72-85.

Sánchez-Martín, M. J., Dorado, M. C., del Hoyo, C., and Rodríguez-Cruz, M. S. (2008). Influence of clay mineral structure and surfactant nature on the adsorption capacity of surfactants by clays. *Journal of Hazardous Materials*, *150*(1), 115–23. doi:10.1016/j.jhazmat.2007.04.093

Sato, H., Ashida, T., Kohara, Y., Yui, M., and Sasaki, N. (1992). Effect of dry density on diffusion of some radionuclides in compacted sodium bentonite. *Journal of Nuclear Science and Technology*, *29*(9), 873–882. doi:10.1080/18811248.1992.9731607

Sawatsky, N., Feng, Y., and Dudas, M. J. (1997). Diffusion of 1 -naphthol and naphthalene through clay materials: Measurement of apparent exclusion of solute from the pore space. *Journal of Contaminant Hydrology*, *27*(1), 25–41.

SERDP and ESTCP. (2006). *Expert Panel Workshop on Reducing the Uncertainty of DNAPL Source Zone Remediation, Final Report.* Retrieved from https://www.serdp-estcp.org/News-and-Events/Conferences-Workshops/Past-ER-Workshops.

Schwarzenbach, R. P., P. M. Gschwend, P. M., and D. M. Imboden, D. M. (2003). *Environmental Organic Chemistry.* 2nd ed. Wiley Interscience, Hoboken, NJ.

Shackelford, C. D. (1991). Laboratory diffusion testing for waste disposal: A review. *Journal of Contaminant Hydrology*, *7*(3), 177–217.

Shen, Y.-H. (2001). Preparations of organobentonite using nonionic surfactants. *Chemosphere*, *44*(5), 989–995. doi:10.1016/S0045-6535(00)00564-6

Sheng, G., and Boyd, S. A. (1998). Relation of water and neutral organic compounds in the interlayers of mixed Ca/trimethylphenylammonium-smectites. *Clays and Clay Minerals*, *46*(1), 10–17.

Silber, J. J., Biasutti, A., Abuin, E., and Lissi, E. (1999). Interactions of small molecules with reverse micelles. *Advances in Colloid and Interface Science*, *82*, 189-252.

Sims, J. E., Elsworth, D., and Cherry, J. A. (1996). Stress-dependent flow through fractured clay till: A laboratory study. *Canadian Geotechnical Journal*, *33*(3), 449–457.

Somasundaran, P., and Krishnakumar, S. (1997). Adsorption of surfactants and polymers at the solid-liquid interface. *Colloids and Surfaces A: Physicochemical and Engineering Aspects*, *123-124*(96), 491–513. doi:10.1016/S0927-7757(96)03829-0

Somasundaran, P., and Huang, L. (2000). Adsorption/ aggregation of surfactants and their mixtures at solid-liquid interfaces. *Advances in Colloid and Interface Science*, *88*(1), 179–208.

Sonon, L. S., and Thompson, M. L. (2005). Sorption of a nonionic polyoxyethylene lauryl ether surfactant by 2:1 layer silicates. *Clays and Clay Minerals*, *53*(1), 45–54. doi:10.1346/CCMN.2005.0530106

Stroo, H. F., Leeson, A., Marqusee, J. A., Johnson, P. C., Ward, C. H., Kavanaugh, M. C., Sale, T. C., Newell, C. J., Pennell, K. D., Lebrón, C. A., and Unger, M. (2012). Chlorinated ethene source remediation: Lessons learned. *Environmental Science and Technology*, *46*(12), 6348–6447.

Tang, C.-S., Shi, B., Liu, C., Zhao, L., and Wang, B. (2008). Influencing factors of geometrical structure of surface shrinkage cracks in clayey soils. *Engineering Geology*, *101*(3-4), 204–217. doi:10.1016/j.enggeo.2008.05.005

Tang, C.-S., Shi, B., Liu, C., Suo, W.-B., and Gao, L. (2011). Experimental characterization of shrinkage and desiccation cracking in thin clay layer. *Applied Clay Science*, *52*(1-2), 69–77. doi:10.1016/j.clay.2011.01.032

Tang, C.-S., Shi, B., Cui, Y.-J., Liu, C., and Gu, K. (2012). Desiccation cracking behavior of polypropylene fiber–reinforced clayey soil. *Canadian Geotechnical Journal*, *49*(9), 1088–1101. doi:10.1139/t2012-067

Thompson, D. (1990). *Hydraulic Evidence of Wisconsinan-aged Open Fractures in a Deep Clayey Till*, M.Sc. thesis, Univ. of Waterloo, Waterloo, Ontario, Canada.

Van Olphen, H., and Fripiat, J. (1979). *Data Handbook for Clay Minerals and Other Non-Metallic Materials,* Pergamon, New York.

Velde, B. (1999). Structure of surface cracks in soil and muds. *Geoderma*, *93*(1-2), 101–124. doi:10.1016/S0016-7061(99)00047-6

Wilke, C., and Chang, P. (1955). Correlation of diffusion coefficients in dilute solutions. *AIChE Journal*, *1*(2), 264–270.

Williams-Daryn, S., and Thomas, R. K. (2002). The intercalation of a vermiculite by cationic surfactants and its subsequent swelling with organic solvents. *Journal of Colloid and Interface Science*, *255*(2), 303–311. doi:10.1006/jcis.2002.8673

Williams-Johnson, M., Eisenmann, C. J., and Donkin, S. G. (1997). *Toxicological Profile for Trichloroethylene*, Agency for Toxic Substances and Disease Registry, Atlanta, GA.

Wilson, J. (1997). Removal of aqueous phase dissolved contamination: Non-chemically enhanced pump-and-treat in *Subsurface Restoration*, Ward, M. R., Cherry, C.H., and Scalf, J.S. (Eds.), Ann Arbor Press, Ann Arbor, MI, 271-285.

Xu, Q., Vasudevan, T. V., and Somasundaran, P. (1991). Adsorption of anionic—nonionic and cationic—nonionic surfactant mixtures on kaolinite. *Journal of Colloid and Interface Science*, *142*(2), 528–534. doi:10.1016/0021-9797(91)90083-K

Young, D. F., and Ball, W. P. (1998). Estimating diffusion coefficients in low-permeability porous media using a macropore column. *Environmental Science and Technology*, *32*(17), 2578–2584. doi:10.1021/es9711324

Zhang, R., and Somasundaran, P. (2006). Advances in adsorption of surfactants and their mixtures at solid/solution interfaces. *Advances in Colloid and Interface Science*, *123-126*, 213–29. doi:10.1016/j.cis.2006.07.004

Zhou, X. (1994). *The Study of Restacked Single Molecular Layer Molybdenum Disulfide with Organic Tetrachloroethylene Included*, B.Sc. thesis, Simon Fraser University, Burnaby, British Columbia, Canada.

Zhu, L., Ren, X., and Yu, S. (1998). Use of cetyltrimethylammonium bromide-bentonite to remove organic contaminants of varying polar character from water. *Environmental Science and Technology*, *32*(21), 3374–3378. doi:10.1021/es980353m

8.0 Publications and Presentations

8.1. Publications

Ayral, D., M. Otero-Diaz, and A. H. Demond, Mechanism of Basal Spacing Reduction in Sodium Smectitic Clay Materials in Contact with DNAPL Wastes, in preparation for submission to *Environmental Science and Technology*.

Ayral, D., and A. H. Demond, Measurement and Estimation of Diffusion of Trichloroethylene in Saturated Low Permeability Soil Materials, in preparation for submission to *Water Resources Research*.

Huang, J., J. A. Christ, M. N. Goltz, and A. H. Demond, Modeling NAPL Dissolution from Pendular Rings in Idealized Porous Media, in review *Water Resources Research*, 2015.

Huang, J. and M. N. Goltz, Analytical Solutions for Transport in Aquifer and Fractured Clay Matrix System, in review *Water Resources Research*, 2015.

Sievers, K., J. Huang, A. H. Demond, and M. N. Goltz, Impact of Cracks in Low Permeability Layers on Dissolved Contaminant Transport in Groundwater, in review *Journal of Hydrologic Engineering*, 2015.

Ayral, D., *Impact of Clay-DNAPL Interactions on the Transport of Chlorinated Solvents in Low Permeability Subsurface Zones*, Ph.D. diss. University of Michigan, 2015.

Bell, J. M., J. Huang, J. A. Christ, A. H. Demond, and M. N. Goltz, Remediation Complications: Subsurface Cracking at Hazardous Waste Sites, *The Military Engineer, 693*, 51-52, January/February 2015.

Ayral D., and A. H. Demond, Estimation of Diffusion Coefficients for Organic Solutes of Environmental Concern in Saturated Clay-Silt Mixtures <u>in</u> L. Wesley, ed., *Clay and Clay Minerals: Geological Origin, Mechanical Properties and Industrial Application*s, Nova Science Publishers, Hauppauge, NY, pp. 45-66.

Ayral, D., M. Otero, M. N. Goltz, and A. H. Demond, Impact of DNAPL contact on the structure of smectitic clay materials, *Chemosphere*, *95*, 181-186, 2014.

Huang, J. and M. N. Goltz, Spatial Moment Equations for a Groundwater Plume with Degradation and Rate-Limited Sorption, *Journal of Hydrologic Engineering, 19*(5), 1053-1058, 2014.

Bell, J. M., *Accounting for Mass Transfer Kinetics when Modeling the Impact of Low Permeability Layers in a Groundwater Source Zone on Dissolved Contaminant Fate and Transport*. M.S. thesis, AFIT/GEM/ENV/14-M08. Graduate School of Engineering and Management, Air Force Institute of Technology (AU), Wright-Patterson AFB OH, March 2013.

Sievers, K.W., *Modeling the Impact of Cracking In Low Permeability Layers in a Groundwater Contamination Source Zone On Dissolved Contaminant Fate and Transport*. M.S. thesis, AFIT/GES/ENV/12-M02. Graduate School of Engineering and Management, Air Force Institute of Technology (AU), Wright-Patterson AFB OH, March 2012.

Miniter, J.M., M.N. Goltz, A.H. Demond, and J. Huang, Diffusion in Clay Layers and Groundwater Remediation, *Air Force Civil Engineer, 19*(3): 22-23, 2011.

Miniter, J. M., *Modeling Enhanced Storage of Groundwater Contaminants Due to the Presence of Cracks in Low Permeability Zones Underlying Contaminant Source Areas*. M.S. thesis, AFIT/GES/ENV/11-M02. Graduate School of Engineering and Management, Air Force Institute of Technology (AU), Wright-Patterson AFB OH, March 2011.

8.2. Presentations:

Ayral, D., M. Otero, and A. Demond, Interactions between chlorinated waste solvents and clay minerals in low permeability subsurface layers. American Geophysical Union Fall Meeting, San Francisco, CA, December 15-19, 2014.

Ayral, D. and A. Demond, Diffusion of DNAPL Components into Low Permeability Layers. American Geophysical Union Fall 2013 Meeting, San Francisco CA, December 9-13, 2013.

Goltz, M. N. and J. Huang, Application of Temporal and Spatial Moments to Analyze Groundwater Contaminant Transport, 2013 World Environmental & Water Resources Congress, Cincinnati, OH, 19-23 May 19-23, 2013.

Otero, M., D. Ayral, J. Shipan, M. N. Goltz, J. Huang, A. H. Demond, Cracking of Clay Due to Contact with Waste Chlorinated Solvents, American Geophysical Union Fall 2012 Meeting, San Francisco CA, December 3-7, 2012.

Ayral, D., M. Otero, S. Chung, M. N. Goltz, J. Huang, A. H. Demond, Enhanced Diffusion of Chlorinated Organic Compounds into Aquitards due to Cracking, American Geophysical Union Fall 2012 Meeting, San Francisco CA, December 3-7, 2012.

Sievers, K., M. N. Goltz, J. Huang, and A. H. Demond, Impact of DNAPL Storage in Cracked Low Permeability Layers on Dissolved Contaminant Plume Persistence, American Geophysical Union Fall 2012 Meeting, San Francisco CA, December 3-7, 2012.

Demond, A. H., Impact of the Interaction of Chlorinated Solvents and Clay in Low Permeability Zones in the Subsurface, Michigan Technological University, Houghton MI, September 24, 2012.

Ayral, D., M. Otero, A. H. Demond, M. N. Goltz, and J. Huang, Diffusion of Chlorinated Organic Contaminants into Aquitards: Enhanced by the Flocculation of Clay?, Graduate Academic Conference, East Lansing MI, March 30, 2012.

Ayral, D., M. Otero, A. H. Demond, M. N. Goltz, and J. Huang, Diffusion of Chlorinated Organic Contaminants into Aquitards: Enhanced by the Flocculation of Clay?, American Geophysical Union Fall 2011 Meeting, San Francisco CA, December 5-9, 2011.

Sievers, K., M. N. Goltz, J. Huang, and A. H. Demond, Modeling the Impact of Cracking in Low Permeability Layers in a Groundwater Contamination Source Zone on Dissolved Contaminant Fate and Transport, American Geophysical Union Fall 2011 Meeting, San Francisco CA, December 5-9, 2011.

Sievers, K. W., M. N. Goltz, J. Huang, and A. H. Demond, Modeling the Impact of Cracking in Low Permeability Layers in a Groundwater Contamination Source Zone on Dissolved

Contaminant Fate and Transport, Partners in Environmental Technology Technical Symposium and Workshop, Washington DC, November 29 – December 1, 2011.

Demond, A. H., M. N. Goltz and J. Huang, Impact of Clay-DNAPL Interactions on Transport of Chlorinated Solvents into Low Permeability Zones, Partners in Environmental Technology Technical Symposium and Workshop, Washington DC, November 29 – December 1, 2011.

Ayral, D., M. Otero, M., and A. Demond, Impact of DNAPLs on the Structure of Clay in the Subsurface, Fall National Meeting of the American Chemical Society, Denver CO, August 28 - 1 September 1, 2011.

Demond, A., D. Ayral, and M. Otero, Impact of Chlorinated Waste Solvents on the Structure of Clay in Subsurface Low Permeability Zones, AEESP Education and Research Conference, Tampa, FL, July 10-12, 2011.

Ayral, D., A. H. Demond, M. N. Goltz, J. Huang, Impact of Chlorinated Solvents on the Structure of Clay in Low Permeability Zones in Groundwater Contamination Source Areas, Partners in Environmental Technology Technical Symposium and Workshop, Washington DC, November 30 – December 2, 2010.

Miniter, J., M. N. Goltz, J. Huang, A. H. Demond, and A. E. Thal, Jr., Modeling the Interaction between Dense Non-Aqueous Phase Liquids (DNAPLs) and Low Permeability Zones in Groundwater Contamination Source Areas, Partners in Environmental Technology Technical Symposium and Workshop, Washington DC, November 30 – December 2, 2010.

Demond, A.H., D. Ayral, and M.N. Goltz, Diffusional Transport of Organic Solutes in Subsurface Clay Lenses and Layers, American Geophysical Union Fall Meeting, San Francisco, CA, December 14-18, 2009.